DEVELOPMENT OF DNA DETECTION SYSTEM USING G-QUADRUPLEX AS CATALYST FOR COLORIMETRIC DETECTION WITH PYRROLIDINYL PEPTIDE NUCLEIC ACID

Miss Somlawan Thipkunthong

A Thesis Submitted in Partial Fulfillment of the Requirements
for the Degree of Master of Science in Chemistry
Department of Chemistry
FACULTY OF SCIENCE
Chulalongkorn University
Academic Year 2022

การพัฒนาระบบการตรวจวัดลำดับเบสของกรดนิวคลีอิกโดยใช้จี-ควอดรูเพล็กซ์เป็นตัวเร่งปฏิกิริยาสำหรับการตรวจวัดเชิงสีร่วมกับพิร์โรลิดินิลเพปไทด์นิวคลีอิกแอซิด

น.ส.โสมลวัณย์ ทิพย์ขุนทอง

วิทยานิพนธ์นี้เป็นส่วนหนึ่งของการศึกษาตามหลักสูตรปริญญาวิทยาศาสตรมหาบัณฑิต
สาขาวิชาเคมี ภาควิชาเคมี
คณะวิทยาศาสตร์ จุฬาลงกรณ์มหาวิทยาลัย
ปีการศึกษา 2565

Thesis Title	DEVELOPMENT OF DNA DETECTION SYSTEM USING G-QUADRUPLEX AS CATALYST FOR COLORIMETRIC DETECTION WITH PYRROLIDINYL PEPTIDE NUCLEIC ACID
By	Miss Somlawan Thipkunthong
Field of Study	Chemistry
Thesis Advisor	Professor TIRAYUT VILAIVAN, Ph.D.

Accepted by the FACULTY OF SCIENCE, Chulalongkorn University in Partial Fulfillment of the Requirement for the Master of Science

..... Dean of the FACULTY OF SCIENCE
(Professor POLKIT SANGVANICH, Ph.D.)

THESIS COMMITTEE

..... Chairman
(Professor ORAWON CHAILAPAKUL, Ph.D.)

..... Thesis Advisor
(Professor TIRAYUT VILAIVAN, Ph.D.)

..... Examiner
(Professor SUMRIT WACHARASINDHU, Ph.D.)

..... External Examiner
(Associate Professor Chittanon Buranachai, Ph.D.)

โสมลวัณย์ ทิพย์ขุนทอง : การพัฒนาระบบการตรวจวัดลำดับเบสของกรดนิวคลีอิกโดยใช้จี-ควอดรูเพล็กซ์เป็นตัวเร่งปฏิกิริยาสำหรับการตรวจวัดเชิงสีร่วมกับพิร์โรลิดินิลเพปไทด์นิวคลีอิกแอซิด. (DEVELOPMENT OF DNA DETECTION SYSTEM USING G-QUADRUPLEX AS CATALYST FOR COLORIMETRIC DETECTION WITH PYRROLIDINYL PEPTIDE NUCLEIC ACID) อ.ที่ปรึกษาหลัก : ศ. ดร.ธีรยุทธ วีไลวัลย์

การตรวจหาลำดับเบสของกรดนิวคลีอิกมีความสำคัญต่อการวินิจฉัยและรักษาโรคทางพันธุกรรมต่างๆ ดังนั้นการพัฒนาวิธีการตรวจวัดที่ทันสมัย ไม่ซับซ้อนและมีประสิทธิภาพยังคงเป็นที่ต้องการอย่างมาก ซึ่งในบรรดาตัวเลือกต่างๆ การตรวจวัดเชิงสีเป็นเทคนิคที่ง่าย ราคาถูก ไม่ต้องใช้เครื่องมือที่ซับซ้อน และสามารถตรวจวัดได้ด้วยตาเปล่า ดังนั้นในงานวิจัยนี้จึงมีแนวคิดที่จะพัฒนาการตรวจวัดเชิงสีสำหรับการตรวจวัดดีเอ็นเอเป้าหมายโดยนำพิร์โรลิดินิลเพปไทด์นิวคลีอิกแอซิด (เอซีพีซีพีเอ็นเอ, acpcPNA) มาใช้ร่วมกับจี-ควอดรูเพล็กซ์/ฮีมิน ดีเอ็นเอไซม์ โครงสร้างจี-ควอดรูเพล็กซ์เกิดจากดีเอ็นเอที่มีลำดับเบสกัวนีนจำนวนมาก ซึ่งในสภาวะที่มีฮีมินจะเกิดการรวมตัวกันเป็นดีเอ็นเอไซม์ ซึ่งมีคุณสมบัติในการเร่งปฏิกิริยาออกซิเดชั่นของสับสเตรต 3,3’,5,5’-tetramethylbenzidine (TMB) ซึ่งไม่มีสีในสภาวะที่มีไฮโดรเจนเปอร์ออกไซด์เป็นตัวออกซิไดซ์ และทำให้เกิดผลิตภัณฑ์ที่มีสีฟ้า นอกจากนี้การเข้าคู่กันของพีเอ็นเอกับลำดับเบสบางส่วนของจี-ควอดรูเพล็กซ์ตามกฎของวัตสัน-คริกจะทำให้เกิดการยับยั้งการเกิดโครงสร้างจี-ควอดรูเพล็กซ์และการทำงานของดีเอ็นเอไซม์ในการเร่งปฏิกิริยาในการเกิดสี แต่เมื่อมีการเข้าคู่กันระหว่างดีเอ็นเอเป้าหมายกับจี-ควอดรูเพล็กซ์ ดีเอ็นเอโพรบโดยไม่มีลำดับเบสคู่สมร่วมกับส่วนของโครงสร้างจี-ควอดรูเพล็กซ์ จะทำให้พีเอ็นเอถูกแทนที่และเกิดโครงสร้างจี-ควอดรูเพล็กซ์ รวมถึงดีเอ็นเอไซม์กลับคืนมา โดยการเกิดและการยับยั้งโครงสร้างจี-ควอดรูเพล็กซ์สามารถยืนยันได้ด้วยเทคนิค CD spectroscopy, gel electrophoresis และ UV-visible spectrophotometry หลักการตรวจวัดเชิงสีนี้ได้ถูกนำมาใช้ในการตรวจหาดีเอ็นเอ โดยมีความจำเพาะต่อลำดับเบสและสามารถตรวจวัดในเชิงปริมาณได้ในช่วงตั้งแต่ 0.25 ถึง 0.025 ไมโครโมลาร์ อีกทั้งมีขีดจำกัดในการตรวจวัดได้ต่ำถึง 7 นาโนโมลาร์ ดังนั้นระบบการตรวจวัดที่ถูกพัฒนาขึ้นนี้จึงมีศักยภาพที่จะนำไปประยุกต์ใช้ในการวินิจฉัยโรคและปัญหาอื่นๆ นอกจากนี้ยังได้นำการขยายสัญญาณด้วยกระบวนการนำดีเอ็นเอเป้าหมายกลับมาใช้ใหม่ (target recycling) ด้วย Exonuclease III ซึ่งสามารถย่อยจี-ควอดรูเพล็กซ์ ดีเอ็นเอโพรบบางส่วน ทำให้ความว่องไวในการตรวจวัดดียิ่งขึ้น อย่างไรก็ตามการนำดีเอ็นเอเป้าหมายกลับมาใช้ใหม่ไม่ประสบผลสำเร็จเนื่องจากการแข่งขันของเอซีพีซีพีเอ็นเอและจี-ควอดรูเพล็กซ์ ดีเอ็นเอโพรบที่ถูกย่อยไปบางส่วน

สาขาวิชา	เคมี	ลายมือชื่อนิสิต .....
ปีการศึกษา	2565	ลายมือชื่อ อ.ที่ปรึกษาหลัก .....

6270207023 : MAJOR CHEMISTRY

KEYWORD: acpcPNA, G-quadruplex/hemin DNAzyme, Colorimetric detection, DNA target recycling, Nucleic acid

Somlawan Thipkunthong : DEVELOPMENT OF DNA DETECTION SYSTEM USING G-QUADRUPLEX AS CATALYST FOR COLORIMETRIC DETECTION WITH PYRROLIDINYL PEPTIDE NUCLEIC ACID. Advisor: Prof. TIRAYUT VILAIVAN, Ph.D.

Nucleic acid sequence detection is very important for many applications such as the diagnosis of genetic diseases. The development of new, simple yet effective methods is still in great demand. Among several options, colorimetric detection is a technique that does not require complicated instruments and allows the detection by naked eyes. In this work, a new colorimetric DNA detection system was developed using the combination of a pyrrolidinyl peptide nucleic acid (acpcPNA) probe and a G-quadruplex/hemin DNAzyme. The G-quadruplex is formed from G-rich DNA sequences, and in the presence of hemin, a DNAzyme is formed which effectively catalyzes the oxidation of the colorless 3,3',5,5'-tetramethylbenzidine (TMB) substrate into the blue oxidized TMB in the presence of H_2O_2. The G-quadruplex formation is inhibited by the partial hybridization with the acpcPNA probe *via* the Watson and Crick base-pairing. Accordingly, the acpcPNA suppresses the DNAzyme activity and also the blue color formation. A strand displacement occurs in the presence of the target DNA, which has a sequence complementary to the G-quadruplex DNA probe but does not directly overlap with the G-quadruplex-forming region. This results in the displacement of the acpcPNA strand leading to the re-formation of the G-quadruplex structure as well as the restoration of the DNAzyme activities. The G-quadruplex disruption and formation were confirmed by CD spectroscopy, gel electrophoresis, and UV-visible spectrophotometry. The principle was successfully applied for colorimetric DNA detection in a sequence-specific fashion with a linearity range from 0.25 μM to 0.025 μM and an LOD of 7 nM. Thus, this developed platform has the potential to be applied for diagnostic applications as well as other problems. To improve the sensitivity further, the target-mediated partial digestion of the G-quadruplex DNA probe by Exonuclease III was proposed to amplify the signal by target recycling. However, the target recycling was not successful due to the competitive binding of the acpcPNA probe to the partially digested G-quadruplex DNA probe.

Field of Study:	Chemistry	Student's Signature .....
Academic Year:	2022	Advisor's Signature .....

ACKNOWLEDGEMENTS

First of all, I would like to thank you every part of me for never giving up and all of the memories and experiences I've had during my master's journey, both good and bad. I would really like to sincerely thank Prof. Dr. Tirayut Vilaivan for supporting my research in every way and for giving me the chance to develop a variety of research skills. In addition, he was exceedingly kind with his time and supportive in helping with the study under his supervision. My sincere appreciation is also extended to Chotima VIlaivan, for helping me. I would like to thank everyone who helped me to finish my research, especially the lovely TV lab family. My moment in the lab is special and joyful.

For my family, I am very appreciative of my mom, my whole family's kindness, and my dogs, as well as their constant support, encouragement, love, caring and healing me. My special thanks as well go to all the friend who have supported me to complete the difficult lectures and encouraged me directly or indirectly.

Finally, I would like to thank Department of Chemistry, Faculty of Science, Chulalongkorn University for the financial supports during my master's journey. I would like to express my appreciation to the members of my thesis committee for their considerate comments and their time.

Somlawan Thipkunthong

TABLE OF CONTENTS

Page

LIST OF FIGURES

LIST OF TABLES

LIST OF ABBREVIATIONS AND SYMBOLS

A	adenine
A^{Bz}	*N*^{6}-benzoyladenine
Ac	acetyl
Ac_2O	acetic anhydride
ACPC	(1*S*,2*S*)-2-amino-1-cyclopentanecarboxylic acid
APS	ammonium persulfate
Boc	*tert*-butoxycarbonyl
Bz	benzoyl
C	cytosine
CD	circular dichroism
cal.	calculated
C^{Bz}	*N*^{4}-benzoylcytosine
CCA	α-cyano-4-hydroxycinnamic acid
DBU	1,8-diazabicyclo[5.4.0]undec-7-ene
DIEA	diisopropylethylamine
DMF	*N,N'*-dimethylformamide
DNA	deoxyribonucleic acid
Exo III	exonuclease III
equiv.	equivalent
FAM	5(6)-carboxyfluorescein
Fmoc	9*H*-fluoren-9-ylmethoxycarbonyl
G	guanine
G-DNA	G-quadruplex deoxyribonucleic acid
G^{Ibu}	*N*^{2}-isobutyrlguanine
HPLC	high performance liquid chromatography
HATU	*O*-(7-azabenzotriazol-1-yl)-*N,N,N',N'*-tetramethyluronium hexafluorophosphate
HOAt	1-hydroxy-7-azabenzotriazole

H_2O_2	hydrogen peroxide
LOD	limit of detection
Lys	lysine
M	molar
MALDI-TOF	matrix assisted laser desorption/ionization time of flight
MeOH	methanol
mg	milligram
min	minute
mL	milliliter
mol	mole
m/z	mass-to-charge ratio
$MgCl_2$	magnesium chloride
nm	nanometer
nmol	nanomole
NH_4OAc	ammonium acetate
PB	phosphate buffer
Pfp	pentafluorophenyl
PCR	Polymerase chain reaction
PNA	peptide nucleic acid or polyamide nucleic acid
RNA	ribonucleic acid
SDS	sodium dodecyl sulfate
T	thymine
TBE	tris-borate-EDTA
TEMED	*N,N,N',N'*-tetramethylethylenediamine
TFA	trifluoroacetic acid
TMB	3,3′,5,5′- tetramethyl benzidine
Tris-HCl	tris hydrochloride
T_m	melting temperature
t_R	retention time
U	unit
UV	ultraviolet

°C	degree celsius
µL	microliter
µmol	micromole
µM	micromolar
%	percent
%w/v	percent weight per volume
ε	molecular extinction coefficient
T_{block}	record block temperature
A_{260}	Absorbance at 260 nm

CHAPTER I

INTRODUCTION

1.1 DNA biosensor

A biosensor is a system that recognizes one or more specific biological targets and generates a measurable signal that can indicate the presence of the target(s) qualitatively and/or quantitatively. One important component of any biosensor is a biomolecule that can recognize the target substrates, such as enzymes, aptamers, antibodies, and nucleic acids. These are collectively referred to as a bioreceptor **(Figure 1.1)**. The specific interaction between the bioreceptor and the target substrate generates some change at the molecular level such as conformational change. Such change will subsequently be transformed into a detectable signal by a transducer. Nucleic acid (DNA/RNA) biosensors are one of the most important classes of biosensors because of the widespread applications of nucleic acid testing. The genetic information, which is stored in the nucleotide sequences, plays an important role in the synthesis of proteins which are essential for the structures and functions of all living organisms. The protein synthesis can be completely stopped or result in completely different proteins with even a minor mutation in the DNA sequence. This may result in genetic disorders. Thus, DNA sequence detection is very important in the diagnosis and treatment of genetic disorders. In addition, DNA sequences are unique to a specific organism, and thus DNA sequences can be reliably used as a barcode or signature to identify a particular species or strain.

DNA sequencing has historically been used to determine DNA sequences, but it requires expensive equipment, time-consuming procedures, and highly qualified workers. Alternatively, the hybridization-based assays *via* the highly specific Watson-Crick base-pairing have been widely applied in probe-based DNA sequence detection. In contrast to other non-nucleic acid targets, the probe sequence can be easily designed using only the primary sequence of the target. Moreover, small amounts of DNA can be easily amplified by techniques such as polymerase chain reaction (PCR) to improve sensitivity by several orders of magnitude. In probe-based DNA

biosensors, the probe-target hybridization is typically coupled with one or more reporting techniques such as fluorescence,[1, 2] colorimetric,[3, 4] or electrochemical detection.[5, 6] The colorimetric detection is an attractive technique because it does not require expensive instruments and could even be operated by naked eye observation under ambient light. For example, the antigen test kits (officially referred to as lateral flow devices) commonly used for pregnancy testing or more recently, COVID-19 detection. These aforementioned colorimetric biosensor platforms are usually designed for non-nucleic acids because the sample preparation was easier. Nonetheless, some nucleic acid test kits have recently been available for home use.[7]

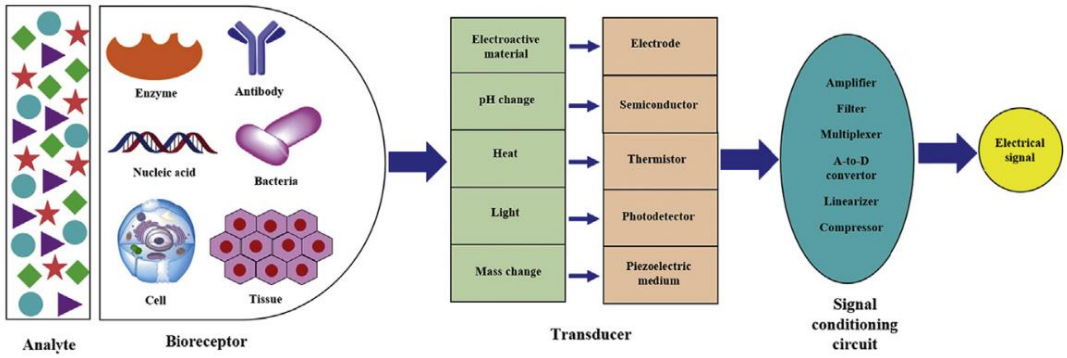

Figure 1.1 Diagram of a biosensor[8] (Reprinted from Elsevier Books, Ali A. Ensafi, Chapter 1 - An introduction to sensors and biosensors, 1-10., Copyright (2019), with permission from Elsevier)

1.2 DNA G-quadruplex

In general, a DNA duplex is formed from the hybridization between nucleobases (A-T, C-G) *via* the Watson-Crick base-pairing **(Figure 1.2)**. However, when the oligonucleotide chain contains a significant number of consecutive guanine bases, they may arrange into a special structure called G-quadruplex. A DNA G-quadruplex is a noncanonical secondary structure, which is formed from four guanine bases *via* the Hoogsteen base pairing.[9] The structure of G-quadruplexes has been extensively studied by UV spectroscopy, nuclear magnetic resonance spectroscopy (NMR), circular dichroism (CD), and biochemical techniques.[10] Typically,

four blocks or three or more consecutive G bases linked together by a few nucleotides are required to form such structures. The four guanine bases are connected together by hydrogen bondings to form a G-tetrad. This structure was further stabilized by base stacking and an alkali metal (or ammonium) ion[11] **(Figure 1.3 (A))**. There are two main types of G-quadruplexes including intramolecular (monomeric) and intermolecular (multimeric) **(Figure 1.3 (B))**. G-quadruplexes are ubiquitous *in vivo* and are thought to have important biological roles.[12] Several planar aromatic molecules can stack on top of the flat end of the G-quadruplex structure to form a stable complex. Certain dyes such as N-methyl mesoporphyrin IX (NMM) and thioflavin T (ThT) can bind to G-quadruplexes and exhibit strong fluorescence enhancement.[13, 14]

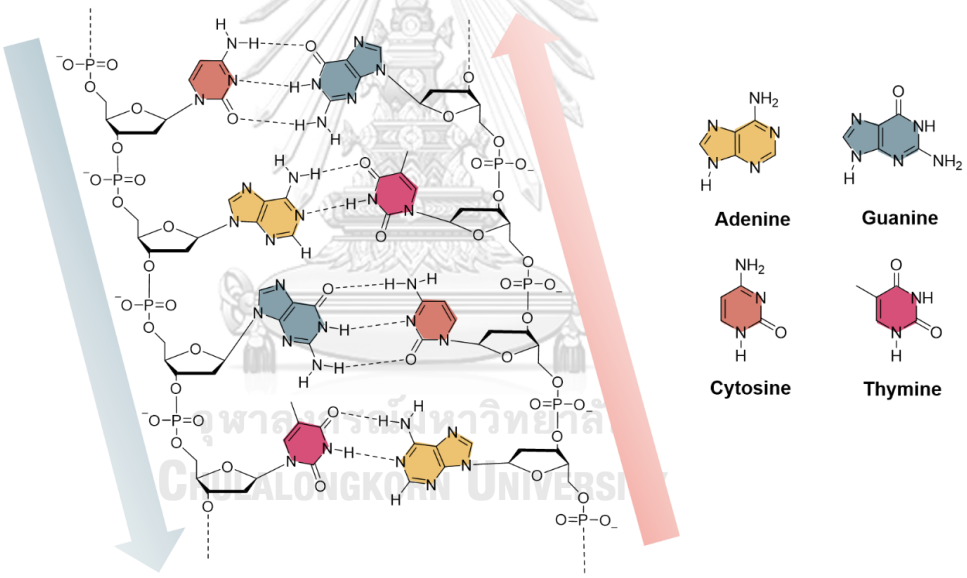

Figure 1.2 Structure of DNA duplex

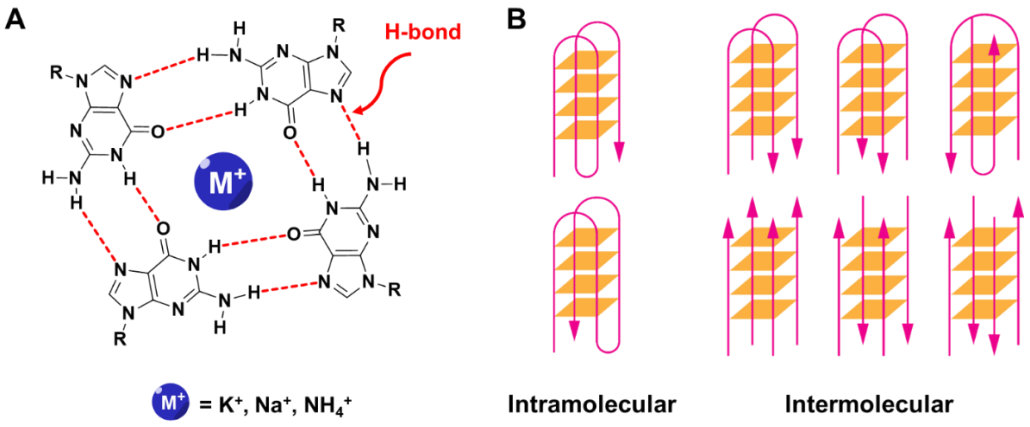

Figure 1.3 (A) Structure of G-quadruplex, (B) Example of intramolecular and intermolecular G-quadruplexes

1.2.1 Detection of DNA by G-quadruplex/hemin DNAzyme

DNAzymes are DNA oligonucleotides that can catalyze a specific chemical reaction similar to natural enzymes and RNA-based ribozymes that are essential for many biologically relevant processes. DNAzymes are generally created by in vitro selection and have found widespread applications.[15] In 1998, The G-quadruplex-enhanced peroxidase activity of hemin was first reported by Travascio and co-workers.[16] The G-quadruplex/hemin DNAzymes have been developed to replace the natural protein-based peroxidases due to their compact size, higher stability, ease of synthesis, and low cost of such a "DNAzyme" system.

Hemin or iron(III)-protoporphyrin IX is a naturally-occurring metal complex that acts as a cofactor in various enzyme-catalyzed processes. It can stack on top of the G-quadruplexes *via* **π-π** interaction to form a stable complex.[17] Such G-quadruplex/hemin complex exhibits peroxidase activities similar to the horseradish peroxidase-hemeprotein. For example, it catalyzes the oxidation of various chromogenic or fluorogenic substrates such as Amplex Red, 3,3′,5,5′-tetramethyl benzidine (TMB), 2,2′-azinobis(3-ethylbenzothiazoline-6-sulfonate) (ABTS) by H_2O_2 to generate colored or fluorescent products.

TMB is one of the most widely used chromogenic substrates in peroxidase reactions due to its high absorption coefficients and non-carcinogenic properties.

Hydrogen peroxide performs as the electron acceptor while the TMB substrate serves as the electron donor. The oxidized TMB may appear in two forms depending on the pH of the solution. The blue oxidized TMB showed the maximum absorbance at 370 nm and 650 nm. Under acidic conditions, the blue oxidation product converts to a more stable yellow diamine form which shows the maximum absorbance at 450 nm as shown in **Figure 1.4**.

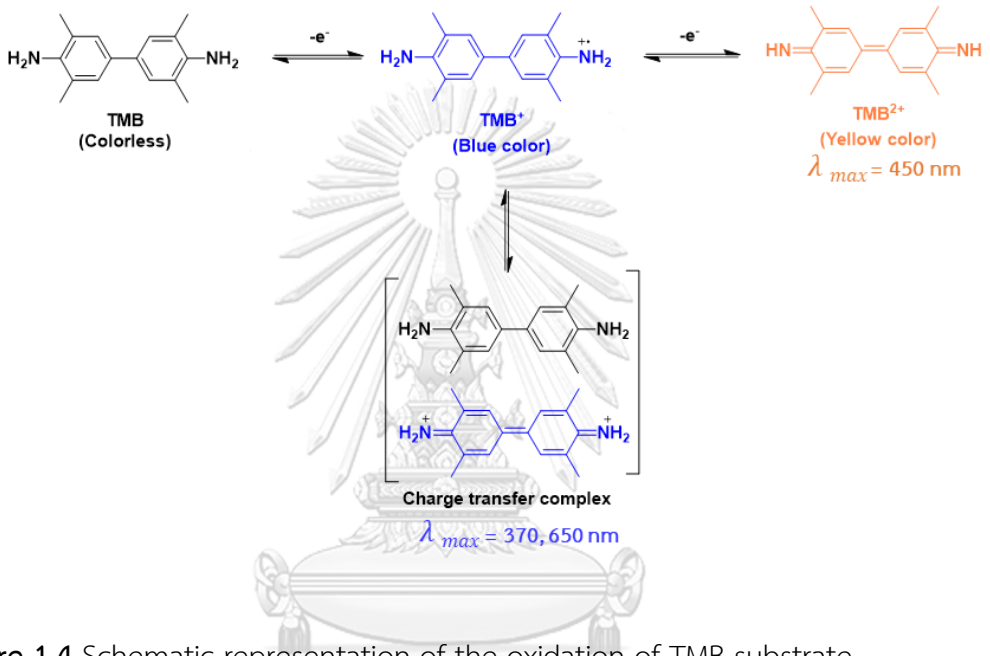

Figure 1.4 Schematic representation of the oxidation of TMB substrate

A proposed mechanism for the catalysis by G-quadruplex/hemin DNAzyme is shown in **Figure 1.5**, The iron(III) ion of hemin is oxidized with H_2O_2 to produce an Fe(IV)=O· radical intermediate or other Fe(IV)=O species, which is the active species that oxidizes the chromogenic or fluorogenic substrates. The signal is generated and the Fe is converted back to Fe(III) species that could enter the next round of the catalytic cycle to convert more substrate molecules to colored or fluorescent products.

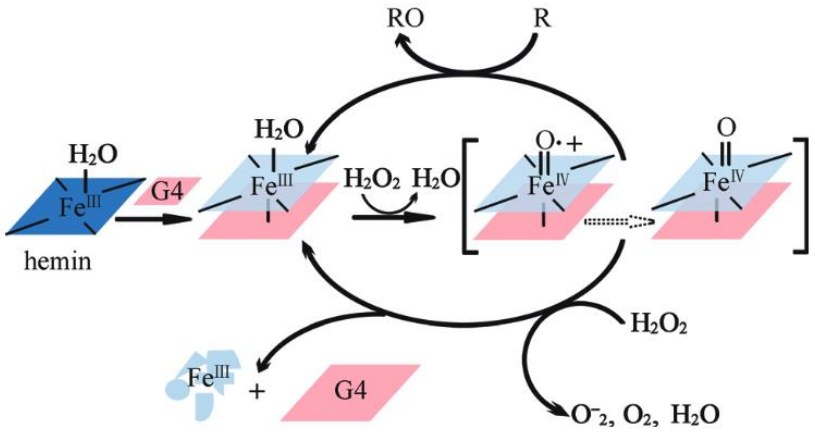

Figure 1.5 A proposed mechanism for the catalysis of G-quadruplex/hemin DNAzyme[18]

In recent years, the G-quadruplex/hemin system has been widely applied in various assays such as metal ion detections,[19] organic molecules detection,[20, 21] nucleic acid detection systems.[22, 23, 24] The significance of using the DNAzyme-based assay is that one binding event can generate several signals due to the catalytic nature of the DNAzyme reaction. As a result, in principle, such DNAzyme-based assay should provide higher sensitivity than conventional non-amplified tests.

In 2012, Zhang and co-workers[25] developed a label-free bifunctional colorimetric oligonucleotide probe for DNA and protein detection. This system consisted of two hairpin "domains" connected together to form a split G-quadruplex DNAzyme. One of the two hairpins was designed to recognize a specific DNA target sequence and another was designed to recognize thrombin, as seen in **Figure 1.6**. In the absence of the target, the two domains are linked to form a G-quadruplex DNAzyme that could catalyze the oxidation of TMB substrate in the presence of hemin. A yellow-colored solution and the absorbance at 450 nm of the oxidized TMB resulted in the absence of the target molecules. In the presence of either or both target molecules, parts of the DNAzyme bound to the target(s), which resulted in the disruption of the G-quadruplex structure. As a result, the colorimetric signal was reduced due to the reduction in the catalytic activity of the DNAzyme.

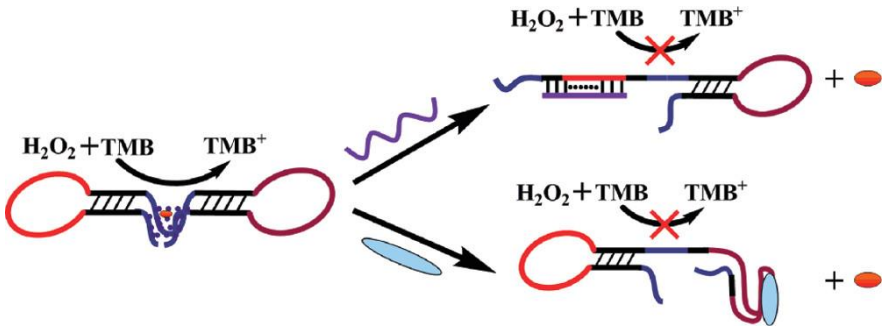

Figure 1.6 Schematic representation of the colorimetric detection of DNA or thrombin protein by the bifunctional oligonucleotide probe[25] (Reprinted (adapted) with permission from {Zhang, L.; Zhu, J.; Li, T.; Wang, E. Bifunctional Colorimetric Oligonucleotide Probe based on a G-Quadruplex DNAzyme Molecular Beacon. *Anal. Chem.* **2011**, *83* (23), 8871-8876.}. Copyright {2011} American Chemical Society.)

However, the above-mentioned system was in a signal-off mode, which was not ideal as it offers limited sensitivity. When the target was present in only small amounts, it is more difficult to measure a small percent reduction of a strong signal. Thus, the color changes cannot be distinguishable.[26] In 2014, Yan and co-worker[24] reported a signal-on detection system for the detection of miRNA by a G-quadruplex DNA. The performance of the detection system was enhanced by the duplex-specific nuclease (DSN)-assisted recycling of the miRNA target. As shown in **Figure 1.7**, the probe for this system consisted of a G-rich DNA and a complementary DNA sequence. The G-rich DNA partially paired with the complementary DNA (cDNA), resulting in the inhibition of the G-quadruplex formation in the absence of DNA target. When the DNA target was present, the complementary DNA probe was fully hybridized with the target miRNA to form the cDNA-target miRNA heteroduplex and release the free G-rich DNA. This G-rich DNA could then fold into the G-quadruplex and bound with the NMM substrate to give a complex with enhanced fluorescence. Furthermore, the DSN enzyme was used to digest the cDNA strand of the cDNA-miRNA heteroduplex, resulting in the release of the free miRNA to hybridize with more cDNA. This result showed that the limit of detection was improved from nM to fM by the enzyme amplification.[27] However, in this case, the potential DNAzyme

activity of the G-quadruplex had not been utilized, and thus the signal amplification relied on the target recycling alone.

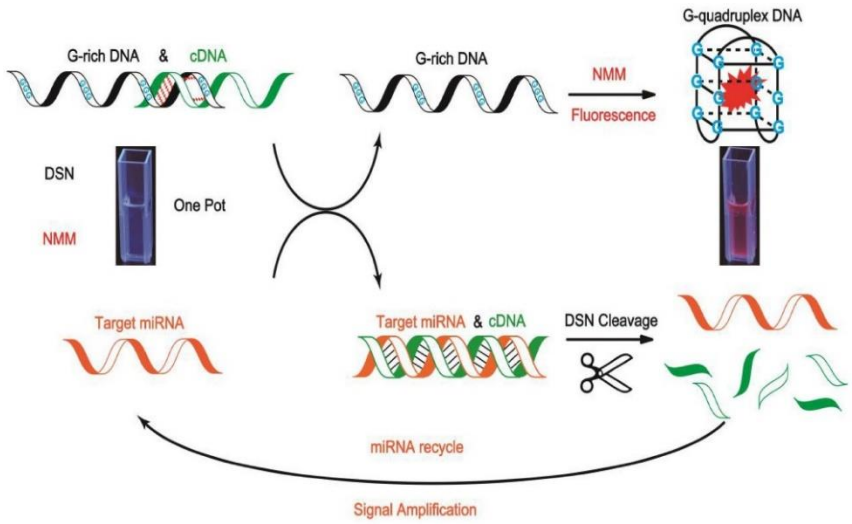

Figure 1.7 Schematic representation of the miRNAs based on DNAzyme molecular beacon combined with target recycling using DSN enzyme[24]

Another interesting example of a colorimetric DNA detecting system based on a DNAzyme molecular beacon (DNAzymeMB) is shown in **Figure 1.8**.[23] The G-rich of DNAzymeMB was split into two parts (at 5' and 3'-terminus) by a blocker complementary DNA. In the absence of the DNA target, the DNAzyme activity was inhibited resulting in no oxidation of the ABTS substrate in presence of H_2O_2. Thus, the solution remained colorless. When the DNA target was present, the blue-green color of oxidized ABTS was generated due to the hybridization of the blocker cDNA and the DNA target resulting in the releasing DNAzymeMB. This DNAzymeMB subsequently formed the binary DNAzyme in the presence of hemin to oxidize the ABTS. To improve the sensitivity of this system further, the DNA primer and DNA polymerase were also included for DNA target recycling. The displacement of the DNA target by the polymerase regenerated the free DNA target that could hybridize with more cDNA. Thus, this work features a double signal amplification strategy using DNAzyme and polymerase-assisted target recycling.

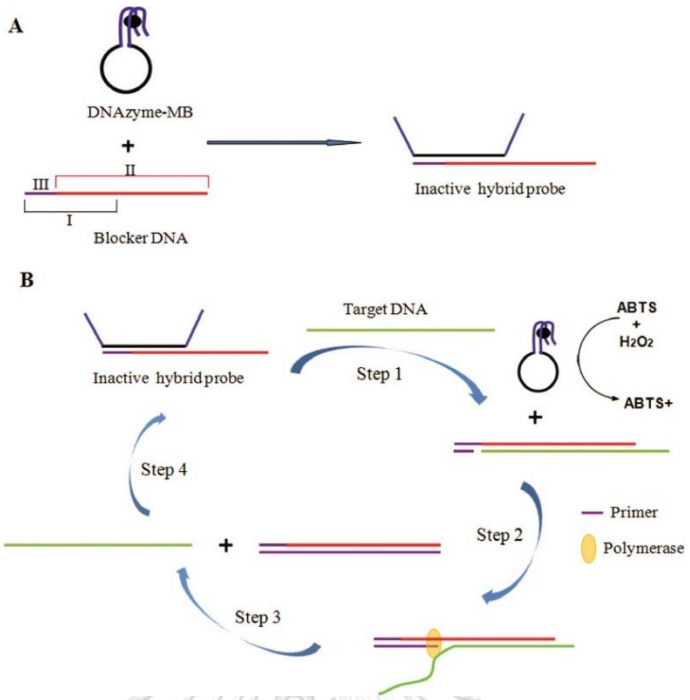

Figure 1.8 The DNA target detection by the combination of DNAzyme molecular beacon (DNAzymeMB) and target recycling by DNA polymerase[23] (Reprinted (adapted) with permission from {Fu, R.; Li, T.; Lee, S. S.; Park, H. G. DNAzyme Molecular Beacon Probes for Target-Induced Signal-Amplifying Colorimetric Detection of Nucleic Acids. *Anal. Chem.* **2011**, *83* (2), 494-500.}. Copyright {2011} American Chemical Society.)

While PCR amplification is typically used to increase the sensitivity of DNA detection, the important limitation is the need for a thermal cycler. Recently, a variety of isothermal nucleic acid amplification methods have been developed. For example, loop-mediated isothermal amplification (LAMP), strand displacement reaction (SDR), hybridization chain reaction (HCR), rolling circle amplification (RCA), and nicking endonuclease signal amplification (NESA).[28-31] In 2018, Zhang and co-worker[32] developed a colorimetric technique for DNA target detection by combining DNAzyme-signal amplification and Exo III assisted-target recycling **(Figure 1.9)**. The unlabeled hairpin DNA molecular beacon (UMB) was designed as the target recognition probe. The G-quadruplex sequence is inactive in the absence of DNA target. The UMB is resistant to catalytic digestion by Exo III because of the 3′-overhang residues. As a result, the ABTS substrate did not get oxidized and

appeared colorless. The stem-loop structure was opened to yield a double-stranded DNA (dsDNA) with a blunt 3′-terminus when the DNA target was added. The G-quadruplex part and the DNA target were then released by the Exo III digestion initiated by the blunt or recessed 3′-terminus. The free DNA target could hybridize with the remaining UMB leading to signal amplification. The released G-quadruplex part was then bound with hemin to catalyze the oxidation of ABTS, producing a blue-green colorimetric signal.

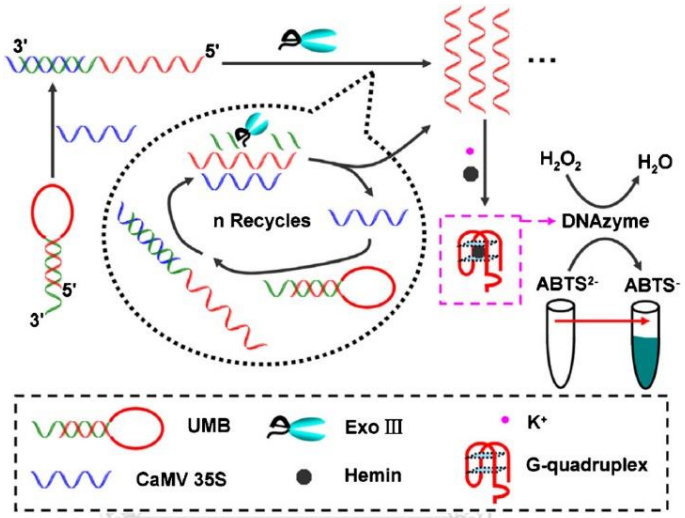

Figure 1.9 Schematic principle of the DNAzyme/Exo III dual-signal amplification strategy for DNA target detection[32] (Li, R.; Zou, L.; Luo, Y.; Zhang, M.; Ling, L. Ultrasensitive Colorimetric Detection of Circulating Tumor DNA Using Hybridization Chain Reaction and the Pivot of Triplex DNA. *Sci. Rep.* **2017**, *7* (1), 44212. Reproduced with permission from Springer Nature.)

1.3 Peptide nucleic acid

Although DNA is widely applied as a probe for DNA sequencing. However, the negatively charged on the DNA backbone contributes to the unfavorable electrostatic repulsion between two DNA strands in the same duplex. Therefore, other synthetic nucleic acid systems have been developed to overcome this problem. Peptide nucleic acid (PNA) is a synthetic nucleic acid mimic with an electrostatically neutral peptide backbone. In the first PNA system developed in 1991 by Nielsen and co-

workers, the sugar-phosphate backbone in natural nucleic acids was totally replaced by an *N*-(2-aminoethyl) glycine backbone **(Figure 1.10)**. [33, 34] This PNA system, which subsequently became known as "aegPNA", has been widely used as a probe for nucleic acid detection due to its many favorable properties over conventional DNA probes. PNA can bind to DNA following the Watson-Crick base-pairing rules similar to DNA-DNA hybridization. Due to the rather flexible structure of PNA, both antiparallel and parallel binding orientations are possible. **(Figure 1.11)**. When compared to DNA-DNA hybrids, PNA-DNA hybrids show higher binding affinity and sequence specificity. Due to the uncharged peptide backbone of the PNA structure, the repulsion between PNA and DNA strands in the duplex was minimized even under low salt conditions. Additionally, PNA is more resistant to nucleases and proteases.[35] The improvement of biostability and specificity towards the DNA target of PNA make it interestingly applied in biotechnology, diagnostics, and therapeutics.[36]

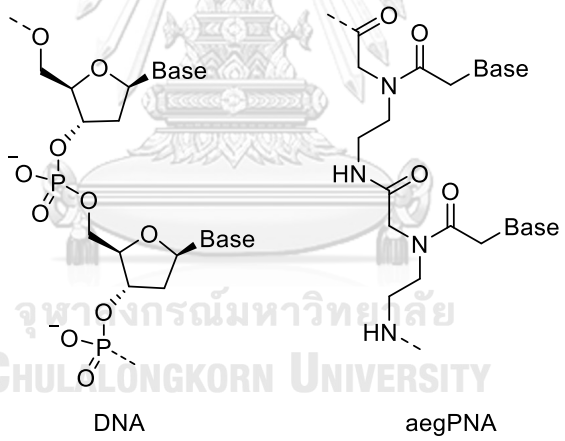

Figure 1.10 Structure of DNA and aegPNA

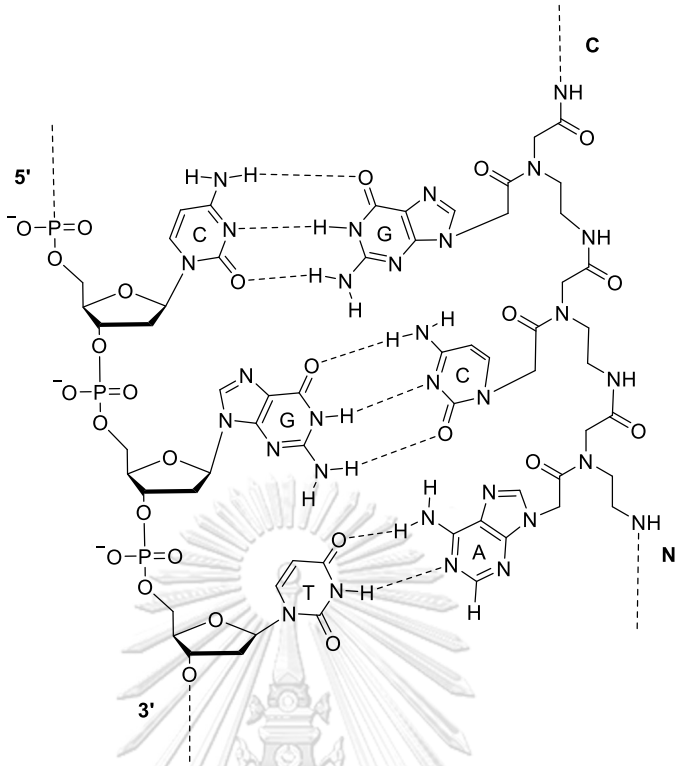

Figure 1.11 The antiparallel orientation of aegPNA-DNA hybridization

During the past few decades, several studies are focused on enhancing the aegPNA's binding properties further.[37] For example, backbone modification at the γ-position of *N*-2-aminoethylglycine backbone by an alkyl group produced a γ-modified PNA.[38] Its exhibits superior binding properties than the original PNA due to the conformational preorganization of γ-PNA induced by the alkyl group with appropriate chirality **(Figure 1.12 (A))**. Furthermore, the incorporation of one or more rings to rigidify the PNA backbone was another effective strategy.[39] In 2005, Vilaivan and co-workers[40-42] developed a new conformationally rigid pyrrolidinyl PNA comprising a D-prolyl-2-aminocyclopentanecarboxylic acid backbone (acpcPNA) **(Figure 1.12 (B))**. This PNA system performs better than aegPNA in terms of binding affinity and specificity towards DNA targets because of the rigidity of the acpcPNA structure. Unlike aegPNA, it also selectively binds to DNA only in the antiparallel orientation. These properties suggest the potential of acpcPNA to apply for many applications that DNA or aegPNA can do and beyond.

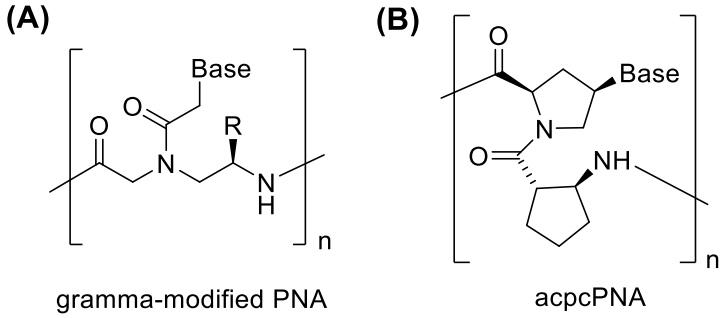

Figure 1.12 Structure of (A) γ-modified PNA, (B) acpcPNA

In an example of PNA application, a reversible supramolecular assembly of a bilingual PNA probe was developed by Heemstra and coworkers for the sensing of DNA/RNA targets.[43] In this work, the fluorophore-modified PNA and a quencher-labeled nucleic acid were required for monitoring hybridization. As shown in **Figure 1.13**, the PNA probe was modified at the γ-positions to form two distinctive hydrophobic and hydrophilic regions. The PNA spontaneously self-assembled into a micelle-like structure. In the presence of a quencher-labeled DNA strand with a sequence complementary to the PNA strand, hybridization occurred, and the micelle structure disintegrated together with the loss of fluorescence due to the quenching effect of the DNA strand. Next, the addition of another nucleic acid strand with a sequence complementary to the DNA strand resulted in the displacement of the PNA probe *via* the toehold-mediated displacement mechanism. This resulted in the re-formation of the PNA micelle and fluorescence signal restoration.

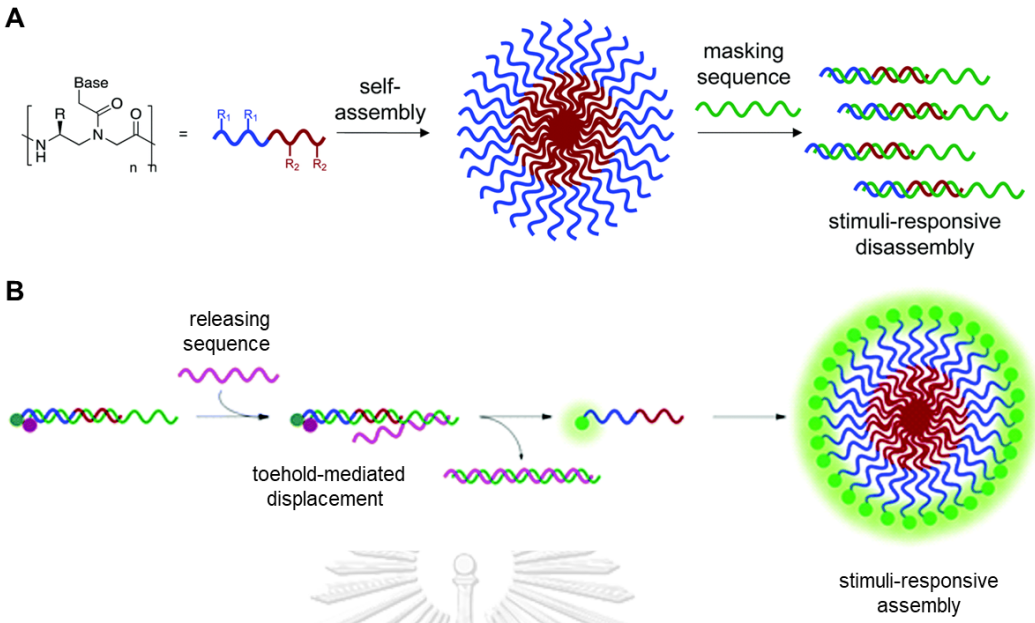

Figure 1.13 (A) The self-assembly of γ-modified PNA probe and the disassembly by the recognition of complementary masking sequence (B) The DNA target detection base on toehold mediated displacement system using of a fluorophore-modified bilingual PNA probe. R_1 = hydrophobic group, R_2 = hydrophilic group, blue line = hydrophobic region of PNA probe, red line = hydrophilic region of PNA probe, green line = masking sequence, pink line = releasing sequence[43] (Used with permission of Royal Society of Chemistry, from Stimuli-Responsive Assembly of Bilingual Peptide Nucleic Acids, Argueta-Gonzalez, H. S.; Swenson, C. S.; Song, G.; Heemstra, J. M., **2022**, *3* (8), 1035-1043.; permission conveyed through Copyright Clearance Center, Inc.)

In another example of the combination of PNA and G-quadruplex DNAzyme for DNA target detection, Kaewarsa and coworkers recently developed an origami paper-based device (oPAD) for prostate cancer-associated (PCA) detection.[44] The acpcPNA probe was first immobilized on the paper device for capturing the DNA marker of the PCA target. The DNA acted as a linker to capture the G-quadruplex DNAzyme reporter on the paper. In a strategically designed system, a single hybridization event caused several G-quadruplex strands to assemble on the same spot on the paper to provide a mechanism for signal amplification **(Figure 1.14)**.

The captured DNAzyme then catalyzed the oxidation of ABTS to give a green-colored product. No color change was observed in the absence of the PCA marker.

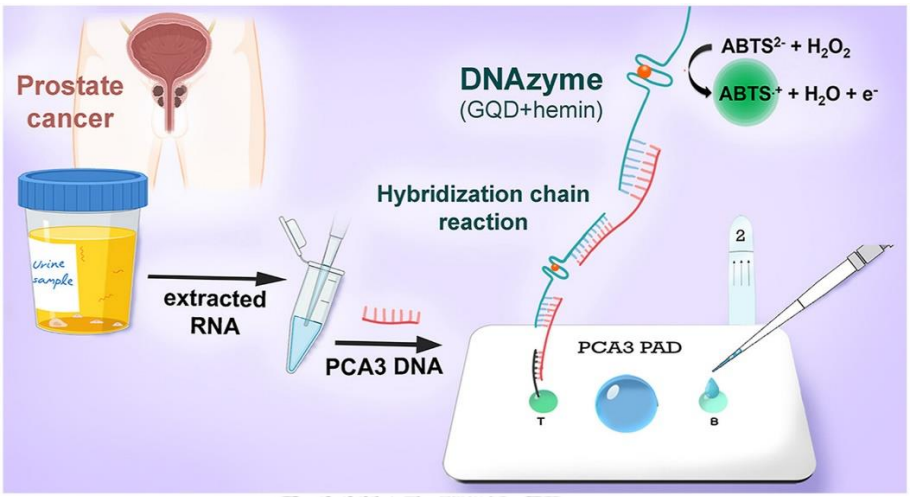

Figure 1.14 The prostate cancer associated (PCA) detection base on the combination of PNA and G-quadruplex probe on the origami paperbased peptide nucleic acid device (oPAD)[44] (Reprinted from Analytica Chimica Acta, 1186, Kaewarsa, P.; Vilaivan, T.; Laiwattanapaisal W., An Origami Paper-Based Peptide Nucleic acid Device Coupled with Label-Free DNAzyme Probe Hybridization Chain Reaction for Prostate Cancer Molecular Screening Test, 339130., Copyright (2021), with permission from Elsevier)

1.4 Objectives of this study

The objective of this work is to develop a new colorimetric detection system for DNA target detection based on the combination of G-quadruplex DNAzyme/acpcPNA probe and signal amplification by Exo III. **Figure 1.15** shows the concept of the colorimetric detection of DNA target according to the proposed strategy. The DNA G-quadruplex (G-DNA) exhibits strong catalytic activity in the oxidation of the colorimetric substrate when combined with hemin. Due to the high affinity and specificity of acpcPNA towards DNA targets, the acpcPNA probe was proposed to inhibit the G-quadruplex formation, thereby attenuating the DNAzyme-catalyzed oxidation of TMB in the presence of H_2O_2. In the presence of the DNA target with a sequence that is complementary to the DNA probe outside the

G-quadruplex forming region, the acpcPNA would be displaced from the DNA probe leading to the re-formation of the G-quadruplex and thus the restoration of the DNAzyme activity. According to this plan, the presence of the DNA target should lead to the appearance of the blue oxidized TMB in the solution (signal-on mode) that should be observable by naked eyes or by UV-vis spectrophotometry. Moreover, an additional Exo III-mediated signal amplification by target recycling will be incorporated to further improve the sensitivity of the detection. By a careful design of the G-DNA probe, the binding of the DNA target will result in a new DNA-DNA duplex with a recessed 3'-terminus. Only the probe strand will be digested by Exo III, resulting in the release of the free DNA target and a partially digested probe that can still form the G-quadruplex. According to this principle, the released DNA target will bind to other G-DNA/acpcPNA probes, inducing further rounds of digestion/target release/DNAzyme activation.

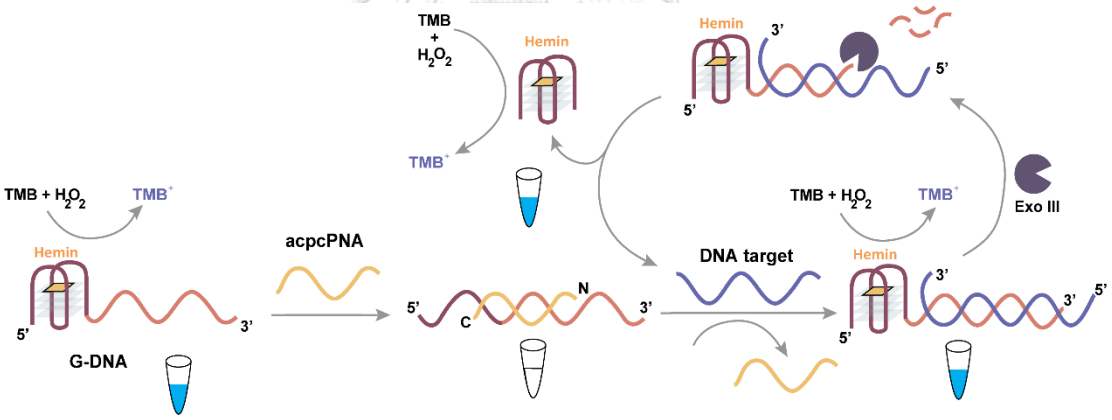

Figure 1.15 The concept of colorimetric detection system for DNA target detection based on the combination of G-quadruplex DNAzyme/acpcPNA probe and signal amplification by Exo III

CHAPTER II

EXPERIMENTAL

2.1. Materials and Method

2.1.1 Materials

The oligonucleotides were purchased from Pacific Science and Ward Medic, and aegPNAs were purchased from Panagene. The sequence of DNA and PNA were shown in **Table 3.2**. Hydrogen peroxide-urea adduct (H_2O_2) and ammonium acetate (NH_4OAc) were purchased from Merck. Hemin was obtained from TCI. 3,3',5,5'-tetramethylbenzidine (TMB) was from Sigma Aldrich. Sodium dodecyl sulfate (SDS) and tris-HCl were from USB corporation. Pure magnesium chloride anhydrous ($MgCl_2$) was obtained from Acros. Nitrogen gas (99.995% purity) was from Labgaz. Milli-Q water was from an ultrapure water system fitted with a Millipak® 40 filter unit 0.22 µm, Millipore. *di*-Sodium phosphate 2-hydrate was from Panreac Quimica SLU. Sodium dihydrogen phosphate from CARLO ERBA. α-cyano-4-hydroxycinnamic acid (CCA) was from Fluka. Exonuclease III (100,000 U/ml, 5,000 units) was from New England Biolabs.

For acpcPNA synthesis, 5(6)-carboxyfluorescein *N*-hydroxylsuccinimide ester (Flu-NHS) was purchased from Thermo Scientific. TentaGel™ S-RAM resin (0.24 mmol/g), 1,8-diazabicyclo[5.4.0]undec-7-ene (DBU), trifluoroacetic acid (TFA), *N*,*N* diisopropylethylamine (DIEA), piperidine, and *O*-(7-azabenzotriazol-1-yl)-*N*,*N*,*N*′,*N*′-tetramethyluronium hexafluoro phosphate (HATU) was from Fluka. 1-Hydroxy-7-azabenzotriazole (HOAt) was purchased from GLBiochem. Thin layer chromatography (TLC) Silica gel 60 F_{254} was obtained from Merck. Anhydrous *N*,*N*-dimethylformamide (DMF) (H_2O ≤ 0.01%) was purchased from RCI Labscan. Fmoc-Lys(Mtt)-OH was from Calibiochem Novabiochem. HPLC grade solvents were purchased from Merck. Nylon membrane filter (47 mm, 0.45 µm) from Vertical Chromatography.

For non-denaturing PAGE experiments, 10x tris-Borate-EDTA (TBE) buffer (890 mM tris base, 890 mM boric acid, and 20 mM EDTA), pH 8.3 (ultrapure grade) was purchased from Vivantis Technologies. 6x loading dye (10 mM tris, 0.03%

bromophenol blue, 0.03% xylene cyanol FF, 60% glycerol, 60 mM EDTA, pH 7.6) was purchased from Thermo Scientific. Acryl/Bis™ solution (40% w/v, 38.67% acrylamide, and 1.33% methylene bis-acylamide in deionized water) 29:1 ultra pure grade was obtained from VWR Life Science. Ammonium persulfate molecular biology grade (ammonium persulfate, APS) was obtained from PanReac AppliChem. *N,N,N',N'*-tetramethylenediamine (TEMED) was from Tokyo Chemical Industry.

2.1.2 Equipment

For the colorimetric detection assay, the absorption spectra were recorded on an EnSight multimode microplate reader (PerkinElmer). CD spectra were recorded on a JASCO J-815 spectropolarimeter (JASCO). The absorption spectrum of DNA or acpcPNA and melting temperature (T_m) measurements were performed on a CARY 100 Bio UV-visible spectrophotometer (Varian). Reverse phase HPLC experiments were performed on a Water Delta 600 HPLC system equipped with a gradient pump and Water 996 photodiode array detector. FreeZone 6 Liter -50C Console Freeze Dryer (LABCONCO) was used for drying of acpcPNA product. The non-denaturing PAGE experiments was performed using gel electrophoresis apparatus (OmniPAGE mini, Cleaver scientific) with generated voltage by a NANOPAC-300 power supply (Cleaver scientific, United Kingdom).

2.2 Synthesis of pyrrolidinyl PNA (acpcPNA)

2.2.1 Synthesis of acpcPNA monomer

All pyrrolidinyl PNA monomers (Fmoc-A^{Bz}-Opfp, Fmoc-C^{Bz}-Opfp, Fmoc-T-Opfp, Fmoc-G^{Ibu}-OH) the β-amino acid spacer (Fmoc-(1*S*,2*S*)-2-aminocycolpentanecarboxylic acid) **(Figure 2.1)** were synthesized according to the literature method[40] by members of Prof. Vilaivan's laboratory.

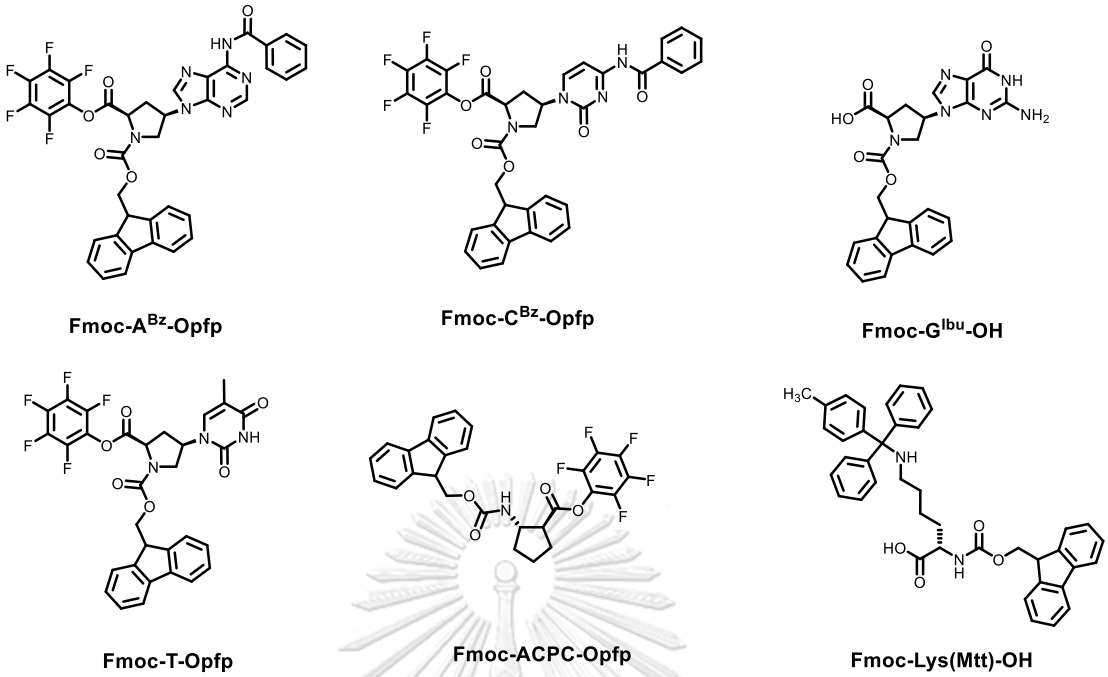

Figure 2.1 Structure of pyrrolidinyl PNA monomers, β-amino acid spacer

2.2.2 Synthesis of acpcPNA on solid phase

TentaGel S-RAM Fmoc resin (1.5 μmol) was used as the solid support for the synthesis of acpcPNA *via* Fmoc-solid phase peptide synthesis. The synthesis was carried out according to Vilaivan and coworkers protocol.[40, 45] The synthesis of acpcPNA began from C-terminus to N-terminus with Lys(Mtt) being added as the first residue. In one round of the synthesis cycle, there are three steps, namely deprotection, coupling, and capping. To generate the active N-terminal amino group, the protecting group (Fmoc) at N-terminus was removed in the deprotection step using 100 μL of stock solution #1 (20% piperidine and 2% DBU in DMF, v/v) under 5 min incubation period. In the coupling step, the resin was immersed in the solution of 4 eq. activated monomer (or spacer) in 30 μL of stock solution #2 (7% DIEA in DMF, v/v) for 30–40 min. The pentafluorophenyl esters (Pfp-activated monomers: Fmoc-A^{Bz}-Opfp, Fmoc-C^{Bz}-Opfp, Fmoc-T-Opfp, Fmoc-ACPC-OPfp) are typically used as the activated monomers. For the coupling of Fmoc-G^{Ibu}-OH or Fmoc-Lys(Mtt)-OH, the free acid required activation by treatment with 4 eq. HATU in 30 μL of stock solution #2. In the capping step, the resin was immersed in 35 μL of stock solution #2

containing 15% acetic anhydride for 5 min to protect the unreacted amino groups from further reactions in the next steps. The three steps were repeated - with extensive washing with DMF at the end of each step - until the desired PNA sequence was obtained. In the case of final residue coupling, the Fmoc N-terminal amine was removed, and the free amino group was capped with acetic anhydride following the same procedure of the capping step. Once completed, the resin was extensively washed with DMF, methanol, and dried. All reactions mentioned above were conducted at ambient temperature.

For the coupling of FAM label at the N-terminus of the acpcPNA with a sequence shown in **Table 3.1**, the activated acpcPNA (0.5 μmol) was immersed in 20 μL solution, containing 5(6)-carboxyfluorescein *N*-hydroxysuccinimide ester (FAM-NHS) (2 mg, 8 equiv.) and 10% DIEA in DMF at room temperature in the absence of light for 3 days. The progress of the reaction was monitored by MALDI-TOF MS. Once completed, the resin was extensively washed with DMF, methanol, and dried.

The nucleobase protecting groups were removed from the synthesized acpcPNA by treating the resin with 1:1 aqueous NH_3 and dioxane (2 mL) at 65 °C for 8 hours. After washing with methanol and drying, the resin was immersed in 500 μL of trifluoroacetic acid (TFA) for 30 min. The process was repeated three times and the TFA was removed under N_2 gas. The acpcPNA was precipitated using 500 μL of diethyl ether, centrifugally washed three times with diethyl ether, and finally dried to obtain the crude acpcPNA as a white solid.

The crude acpcPNA was dissolved in water (100-200 μL) and purified by reverse phase HPLC. The conditions were as follow column: ACE 5 C18-AR, 150 x 4.6 mm; mobile phase: a gradient of 0.1% TFA in methanol (A) and 0.1% TFA in Milli-Q (B) (10-90% of (A), 5-90 minutes); flow rate: 0.5 mL/min. Fractions containing pure acpcPNAs were collected and combined with the aid of MALDI-TOF mass spectrometry. The combined fractions were dried using a freeze-dryer and dissolved in 150 μL of Milli-Q water. The purified acpcPNAs were characterized using MALDI-TOF mass spectrometer employing **α**-cyano-4-hydroxycinnamic acid (CCA) matrix.

To determine the concentration of the acpcPNA stock solution, 1 μL of acpcPNA stock was added to 800 μL of 10 mM sodium phosphate buffer pH 7.0 in a

quartz cuvette (10 mm pathlength). The absorbance spectra were measured using UV-visible spectrophotometry from 200 to 800 nm. The concentration of acpcPNA was achieved from equations 1 and 2.

$$OD_{260} = \frac{\mathbf{A_{260} \times total\ volume\ (\mu L)}}{\mathbf{volume\ of\ acpcPNA\ (\mu L)}} \quad (1)$$

$$\text{Concentration of acpcPNA (}\mu\text{M)} = \frac{\mathbf{OD_{260} \times 1000}}{\boldsymbol{\varepsilon}} \quad (2)$$

$\boldsymbol{\varepsilon}$ (molecular extinction cofficient) was calculated from Vilaivan's website (http://www.chemistry.sc.chula.ac.th/pna/pna.asp)

The purity of the purified acpcPNA was verified by reverse phase HPLC using Water Delta 600 HPLC system equipped with a gradient pump and Water 996 photodiode array detector. The conditions were as follow column: UPS C18, 4.6 x 50 mm; mobile phase: a gradient of 0.1% TFA in methanol (A) and 0.1% TFA in Milli-Q (B) (10-90% of (A), 5-60 minutes); flow rate: 0.5 mL/min.

2.3 Melting temperature analysis (T_m)

The sample solution was prepared in a quartz cuvette (10 mm path length). Unless otherwise specified, 800 µL solution contained the acpcPNA and/or G-DNA (1 µM) and/or complementary DNA (1 µM) in 32 µL of 0.5% w/v SDS, 32 µL of 5 M NH_4OAc in 80 µL of 660 mM Tris-HCl buffer, 6.6 mM $MgCl_2$. The final concentrations of SDS = 0.02% w/v, NH_4OAc = 200 mM in 66 mM Tris-HCl buffer, 0.66 mM $MgCl_2$. The absorbance was monitored at 260 nm from 20 ºC to 90 ºC (heating rate of 1.0 ºC/min) by UV-visible spectrophotometry. The temperature correction was performed by using the linear equation 3, whereby T_{block} was the record block temperature. The data smoothing and derivatization were performed through KaleidaGraph 4.0 (Synergy Software). The normalized graph was plotted between correct temperature (x-axis) and normalized temperature at A_{260} (y-axis), the normalized temperature was achieved by dividing the value of each temperature by

the starting absorbance. The melting temperature (T_m) was calculated from the maximum value of the first derivative plot.

$$\text{Correct temperature} = (0.9696 \times T_{block}) - 0.8396 \quad (3)$$

2.4 Circular dichroism analysis (CD)

The sample solution (total volume = 800 µL) was prepared by mixing acpcPNA and G-DNA and 80 µL of 660 mM Tris-HCl buffer, 6.6 mM $MgCl_2$, pH 8.0 and deionized water to give the final concentration of acpcPNA = 2 µM and G-DNA = 1 µM in 66 mM Tris-HCl buffer with 0.66 mM $MgCl_2$ in 1.5 mL microcentrifuge tube. The solution was incubated for 20 minutes. In the experiments containing the DNA target, the DNA target was added to the mixture (final concentration = 3 µM) and incubated for 20 minutes before adding the acpcPNA. Next, 32 µL of 5 M NH_4OAc (200 mM) was added and solution was incubated for another 20 minutes. The solution was transferred to a quartz cell (10 mm path length) and the CD spectrum was measured from 200 to 400 nm (4 repetitions, scanning rate = 100 nm/min). The solutions of single-stranded acpcPNA or DNA at the same concentration in 200 mM NH_4OAc, 66 mM Tris-HCl buffer, 0.66 mM $MgCl_2$ were used as control samples. All CD spectra were subtracted by the CD spectrum of a blank sample (buffer + salt).

2.5 Gel electrophoresis experiments

Non-denaturing PAGE was used to confirm the G-quadruplex formation and studied the effect of acpcPNA with G-DNA, including the effect of DNA target with G-DNA/acpcPNA probes. To prepare 17% polyacrylamide gel, *N,N,N',N'*-tetramethylenediamine (TEMED) (10 µL), and ammonium persulfate (10 mg) were immediately added to a solution of acrylamide/*N,N'*-methylenebis(acrylamide) solution (29:1), 40% (w/v) (5 mL), 10x Tris borate-EDTA buffer (TBE) (1 mL), and Milli-Q water (3 mL). The mixture was rapidly transferred to the gel electrophoresis apparatus and left until the gel was completely polymerized (30-60 minutes). The sample was prepared by mixing acpcPNA (0.8 nmol) and/or G-DNA (0.4 nmol) and/or DNA target (1.2 nmol) with 0.8 µL of 5 M NH_4OAc (200 mM) and 2 µL of 660

mM Tris-HCl buffer, 6.6 mM $MgCl_2$ and the final volume was adjusted to 20 µL by Milli-Q water to give the final solution with 66 mM Tris-HCl and 0.66 mM $MgCl_2$.

To study the effect of Exo III with G-DNA/PNA in the presence of the DNA target, the order of DNA target (1.2 nmol), PNA (0.8 nmol), and NH_4OAc (200 mM) addition was the same as in the colorimetric assay **(section 2.6)**. 1 µL of 5 U/µL Exo III in 25 mM HEPES buffer, pH 8.0 (5 U Exo III) was added to the solution and incubated at 40 °C for 30 minutes. The volume of the solution was adjusted to 20 µL with Milli-Q water. To the sample was added 2 µL of 6x loading dye (0.5x loading dye) (total volume = 22 µL). Next, 10 µL of the sample was loaded onto the gel. The electrophoresis experiments were performed for 90 min at a constant voltage of 100 V. The gel was visualized by UV-shadowing by placing it over a PVC-wrapped 20 x 20 cm TLC plate coated with silica gel GF254. Next, it was viewed under UV light (254 nm), and the photograph was taken using a Canon EOS M digital camera. In the case of FAM-acpcPNA, FAM-DNA, and TAMRA-DNA, the gel was imaged under a UV transilluminator (365 nm) with a yellow filter or by UV shadowing (254 nm) without the yellow filter. The photograph of the gel in **Figure 3.16** was taken under LED white light.

2.6 Colorimetric detection

Different DNA targets (1.5 µL of 25 µM DNA target) were incubated with 1.5 µL of 25 µM G-DNA, 15 µL of 660 mM Tris-HCl buffer, 6.6 mM $MgCl_2$ in a 96 well microplate for 20 min (total volume = 18 µL). Next, 3 µL of 25 µM acpcPNA (2 equiv) was added to the solution and incubated for further 20 min (total volume = 21 µL). Then, 6 µL of 5 M NH_4OAc, 6 µL of 0.5% SDS, 1.5 µL of 5 mM TMB and 1.5 µL of 1.25 µM hemin were added to the mixture in that order. The total volume was adjusted to 147 µL using Milli-Q water to give the final concentrations of DNA target = 0.25 µM, G-DNA = 0.25 µM, acpcPNA = 0.5 µM, NH_4OAc = 200 mM, SDS = 0.02% w/v, TMB = 0.05 mM, hemin = 0.0125 µM in 66 mM Tris-HCl buffer with 0.66 mM $MgCl_2$, and the solution was incubated for another 20 minutes. Finally, 3 µL of 250 mM urea-H_2O_2 (5 mM) was added. After incubation for another 10 minutes, the absorption spectra (300 to 800 nm) or the absorbance at 680 nm were measured using the

multimode microplate reader. The same samples were also prepared in a 0.2 mL PCR tube for imaging under white light using a Canon EOS M digital camera. In the specificity experiments, p-values were calculated in Microsoft Excel using the paired two sample for means (t-test) mode with a 95% level of confidence. One of the samples was the complementary and the other was the mismatched DNA. A statistically significant difference was concluded when the p-value was < 0.05.

2.7 Sensitivity

In a 96 well microplate, various concentrations of the DNA target (1.5-15 µL of 2.5 µM DNA target) were incubated with 1.5 µL of 25 µM G-DNA(inter) in 15 µL of 660 mM Tris-HCl buffer, 6.6 mM $MgCl_2$ for 20 min (total volume = 16.5-30 µL). Next, 3 µL of 25 µM acpcPNA-C3 (2 equiv) was added to the solution and incubated for 20 min (total volume = 19.5-33 µL). Followed by 6 µL of 5 M NH_4OAc, 6 µL of 0.5% w/v SDS, 1.5 µL of 5 mM TMB and 1.5 µL of 1.25 µM hemin were added into the solution and incubated for another 20 min. The total volume was adjusted to 147 µL by Milli-Q water to give the final concentrations of DNA target = 25-250 nM, G-DNA(inter) = 0.25 µM, acpcPNA-C3 = 0.5 µM, NH_4OAc = 200 mM, SDS = 0.02%, TMB = 0.05 mM, hemin = 0.0125 µM in 66 mM Tris-HCl buffer with 0.66 mM $MgCl_2$, and the solution was incubated for another 20 minutes. Finally, 3 µL of 250 mM urea-H_2O_2 (5 mM) was added. The absorption spectra were measured on multimode microplate reader after 10 minutes. The experiments were repeated three times for each concentration. The linear calibration curve was constructed by plotting the relationship between concentration of DNA target (x-axis) and absorbance at 680 nm (y-axis). The limit of detection (LOD) was calculated from equation 4.

$$\text{Limit of detection} = \frac{3 \times \text{SD}}{\text{Slope}} \quad (4)$$

2.8 Target recycling

The Exo III target recycling procedure was adapted from the literature.[32, 46] In a 0.2 mL PCR tube, the 0.8 µL of 25 µM DNA target was incubated with 2 µL of 25 µM G-DNA(inter) in 20 µL of 660 mM Tris-HCl buffer, 6.6 mM $MgCl_2$ at room temperature for 20 min (total volume = 22.8 µL). Next, 4 µL of 25 µM acpcPNA-C3 (2 equiv) was added to the solution and incubated for 20 min (total volume = 26.8 µL). Then, 1 µL of 0.5 U Exo III (0.5 U) was added to the solution (total volume = 27.8 µL) and incubated at 40 °C for 30 minutes. The reaction was cooled down to room temperature for 10 minutes. Then, 8 µL of 5 M NH_4OAc, 8 µL of 0.5% w/v SDS, 2 µL of 5 mM TMB and 2 µL of 1.25 µM hemin were added into the solution (total volume = 47.8 µL) and incubated for another 20 min at room temperature. The total volume was adjusted to 196 µL by Milli-Q water to give the final concentrations of DNA target = 0.10 µM, G-DNA(inter) = 0.25 µM, acpcPNA-C3 = 0.5 µM, Exo III = 0.5 U, NH_4OAc = 200 mM, SDS = 0.02% w/v, TMB = 0.05 mM, hemin = 0.0125 µM in 66 mM Tris-HCl buffer with 0.66 mM $MgCl_2$, and the solution was incubated for another 20 minutes. Finally, 4 µL of 250 mM urea-H_2O_2 (5 mM) was added. After 10 minutes, 150 µL of the reaction mixture was transferred to a 96 well microplate. The absorption at 680 nm was measured using multimode microplate reader.

CHAPTER III

RESULTS AND DISCUSSION

3.1 Synthesis and characterization of peptide nucleic acid probes

All acpcPNA probes used in this work were synthesized on Tentagel S RAM resin (1.5 μM) with one lysine amide residue included at the C-terminus for water solubility improvement following the literature procedure. For FAM-acpcPNA synthesis, the PNA was modified at the N-terminus by 5(6)-carboxyfluorescein *N*-hydroxysuccinimide ester (FAM) *via* amide bond formation. The FAM-acpcPNA was used in experiment **section 2.2.2** for the study of interactions between G-DNA, acpcPNA and DNA target. In all cases, the acpcPNA probes were cleaved from the solid support using 90% TFA and purified by reverse phase HPLC. The purified acpcPNAs were characterized by MALDI-TOF mass spectrometry using α-cyano-4-hydroxycinnamic acid (CCA) as a matrix. **Table 3.1** shows that the observed and predicted molecular weights of pure acpcPNAs were in good agreement. The quality of acpcPNA probes was also further confirmed using reverse phase HPLC to be more than 90% purity in all cases. The mass spectra and chromatograms of the synthesized acpcPNA are shown in **Figures A1-A5**.

Table 3.1 Characterization data of all acpcPNAs used in this study

Name	Sequence (N → C)	*m/z* cal.	*m/z* found.	t_R (min)	%yield
acpcPNA-C2	Ac-C TCG TTA CCT-LysNH_2	3484.8	3483.7	30.3	18
acpcPNA-C3	Ac-C TCG TTA CCC AA-LysNH_2	4152.5	4151.7	30.9	26
FAM-acpcPNA-C3	FAM-C TCG TTA CCC AA-LysNH_2	4469.8	4469.4	30.6	23
acpcPNA-C5	Ac-C TCG TTA CCC CC-LysNH_2	4104.4	4103.7	29.2	19
acpcPNA-C3GC	Ac-CG TTA CCC GC-LysNH_2	3494.8	3494.9	27.9	30

Table 3.2 G-DNA and PNA sequences[a]

Name	DNA sequence
G-DNA(intra$(GGG)_4$)	5'-T GGG TA GGG C GGG TT GGG TAA CGA GTT CCG TGA CGC-3'
G-DNA(intra$(GGG)_3$)	5'-T GGG TA GGG C GGG TAA CGA GTT CCG TGA CGC-3'
G-DNA(inter)	5'-GG GGG TAA CGA GTT CCG TGA CGC-3'
DNA target	3'-TT TTT ATT GCT CAA GGC ACT GCG TAC CG-5'
Single base mismatched DNA 1	3'-TT TTT ATT GCT CAA GGC ACT CCG TAC CG-5'
Single base mismatched DNA 2	3'-TT TTT ATT GCT CAA CGC ACT GCG TAC CG-5'
Single base mismatched DNA 3	3'-TT TTT ATA GCT CAA GGC ACT GCG TAC CG-5'
Double base mismatched DNA 1	3'-TT TTT ATA GCT GAA GGC ACT GCG TAC CG-5'
Double base mismatched DNA 2	3'-TT TTT ATT GCT CAA GGG ACT CCG TAC CG-5'
Double base mismatched DNA 3	3'-TT TTT ATT GCT GAA GGG ACT GCG TAC CG-5'
Triple base mismatched DNA	3'-TT TTT ATA GCT CAA CGC ACT CCG TAC CG-5'
Non-DNA target	3'-TTC TTT CTT GCC CAC GCT TGT TTG TTC GC-5'
Name	**PNA sequence (C → N)**
acpcPNA-C2	NH_2-Lys-TCC ATT GCT C-Ac
acpcPNA-C3, aegPNA-C3	NH_2-Lys-AA CCC ATT GCT C-Ac
FAM-acpcPNA-C3	NH_2-Lys-AA CCC ATT GCT C-FAM
acpcPNA-C5, aegPNA-C5	NH_2-Lys-CC CCC ATT GCT C-Ac
acpcPNA-C3GC	NH_2-Lys-CG CCC ATT GC-Ac

[a]The binding regions for the DNA targets are highlighted. The binding regions for the acpcPNA probe are underlined. Mismatched bases are shown in red. Non-pairing bases are presented in normal text.

3.2 Inhibition of G-quadruplex DNAzyme by acpcPNA probes

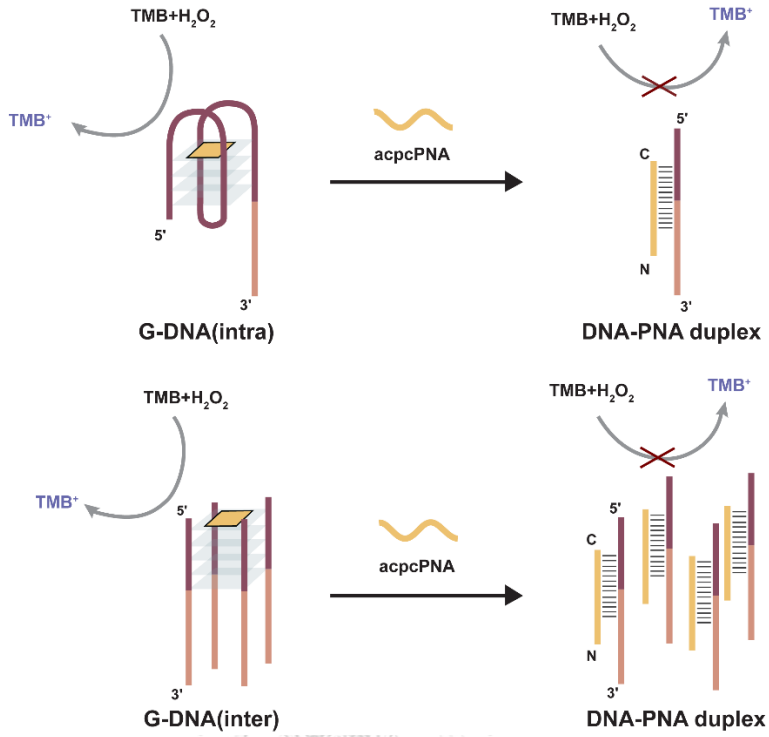

Figure 3.1 The proposed inhibition of intramolecular and intermolecular G-quadruplex DNAzyme by acpcPNA

As shown in **Figure 3.1**, the combination of a DNA G-quadruplex – either intramolecular or intermolecular – and hemin can catalyze the oxidation of TMB in the presence of H_2O_2 by acting as a DNAzyme that mimics the peroxidase enzyme.[25, 47] Thus, the blue-colored product was obtained and the absorbance at 680 nm increased. According to our design, it was proposed that the formation of intramolecular or intermolecular G-quadruplexes should be inhibited by the Watson-Crick base-pairing with the acpcPNA strand. Accordingly, no G-quadruplex DNAzyme is available to convert the substrate into the blue product, thus the solution should remain colorless.

3.2.1 The inhibition of intramolecular G-quadruplex DNAzyme

For the inhibition of intramolecular G-quadruplex DNAzyme by acpcPNA, two different sequences of intramolecular G-quadruplexes were studied. The acpcPNA was designed to inhibit the G-quadruplex formation by binding to parts of the G-quadruplex forming sequence at 5'-terminus. As shown in **Figure 3.2 (A)**, The blue-colored solution was obtained in **Tube 2** and the absorbance at 680 nm increased **(Spectrum 2)** when compared with the condition without G-DNA(intra$(GGG)_4$) **(Spectrum 1)**. The result confirmed that the sequence G-DNA(intra$(GGG)_4$) can form an intramolecular G-quadruplex[48] as shown by the ability to catalyze the oxidation of TMB in the presence of hemin. In the presence of acpcPNA-C3, the blue-colored product was still observed **(Tube 3)**. Thus, the acpcPNA-C3 bearing the CCCAA sequence at its C-terminus could not inhibit the intramolecular G-quadruplex formation. Next, the G-DNA(intra$(GGG)_3$) sequence which consisted of three repeat units of GGG at the 5'-terminus could also form G-triplex[49-51] which showed similar DNAzyme activity as G-DNA(intra$(GGG)_4$) to give the blue solution as shown in **Tube 2 (Figure 3.2 (B))**. In the presence of acpcPNA-C3GC in which the two C-terminal AA bases of acpcPNA-C3 were replaced by CG base to increase the base pairing stability, the intensity of the blue color and the absorbance were slightly decreased but were still higher than those of the solution without G-DNA as shown in **Tube 1 (Figure 3.2 (B))**. These results indicated that both acpcPNA-C3 and acpcPNA-C3GC could not completely inhibit the intramolecular G-quadruplex formation.

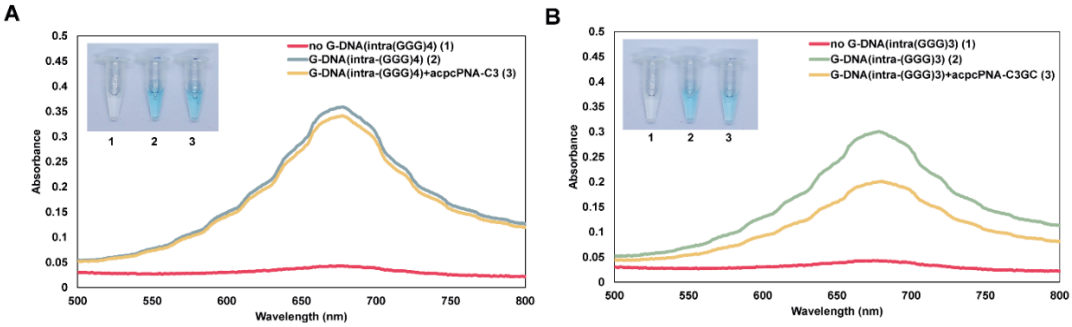

Figure 3.2 Photographs and UV-vis spectra of the DNAzyme-catalyzed oxidation of TMB (0.05 mM) by (A) DNA(intra$(GGG)_4$), (B) DNA(intra$(GGG)_3$) in the presence of H_2O_2 (5 mM), hemin (0.0125 μM), NH_4OAc (200 mM), SDS (0.02 %w/v) in 66 mM Tris-HCl buffer, 0.66 mM $MgCl_2$, pH 8.0 with (1) no G-DNA(intra), (2) G-DNA(intra), (3) G-DNA(intra)+acpcPNA. The concentrations of G-DNA(intra) = 0.25 μM, acpcPNA = 0.50 μM

3.2.2 The inhibition of intermolecular G-quadruplex DNAzyme

In this experiment, an intermolecular G-quadruplex DNA sequence with five guanine bases at the 5'-terminus (G-DNA(inter)) was used as the probe. As an inhibitor, the acpcPNA probe with varying numbers of cytosine bases at the C-terminus was evaluated. **Figure 3.3 (A)** showed that G-DNA(inter), when complexed with hemin, could oxidize the TMB to get a blue-colored solution **(Tube 2)**, and the absorbance at 680 nm was increased by 6-fold **(Spectrum 2)**. This suggested that the G-DNA(inter) could form an intermolecular G-quadruplex that can interact with hemin *via* **π-π** interaction to form a catalytically active DNAzyme.[17] In the presence of acpcPNA-C3 or acpcPNA-C5, the DNAzyme-catalyzed TMB oxidation was suppressed as shown by the colorless solution **(Tubes 3, 4)**, resulting in the decrease of the absorbance at 680 nm **(Spectrum 3, 4)** to the same level as the background TMB oxidation in the absence of G-DNA(inter) **(Tube 1, Spectrum 1)**. The results indicated that complete suppression of the DNAzyme activity required at least 2 equiv. of the acpcPNA inhibitor probe that carried at least three cytosine bases at the C-terminus. As illustrated by the blue-colored solution in **Tube 5** and

Spectrum 5, acpcPNA-C2 with carried only two cytosine bases at the C-terminus was unable to effectively inhibit the intermolecular DNA G-quadruplex formation. Thus, acpcPNA-C3 was selected as the inhibitor probe to be used with G-DNA(inter) DNAzyme for further experiments. Interestingly, it is important to note that the NH_4OAc must be added last since the G-quadruplex formation was not inhibited by the PNA when the NH_4OAc was added before the addition of acpcPNA-C3. This is presumably due to the slow kinetics of the G-quadruplex unfolding even though the T_m of G-DNA(inter)/acpcPNA-C3 (56.5 °C) was significantly higher than that of G-DNA(inter) (48 °C) under the experimental conditions (200 mM NH_4OAc, 0.02 % SDS, 66 mM Tris-HCl buffer, 0.66 mM $MgCl_2$, pH 8.0). On the other hand, the T_m of G-DNA(inter) was not observable under the condition without NH_4OAc, as shown in **Figure 3.3 (B)** indicating the important role of the ammonium ion. According to **Figure 3.3 (C)**, when a DNA strand with the same sequence as the acpcPNA was used as the inhibitor strand, the blue color was still observed demonstrating that DNA did not bind sufficiently strong to inhibit the intermolecular G-quadruplex formation.

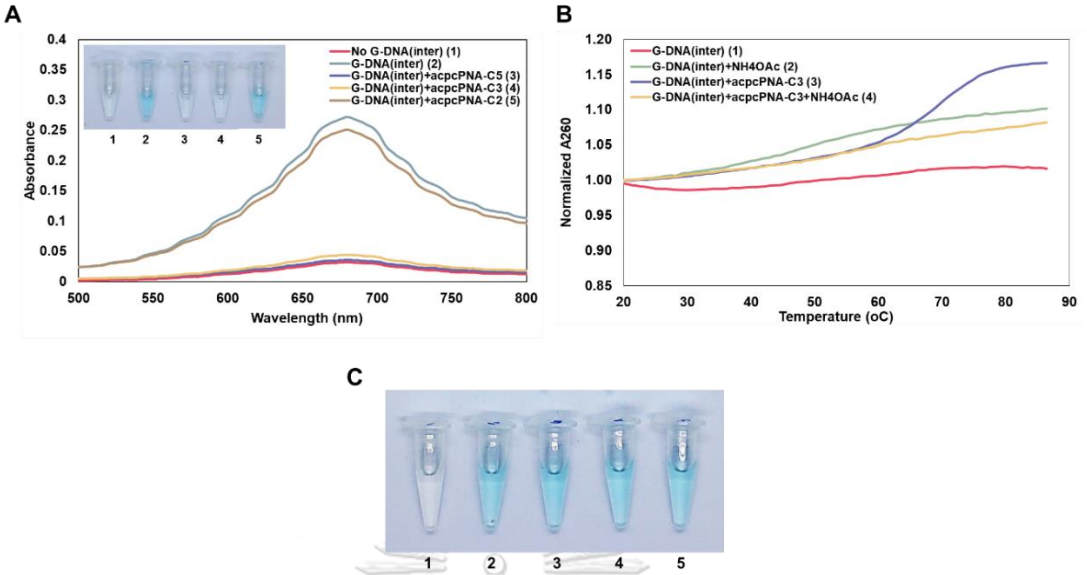

Figure 3.3 (A) Photographs and UV-vis spectra of the DNAzyme-catalyzed oxidation of TMB (0.05 mM) in the presence of H_2O_2 (5 mM), hemin (0.0125 μM), NH_4OAc (200 mM), SDS (0.02 %w/v) in 66 mM Tris-HCl buffer, 0.66 mM $MgCl_2$, pH 8.0 with (1) no G-DNA(inter), (2) G-DNA(inter), (3) G-DNA(inter)+acpcPNA-C5, (4) G-DNA(inter)+acpcPNA-C3, (5) G-DNA(inter)+acpcPNA-C2. The concentrations of G-DNA(inter) = 0.25 μM, acpcPNA or DNA = 0.50 μM (B) Melting temperature of (1) G-DNA(inter) with NH_4OAc, (2) G-DNA(inter)+acpcPNA-C3 without NH_4OAc, (3) G-DNA(inter)+acpcPNA-C3 with NH_4OAc in 66 mM Tris-HCl buffer, 0.66 mM $MgCl_2$, pH 8.0. The concentration of NH_4OAc = 200 mM. and (C) Photographs of the DNAzyme-catalyzed oxidation of TMB with (1) no G-DNA(inter), (2) G-DNA(inter), (3) G-DNA(inter)+DNA-C5, (4) G-DNA(inter)+DNA-C3, (5) G-DNA(inter)+DNA-C2. The concentrations of DNA = 0.50 μM

3.3 Conditions optimization for the DNAzyme-calalyzed reactions and their inhibition

3.3.1 Effect of sodium dodecyl sulfate (SDS) concentration

Because of the instability and low solubility in water of the blue oxidized TMB product, sodium dodecyl sulfate (SDS) – a negatively charged surfactant – has been previously employed to solve the problem.[52-54] The positively charged oxidized TMB was stabilized by electrostatic interaction with the negatively charged SDS resulting in

an extended lifetime of the blue coloration. As shown in **Figures 3.4 (A) and 3.5 (A)**, the intensity of the blue color in the solution as well as the absorbance at 680 nm increased with increasing SDS concentrations from 0.005 %w/v to 0.02 %w/v. The values slightly decreased after 0.02 %w/v indicating that the [SDS] = 0.02 %w/v was optimal. High concentrations of SDS may inhibit the catalytic activity of the DNAzyme due to the competing hydrophobic and electrostatic interactions between SDS and hemin.

3.3.2 Effect of different salts

The structure of G-quadruplex could be stabilized by several monovalent or divalent cations including K^+, Na^+, Mg^{2+}, or NH_4^+.[55, 56] Moreover, the conformation and stabilization of DNA G-quadruplexes are affected by the type of metal ion.[57] In this study, the effects of different metal salts were investigated at the same concentration of 200 mM. The maximum blue color intensity was produced in the presence of NH_4OAc as shown in **Figure 3.4 (B)**. Thus, 200 mM NH_4OAc was used for all subsequent reactions. However, the CD spectrum of G-DNA(inter) still showed a negative band at 245 nm and a positive band at 265 nm both in the absence and presence of salts as shown in **Figure A6**. The results indicated that the parallel G-quadruplex structure can form in 66 mM Tris-HCl buffer, 0.66 mM $MgCl_2$, pH 8.0 in the absence of NH_4OAc. However, the DNAzyme activity was observed only in the presence of NH_4OAc.

3.3.3 Effect of H_2O_2 concentration

For TMB oxidation, H_2O_2 was required as the stoichiometric oxidizing agent. In the next experiment, the concentration of H_2O_2 (added in the form of urea-hydrogen peroxide complex, which was easier to control the dose than liquid H_2O_2) was studied at the concentrations of G-DNA(inter) = 0.25 μM, TMB = 0.05 mM, hemin = 0.0125 μM, NH_4OAc = 200 mM, SDS = 0.02% w/v. As the H_2O_2 concentration increased, the intensity of the blue color in the solution and the absorbance at 680 nm increased, as illustrated in **Figures 3.4 (C), 3.5. (B)**. When the concentration of

H_2O_2 reached 5 mM, the blue coloration reached the maximum value and remained constant. As a result, $[H_2O_2]$ = 5 mM was selected.

3.3.4 Effect of ratios of G-DNA(inter) and hemin

Next, the ratio of G-DNA(inter) and hemin was investigated to find the optimal value that gave the maximum DNAzyme activity. In the absence of G-DNA(inter), TMB was slightly oxidized by hemin, which contributed to some background signals. Thus, the concentration of G-DNA(inter) was varied while the concentration of hemin was fixed at 0.0125 μM - a concentration at which no significant background was observed - and the concentrations of TMB = 0.05 mM, H_2O_2 = 5 mM, NH_4OAc = 200 mM, SDS = 0.02% w/v were used. As shown in **Figure 3.4 (D), 3.5 (C).** the intensity of the blue color and absorbance at 680 nm increased with increasing G-DNA(inter) concentration and reached a plateau at concentrations above 0.25 μM. Thus, the ratio of G-DNA(inter): hemin at 20:1 was selected for further experiments.

3.3.5 Effect of acpcPNA-C3 concentration

Next, the effect of acpcPNA-C3 concentration on the inhibition of the G-quadruplex DNAzyme deriving from G-DNA(inter) was studied. With the concentrations of G-DNA(inter) = 0.25 μM, TMB = 0.05 mM, H_2O_2 = 5 mM, hemin = 0.0125 μM, NH_4OAc = 200 mM, SDS = 0.02 %w/v, the concentration of acpcPNA-C3 was varied in the range from 0.125 μM to 0.75 μM. The results in **Figures 3.4 (E) and 3.5 (D)** showed that a complete colorless solution was observed when the concentration of the acpcPNA-C3 was at least 0.50 μM. As a result, this concentration of acpcPNA-C3 probe, which converted to 2 equiv. relative to that of G-DNA(inter), was selected for further experiments. Under the optimal condition, the blue color remained stable for at least 60 minutes.

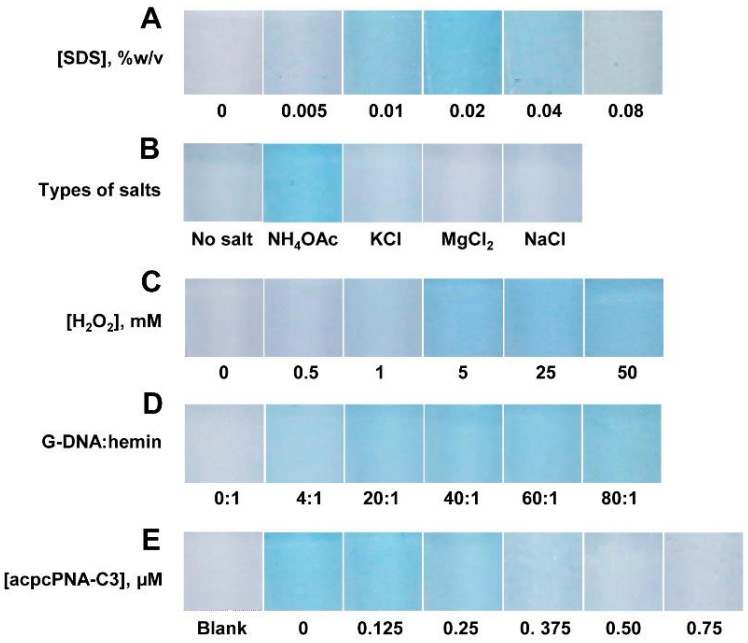

Figure 3.4 Photographs of (A) the effect of SDS concentration, (B) the effect of different salts, (C) the effect of H_2O_2 concentration, (D) the effect of G-DNA(inter):hemin ratio at the fixed concentration of hemin = 0.0125 µM, (E) the effect of acpcPNA-C3 concentration. The concentrations of TMB = 0.05 mM, hemin = 0.0125 µM in 66 mM Tris-HCl buffer, 0.66 mM $MgCl_2$, pH 8.0

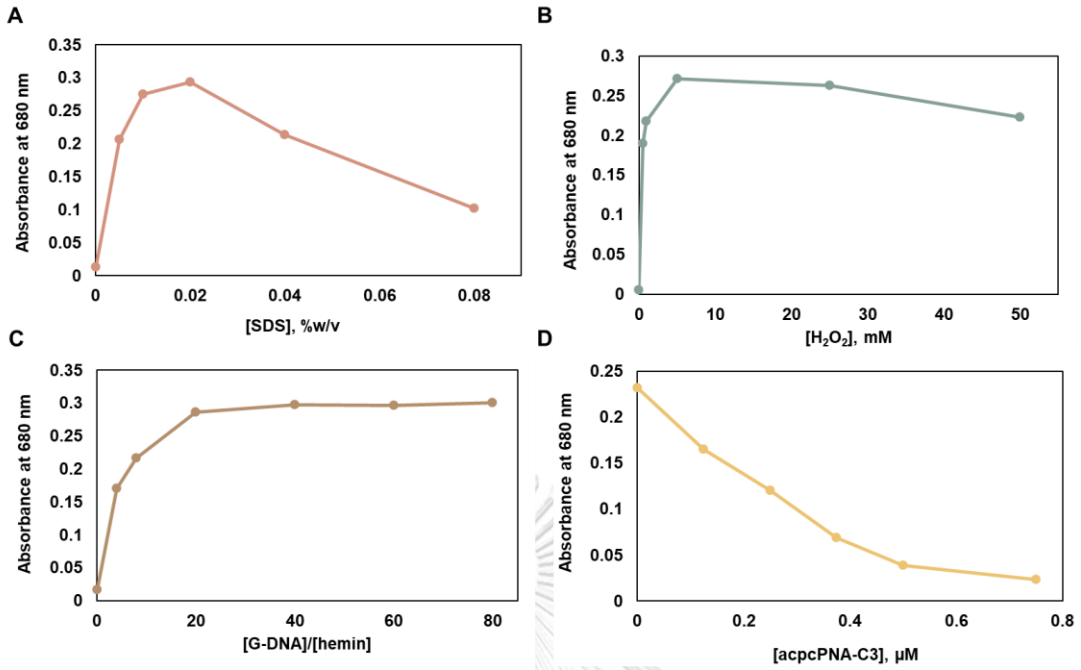

Figure 3.5 The plots between the absorbance at 680 nm and (A) SDS concentration, (B) H_2O_2 concentration, (C) G-DNA(inter):hemin ratio at the fixed concentration of hemin = 0.0125 μM, (D) acpcPNA-C3 concentration. The concentrations of TMB = 0.05 mM, hemin = 0.0125 μM in 66 mM Tris-HCl buffer, 0.66 mM $MgCl_2$, pH 8.0

3.4 Restoration of the DNAzyme activity by DNA target displacement

3.4.1 Preliminary study of the DNA target displacement

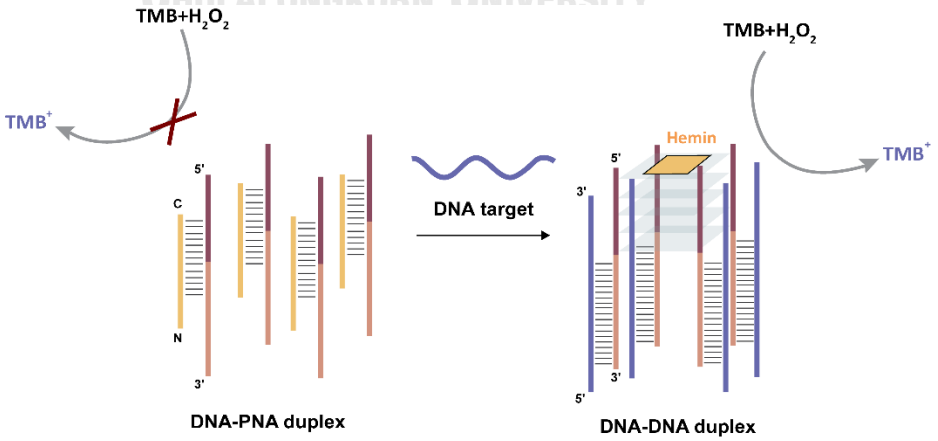

Figure 3.6 The restoration of G-quadruplex DNAzyme by the strand displacement of DNA target

Next, the restoration of DNAzyme activities was investigated in the presence of a DNA target. According to the design principle, the DNA target should bind to the PNA-blocked DNAzyme with a concomitant displacement of the acpcPNA probe. This would enable the formation of G-quadruplex DNAzyme again and thus the DNAzyme activity should be restored **(Figure 3.6)**. Unexpectedly, the restoration of DNAzyme activity did not occur when acpcPNA-C3 was treated with G-DNA(inter) followed by the addition of DNA target as shown in **Tube 4, Figure 3.7 (A)**. This suggests the slow kinetics of the strand displacement of acpcPNA-C3 by the DNA target hybridization. To overcome this problem, the excess DNA target (0.75 μM) was treated with G-DNA(inter) in 66 mM Tris-HCl buffer, 0.66 mM $MgCl_2$, pH 8.0 for 20 minutes prior to the addition of acpcPNA-C3 followed by the addition of NH_4OAc, SDS, TMB and hemin. After incubation for 20 min, the blue color was observed and the maximum absorbance at 680 nm was increased, as shown in **Figure 3.7 (B)**. The results indicated that DNAzyme activity was restored suggesting the re-formation of the G-quadruplex in the presence of the DNA target. Attempts were also made to increase the salt concentration with the aim to decrease the acpcPNA-DNA hybrid stability and increase the DNA-DNA hybrid stability. Although the T_m of G-DNA(inter)/DNA target (69 °C) was significantly higher than that of G-DNA(inter)/acpcPNA-C3 duplex (56.5 °C) in 200 mM NH_4OAc, 0.02% SDS, 66 mM Tris-HCl buffer, 0.66 mM $MgCl_2$, pH 8.0 **(Figure 3.7 (C))**, the restoration of the DNAzyme activity by DNA target displacement was still not observed. Thus, the pre-hybridization between the G-DNA(inter) and the DNA target was necessary. Moreover, attempts were made to reduce the stability of G-DNA(inter)/acpcPNA-C3 duplex by reducing the number of complementary bases between the G-DNA(inter) probe and acpcPNA-C3 using sequences shown in **Table A1**. The results in **Figure A9 (A)** showed that the DNAzyme activity was not successfully suppressed in this case. The attempt to increase the G-DNA(inter)-DNA target hybrid stability by increasing the number of complementary bases between G-DNA(inter) and the DNA target was also unsuccessful. The restoration of DNAzyme activity still did not occur **(Figure A9 (B))**.

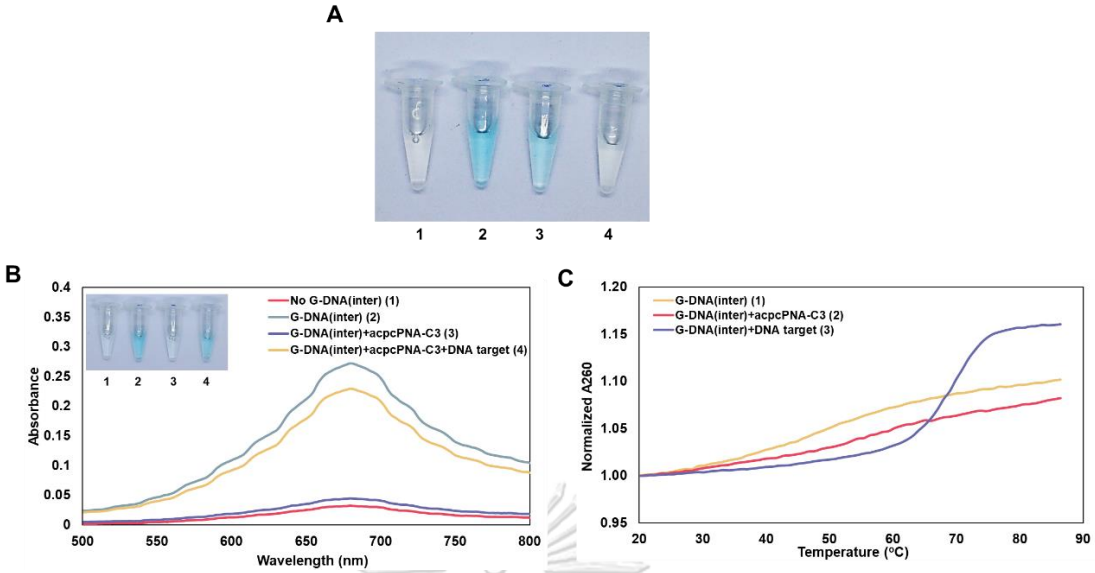

Figure 3.7 (A) Photographs of variation of order between acpcPNA and DNA target for the restoration of DNAzyme activity with (1) no G-DNA(inter), (2) G-DNA(inter), (3) G-DNA(inter)+DNA target+20 min incubation before acpcPNA-C3 addition (4) G-DNA(inter)+acpPNA-C3+10 min incubation before DNA target addition. (B) Photographs and UV-vis spectra of the DNAzyme-catalyzed oxidation of TMB (0.05 mM) in the presence of H_2O_2 (5 mM), hemin (0.0125 μM), NH_4OAc (200 mM), SDS (0.02 %w/v) in 66 mM Tris-HCl buffer, 0.66 mM $MgCl_2$, pH 8.0 with (1) no G-DNA(inter), (2) G-DNA(inter), (3) G-DNA(inter)+acpcPNA-C3, (4) G-DNA(inter)+DNA target+20 min incubation before acpcPNA-C3 addition. The concentrations of G-DNA(inter) = 0.25 μM, acpcPNA-C3 = 0.50 μM, DNA target = 0.75 μM. (C) Melting temperature of (1) G-DNA(inter), (2) G-DNA(inter)/acpcPNA-C3 duplex and (3) G-DNA(inter)/DNA target duplex in 66 mM Tris-HCl buffer, 0.66 mM $MgCl_2$, pH 8.0., 200 mM NH_4OAc, 0.02% SDS. The concentration of G-DNA(inter) = acpcPNA-C3 = DNA target = 1 μM

3.4.2 Characterization of formation of DNA G-quadruplex and its inhibition

The formation of the G-quadruplex and its inhibition were studied mechanistically using CD spectroscopy and gel electrophoresis.[58, 59] The formation of a parallel-stranded G-quadruplex was indicated by the CD spectrum of G-DNA(inter), which showed a negative band around 245 nm and a positive band around 265 nm **(Spectrum 1, Figure 3.8)**.[60] In contrast, the CD spectrum of G-DNA(inter) in the

presence of acpcPNA-C3 showed only a negative band at 245 nm **(Spectrum 3, Figure 3.8)** indicating that the formation of G-DNA(inter) was inhibited. However, the CD spectra of the G-DNA(inter) in the presence of DNA target with or without acpcPNA-C3 were similar, displaying a negative band at 245 nm and a positive band at 280 nm. Thus, the restoration of G-quadruplex of G-DNA(inter) by the presence of DNA target could not be clearly confirmed by this technique.

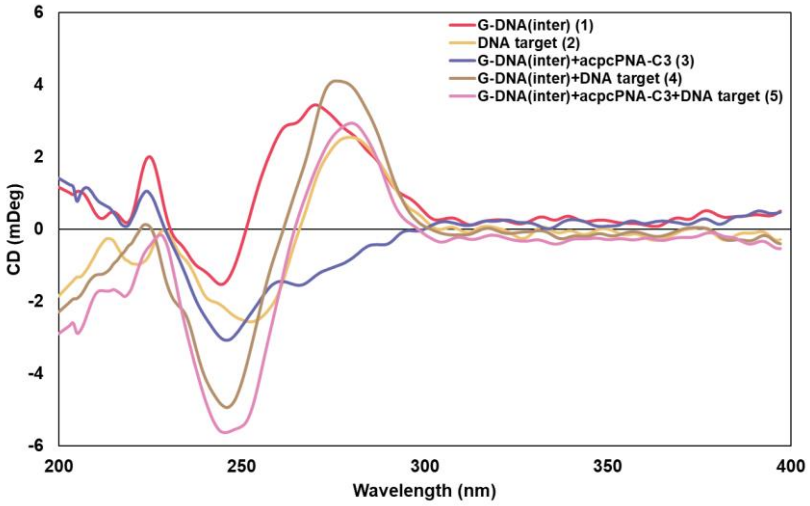

Figure 3.8 CD spectra of (1) G-DNA(inter), (2) DNA target, (3) G-DNA(inter)+acpcPNA-C3, (4) G-DNA(inter)+DNA target, (5) G-DNA(inter)+acpcPNA-C3+DNA target. The concentrations of G-DNA(inter) = 1 μM, acpcPNA-C3 = 2 μM, DNA target = 3 μM, NH_4OAc = 200 mM in 66 mM Tris-HCl buffer, 0.66 mM $MgCl_2$, pH 8.0

Next, non-denaturing PAGE was used to confirm the inhibition of G-quadruplex formation in G-DNA(inter) by hybridization with acpcPNA as well as the restoration of G-quadruplex following the acpcPNA displacement by the DNA target. According to **Figure 3.9**, a band at the baseline demonstrated that the G-DNA(inter) formed a G-quadruplex structure under the experimental conditions (lane 1).[61] In the presence of acpcPNA-C3, a faster-moving sharp band of G-DNA(inter)/acpcPNA-C3 complex was observed (lane 3). The results indicated that the G-DNA(inter) was hybridized to acpcPNA-C3 and the G-quadruplex was destroyed. In the presence of DNA target, the smearing band was observed (lane 5) similar to the band of

G-DNA(inter)/DNA target (lane 4). The results confirmed the re-formation of the G-quadruplex structure. However, another fast-moving sharp band also appeared in lanes 4 and 5. This result suggested that the G-DNA(inter)/DNA target duplex could also exist in the unassociated (non-G-quadruplex) form.

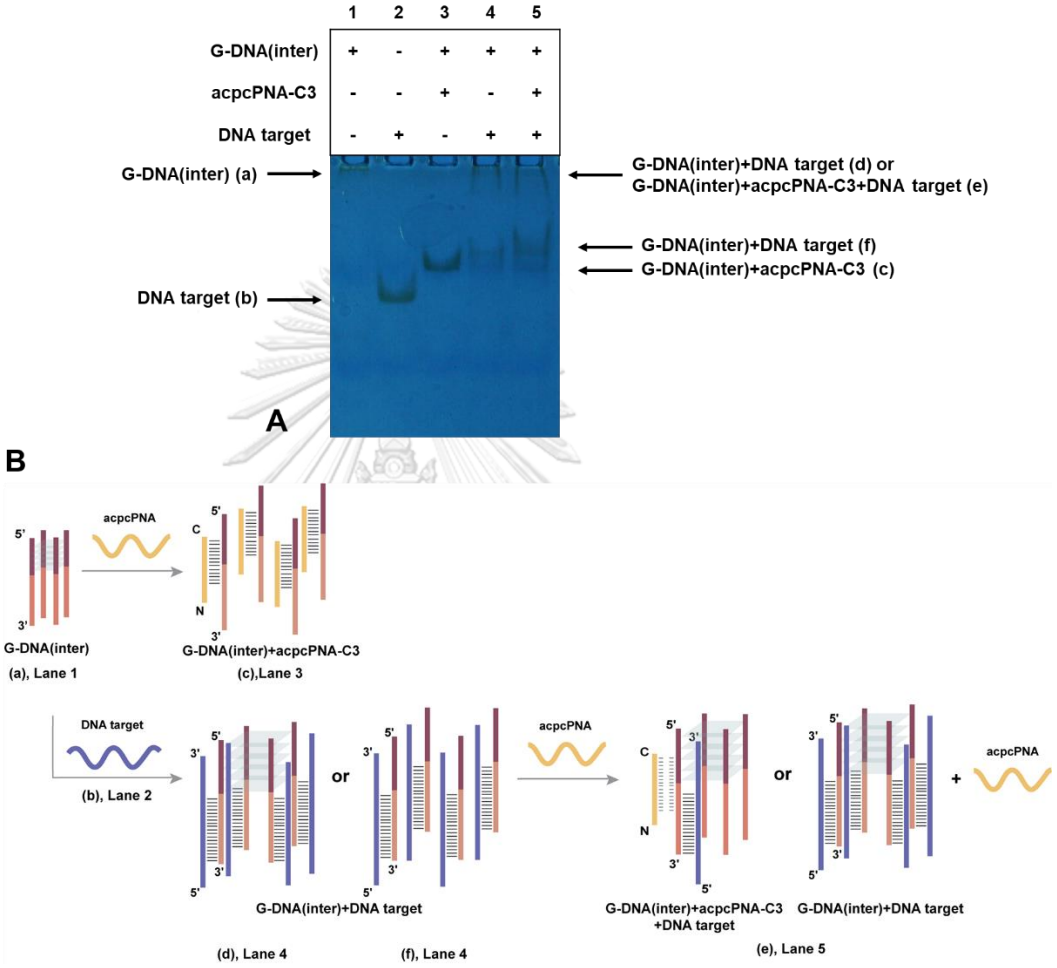

Figure 3.9 Non-denaturing PAGE of the DNA target detection by G-DNA(inter)/acpcPNA-C3 probe combination, lane 1: G-DNA(inter), lane 2: DNA target, lane 3: G-DNA(inter)+acpcPNA-C3, lane 4: G-DNA(inter)+DNA target, lane 5: G-DNA(inter)+acpcPNA-C3+DNA target under UV light. The quantities of G-DNA(inter) = 0.4 nmol, acpcPNA-C3 = 0.8 nmol, DNA target = 1.2 nmol in NH_4OAc = 200 mM in 66 mM Tris-HCl buffer, 0.66 mM $MgCl_2$, pH 8.0 (total volume = 10 µL)

3.5 Performance of DNA target sensor by G-DNA(inter)/acpcPNA-C3

3.5.1 Specificity

The DNAzyme activity was successfully restored in the presence of the complementary DNA target. To confirm that the sensor is specific to only the complementary DNA target sequence, the color restoration experiments in the presence of single mismatched (smDNA), double mismatched (dmDNA), triple mismatched (tmDNA), and non-DNA target sequences with sequences shown in **Table 3.2** were also performed. The specificity of this sensing system was evaluated by monitoring the absorbance at 680 nm. As shown in **Figure 3.10**, the DNAzyme activity was suppressed by 80% in the presence of acpcPNA-C3. Thus, the absorbance was similar to the blank and the solution appeared colorless. The absorbance values in the presence of smDNA2 were statistically lower than the complementary DNA target (p-value = 0.004) while the smDNA 1 and smDNA 3 gave a similar or even higher response (in the case of smDNA 3). The high signals in the case of smDNA 1 and smDNA 3 are not unexpected considering the location of the mismatch which were close to the 5'- and 3'-termini in the cases of smDNA 1 and smDNA 3, respectively. Nonetheless, there is no obvious correlation between the color change and thermal stabilities of different mismatches (T_m of the G-DNA(inter)/smDNA duplexes (smDNA 1 = 53.5 °C; smDNA 2 = 52.5 °C; smDNA 3 = 65.5 °C) **(Figure A7, Table 3.3)** compared to complementary DNA target (69 °C) under the optimal conditions (200 mM NH_4OAc, 0.02 %w/v SDS, 66 mM Tris-HCl buffer, 0.66 mM $MgCl_2$, pH 8.0).

In the case of dmDNAs, the absorbance values from dmDNA 1 and 2 were obviously lower than the complementary DNA. The absorbance from the dmDNA 3 experiment was higher than the other dmDNAs, but the value is statistically smaller than the complementary case (p-values = 0.007). Thus, all dmDNA can be distinguished from complementary DNA. Again, there is no apparent correlation between the color intensity and T_m of G-DNA(inter)/dmDNA hybrids. It appears that the competition between acpcPNA and DNA target binding to the G-DNA(inter) probe was quite complicated and could not be accounted for by the thermal stability data alone. Experiments with tmDNA and non-complementary DNAs gave signals that

were indistinguishable from the blank experiments, and the difference from complementary DNA target sequences was quite obvious. As a result, although the discrimination between mismatched and complementary DNA targets was not quite satisfactory, at least the DNAzyme activity restoration was successfully demonstrated to be specific to the DNA target sequence. In all cases, the blue color observed by naked eyes are consistent with the absorbance – i.e. the higher the absorbance value, the stronger the blue color. One possible reason for the relatively poor performance in single mismatch discrimination is that the specificity in this case relies on the formation of DNA-DNA hybrid rather than PNA-DNA hybrid. Since the DNA-DNA hybrid region is quite long in order to gain sufficient binding strength to compete with the PNA probe, the mismatch discrimination is naturally compromised.

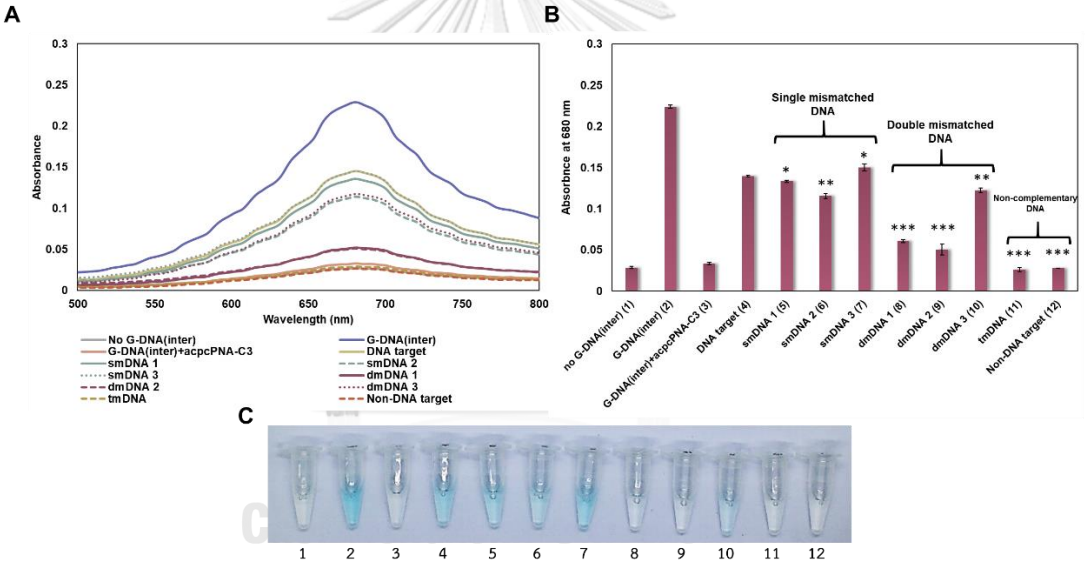

Figure 3.10 Specificity study of G-DNA(inter)/acpcPNA-C3 sensor. UV-vis spectra (A), Bar graph (B) and Photographs (C) of the DNAzyme-catalyzed oxidation of TMB (0.05 mM) in the presence of G-DNA(inter) (0.25 μM), acpcPNA-C3 (0.5 μM), DNA target (0.25 μM), H_2O_2 (5 mM), hemin (0.0125 μM), NH_4OAc (200 mM), SDS (0.02 %w/v) in 66 mM Tris-HCl buffer, 0.66 mM $MgCl_2$, pH 8.0 with (1) no G-DNA(inter), (2) G-DNA(inter), (3) G-DNA(inter)+acpcPNA-C3, (4) comDNA, and (5) smDNA 1, (6) smDNA 2, (7) smDNA 3, (8) dmDNA 1, (9) dmDNA 2, (10) dmDNA 3, (11) tmDNA, (12) non-DNA target. * not statistically significant different (p>=0.05), ** statistically significant different (p<0.05), *** very different.

Table 3.3 T_m of duplexes of G-DNA(inter) with DNA target or mismatched DNA

Name	T_m (°C)
G-DNA(inter)/DNA target duplex	69.0
G-DNA(inter)/smDNA 1 duplex	53.5
G-DNA(inter)/smDNA 2 duplex	52.5
G-DNA(inter)/smDNA 3 duplex	65.5
G-DNA(inter)/dmDNA 1 duplex	59.0
G-DNA(inter)/dmDNA 2 duplex	47.5
G-DNA(inter)/dmDNA 3 duplex	59.0
G-DNA(inter)/tmDNA duplex	-
G-DNA(inter)/non-DNA target duplex	-

3.5.1.1 Comparison of selectivity of acpcPNA and aegPNA probes

From the previous experiments, the acpcPNA-C3 probe could effectively inhibit the DNAzyme activity of G-DNA(inter). In addition, the sensing system consisting of G-DNA(inter)/acpcPNA-C3 could discriminate between the DNA target and mismatched DNA targets. To compare the performance of the sensing system of acpcPNA with aegPNA probes, the experiments were performed on G-DNA(inter)/acpcPNA-C5 and G-DNA(inter)/aegPNA-C5. The PNA-C5 probes were compared because the aegPNA were only available with C5 tail, and it was thought that increasing the number of cytosine bases at the C-terminus should enhance the PNA's quenching ability of the DNAzyme activity further. As shown in **Figure 3.11**, the acpcPNA-C5 probe could also suppress the DNAzyme activity of the G-DNA(inter) probe well, and the pair showed similar specificity to the G-DNA(inter)/acpcPNA-C3 system. The aegPNA-C5 probe could also similarly suppress the DNAzyme activity of the G-DNA(inter) probe. In the specificity test of the acpcPNA-C5 system, the signals were relatively high in most single mismatched cases, especially the smDNA 3 which showed an even higher signal than the complementary DNA target which was consistent with the previous experiments with acpcPNA-C3. In the case of double mismatched DNAs, the signals were easily distinguishable from the complementary DNA target. Only the dmDNA 3 showed similar absorbance to the comDNA

(p-value = 0.05). The experiments with triple mismatched and non-complementary DNAs show signals that were similar to the blank experiments suggesting that the restoration of the DNAzyme activity requires a specific DNA target. In the case of aegPNA-C5 system, only dmDNA 2, tmDNA, and non- DNA target showed significantly smaller absorbances than the complementary DNA target. Furthermore, the signal from dmDNA 2 was still relatively high compared to the complementary DNA target. The results suggested that the G-DNA(inter)/acpcPNA-C5 sensing system performed better than the G-DNA(inter)/aegPNA-C5 sensing system in terms of specificity.

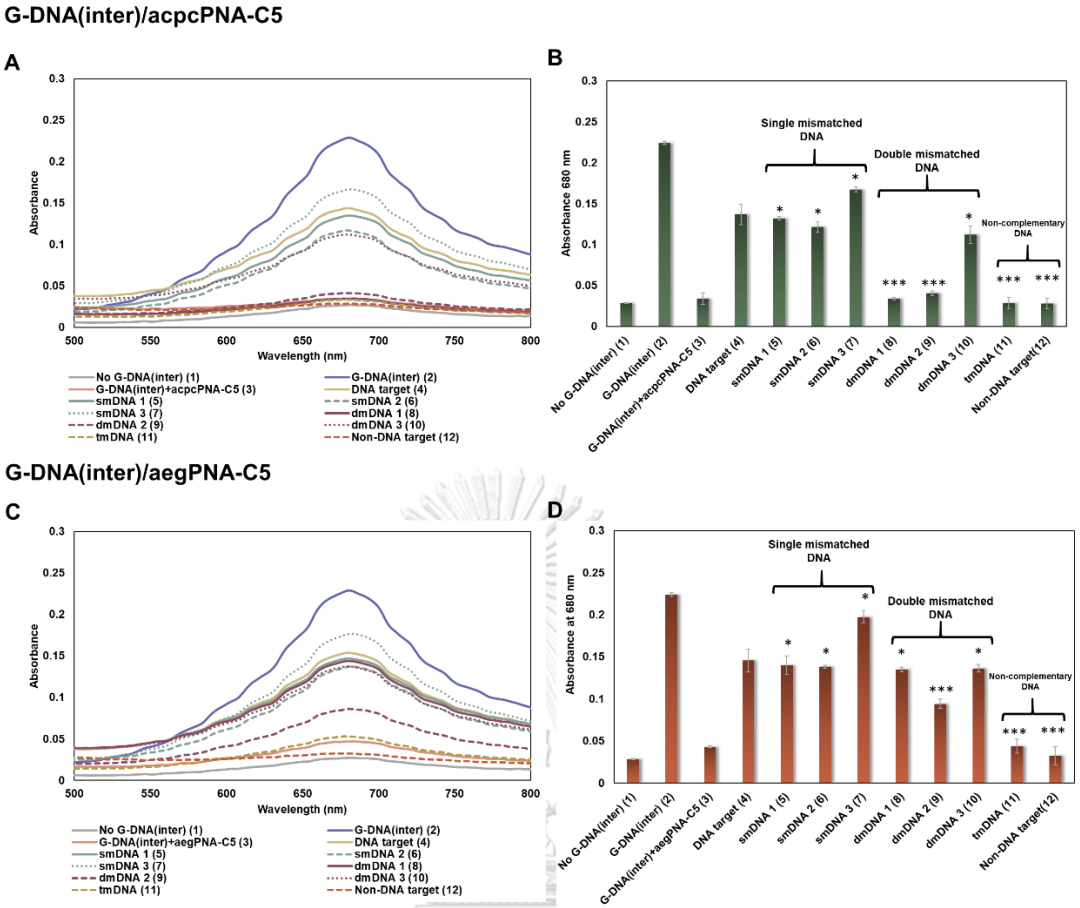

Figure 3.11 Specificity study of G-DNA(inter)/acpcPNA-C5 sensor and G-DNA(inter)/aegPNA-C5 sensor. UV-vis spectra (A), (C), Bar graph (B), (D) of the DNAzyme-catalyzed oxidation of TMB (0.05 mM) in the presence of H_2O_2 (5 mM), hemin (0.0125 μM), NH_4OAc (200 mM), SDS (0.02 %w/v) in 66 mM Tris-HCl buffer, 0.66 mM $MgCl_2$, pH 8.0 with (1) no G-DNA(inter), (2) G-DNA(inter), (3) G-DNA(inter)+acpcPNA-C3, (4) comDNA, and (5) smDNA 1, (6) smDNA 2, (7) smDNA 3, (8) dmDNA 1, (9) dmDNA 2, (10) dmDNA 3, (11) tmDNA, (12) non-DNA target. * not statistically significant different (p>=0.05), ** statistically significant different (p<0.05), *** very different.

3.5.2 Sensitivity

To study the sensitivity of the G-DNA(inter)/acpcPNA-C3 sensing system for the detection of DNA target, different concentrations of DNA target were incubated with G-DNA(inter) in 66 mM Tris-HCl buffer, 0.66 mM $MgCl_2$, pH 8.0 for 20 minutes.

Next, the acpcPNA-C3 was added to the mixture and left for 20 minutes followed by the addition of NH_4OAc, SDS, TMB, and hemin and incubated for 20 minutes. As shown in **Figure 3.12** the absorbance at 680 nm was still clearly observed when the amount of the DNA target was decreased from 0.25 μM to 0.025 μM. A linear relationship between the absorbance at 680 nm and the DNA target concentration was obtained (y = 0.0005x + 0.0413) with R^2 = 0.9937. Based on the limit of detection (LOD) of 3SD(blank)/slope, the sensor could detect the DNA target down to at least 7 nM. The sensitivity of this DNA sensing system was on the high side, but still compared well to several other DNA detection systems based on colorimetric or fluorescence detection without signal amplification, including Hg^{2+}-hairpin probe (10 nM)[62], AuNP on metal–organic frameworks (11 nM)[63], graphene oxide for DNA sensing (12 nM)[64], and quantum dots based DNA sensing system (17 nM).[65]

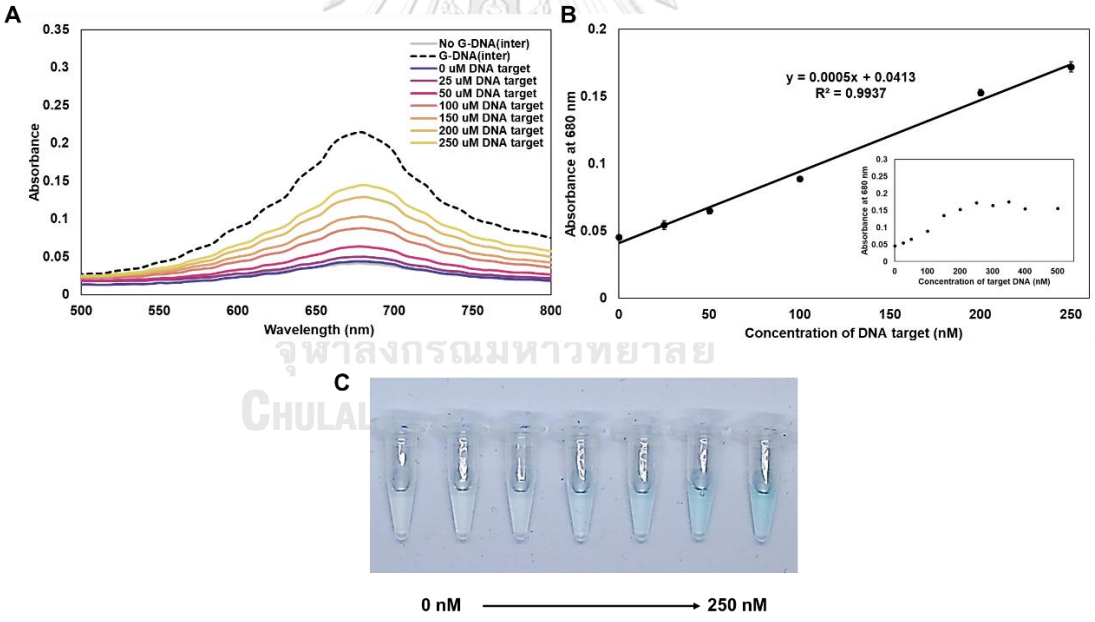

Figure 3.12 Sensitivity study of G-DNA(inter)/acpcPNA-C3 sensor. (A) UV-vis spectra, (B) The calibration graph, (C) Photographs of the DNAzyme-catalyzed oxidation of TMB (0.05 mM) in the presence of G-DNA(inter) (0.25 μM), acpcPNA-C3 (0.50 μM), DNA target (25-250 nM), H_2O_2 (5 mM), hemin (0.0125 μM), NH_4OAc (200 mM), SDS (0.02 %w/v) in 66 mM Tris-HCl buffer, 0.66 mM $MgCl_2$, pH 8.0 with different concentration of DNA target

3.6 DNA target recycling by Exonuclease III

3.6.1 Principle of signal amplification using Exo III

In order to increase the sensitivity of the DNA detection system further, it was coupled to an Exo III mediated target recycling scheme according to the principle shown in **Figure 3.13** Exo III is an enzyme that is widely used to improve the sensitivity of numerous sensing systems.[66-68] Due to the selectivity for cleaving double strand DNA with blunt or recessed 3′-termini by removal of mononucleotides from 3′-hydroxyl termini. In this work, Exo III was used to digest the duplex of G-DNA(inter) and DNA target for target recycling. In the presence of DNA target, the acpcPNA would be displaced by the DNA target to form a G-DNA(inter)/DNA target duplex whereby the G-DNA(inter) probe carried a 3'-recessed end. Thus, this DNA duplex would be susceptible to digestion by Exo III from the 3'-terminus of the G-DNA(inter) probe. Such digestion would release the free G-quadruplex as well as the DNA target. The free G-quadruplex could then combine with hemin to catalyze the oxidation of the TMB substrate. The released DNA target could bind more G-DNA(inter) probes and thus generate more signals.

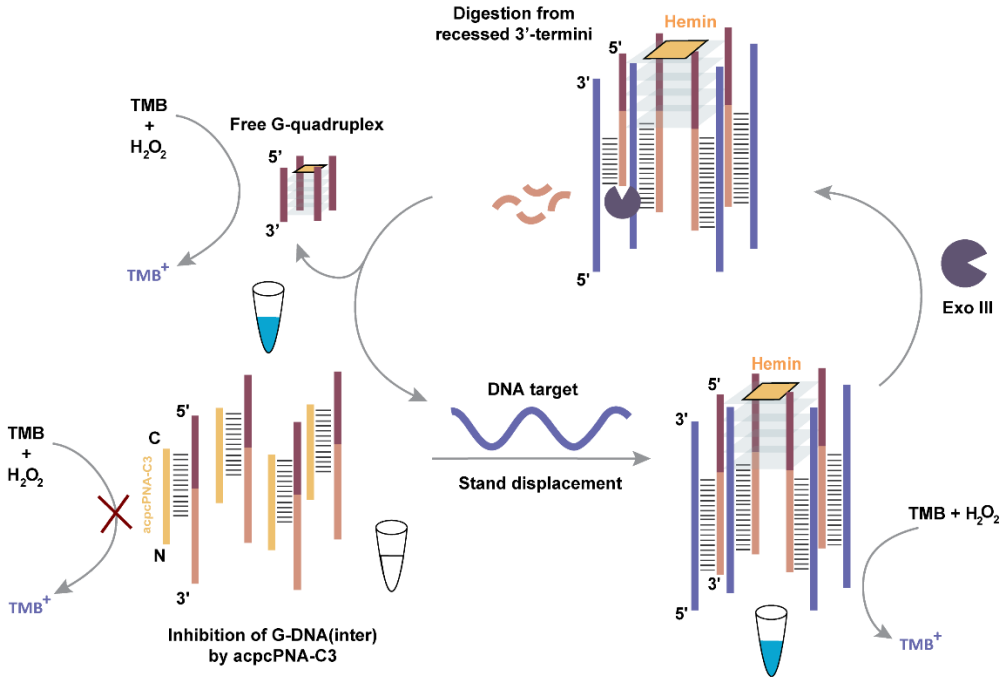

Figure 3.13 The proposed principle of target recycling by Exo III

3.6.2 Effect of Exo III amounts

In the previous experiments, the addition of acpcPNA-C3 to the G-DNA(inter) probe before the DNA target resulted in an unsuccessful restoration of the blue coloration and the absorbance at 680 nm **(Figure 3.14, Tube #4 and Graph #4)**, indicating that the restoration of the DNAzyme activity could not occur due to the slow kinetics of the strand displacement. However, once the G-DNA inter probe is digested by Exo III, the blue color should be recovered. As shown in **Tube #5** and **Graph #5**, the blue color was observable in the presence of only G-DNA(inter) and 0.5 U Exo III. The optimal molar ratio of DNA to the enzyme was determined as 38 pmol DNA: 0.5 U Exo III by non-denaturing PAGE **(Figure A8)**. Moreover, the blue color and the absorbance at 680 nm showed similar results at higher Exo III units **(Tubes and Graphs #7, #9)**. This indicated that the Exo III could not degrade the single-stranded G-DNA(inter) probe and thus the DNAzyme was still active. However, no blue coloration was observed in presence of acpcPNA-C3, DNA target, and 0.5 U Exo III **(Tube #6 and Graph #6)** or higher **(Tubes and Graphs #8, #10)**. The results showed that the target recycling did not occur as planned.

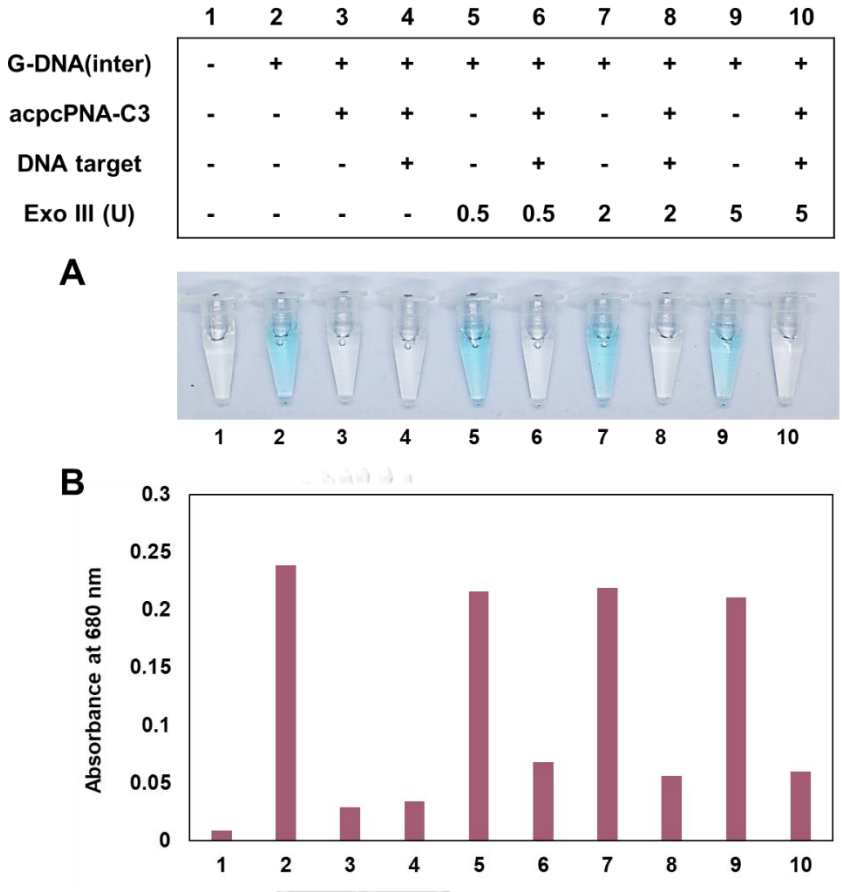

Figure 3.14 (A) Photographs and (B) Bar graph of the DNAzyme-catalyzed oxidation of TMB (0.05 mM) in the presence of H_2O_2 (5 mM), hemin (0.0125 μM), NH_4OAc (200 mM), SDS (0.02 %w/v) in 66 mM Tris-HCl buffer, 0.66 mM $MgCl_2$, pH 8.0 with (1) no G-DNA(inter), (2) G-DNA(inter), (3) G-DNA(inter)+acpcPNA-C3, (4) G-DNA(inter)+acpcPNA-C3+DNA target, G-DNA(inter)+ (5) 0.5 U, (7) 2 U, (9) 5 U Exo III, G-DNA(inter)+acpcPNA-C3+DNA target + (6) 0.5 U, (8) 2 U, (10) 5 U Exo III with incubation for 30 minutes at 40 °C. Conditions: G-DNA(inter) (0.25 μM), acpcPNA-C3 (0.5 μM), DNA target (0.10 μM)

Non-denaturing PAGE was used to investigate the interaction of Exo III on the G-DNA(inter)/acpcPNA-C3 system in the absence and presence of the DNA target. As shown in **Figure 3.15**, lanes 1 and 6 showed a band at the baseline suggesting that the intermolecular G-quadruplex structure was formed from the G-DNA(inter) probe both in the absence and presence of Exo III. In the presence of acpcPNA-C3 inhibitor probe, a sharp band deriving from the G-DNA/acpcPNA-C3 complex was

observed (lanes 3 and 8). The result confirmed that the complex of G-DNA(inter)/acpcPNA-C3 was not digested by Exo III. In the presence of DNA target without the acpcPNA-C3, several bands were observed in the absence of Exo III. These include the excess DNA target band (with the highest mobility), the target-probe hybrid bands, and a baseline band (G-quadruplex structure). In the presence of Exo III, the target-probe hybrid bands disappeared and only the excess DNA target band and the baseline band were observed (lane 9). The results confirmed that the G-DNA(inter)/DNA target hybrid was successfully digested under this condition. In the presence of all components (G-DNA(inter)/acpcPNA-C3/DNA target), several bands were also observed similar to the case without acpcPNA-C3 as shown in lane 5. However, there are some additional low-mobility bands that may be associated with more complex structures such as ternary complexes between G-DNA(inter)/acpcPNA-C3/DNA target. In the presence of Exo III, these complex bands disappeared and only the excess DNA target band and a new band with slightly higher mobility than the G-DNA(inter)/acpcPNA-C3 duplex were observed (lane 10). Based on the experimental evidence, it was proposed that the complex between a partially digested G-DNA(inter) and acpcPNA-C3 might re-form when the DNA target was released from the partially digested G-DNA(inter) probe, leading to the unsuccessful restoration of the DNAzyme activity as originally planned.

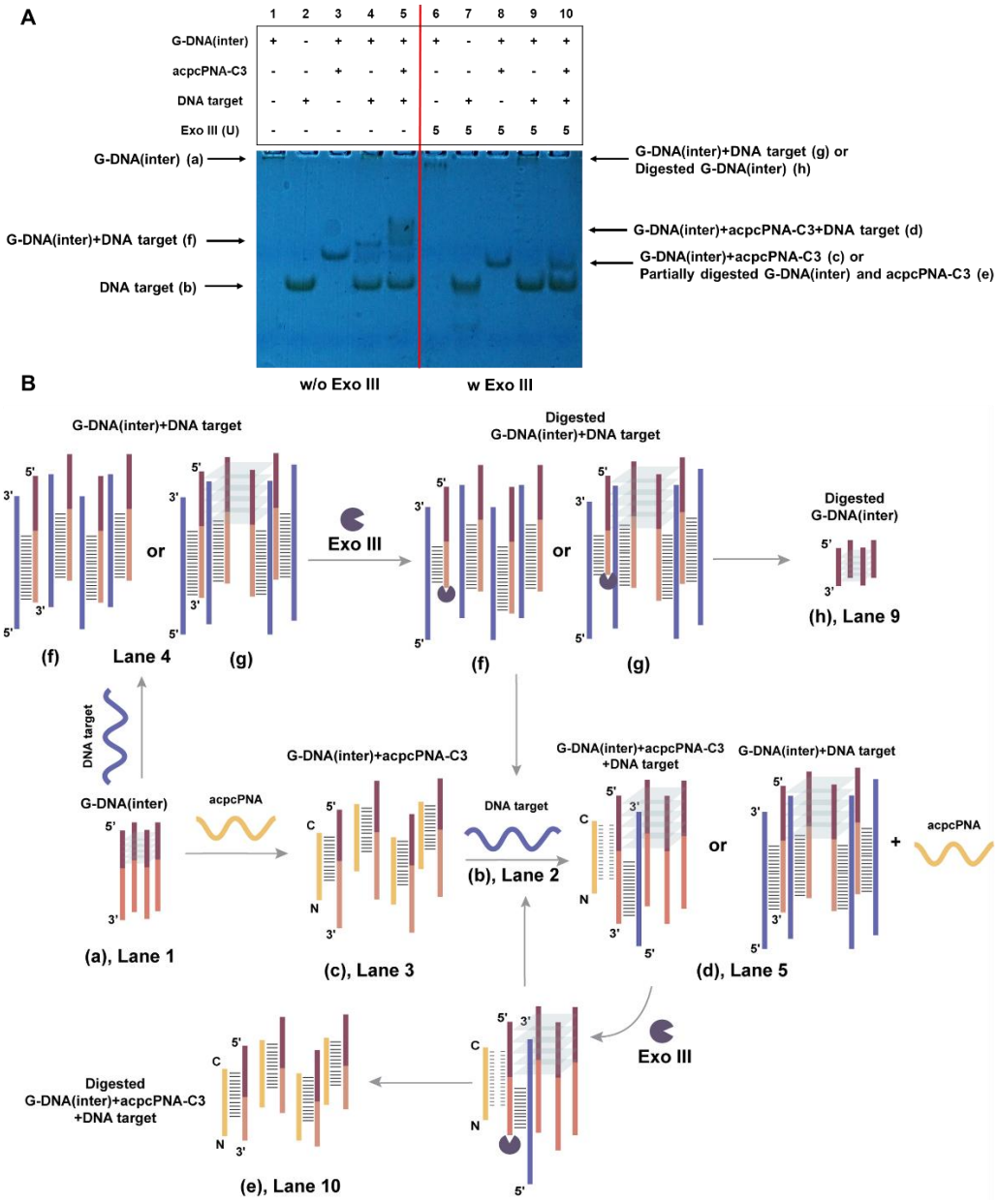

Figure 3.15 Non-denaturing PAGE of the DNA target recycling with G-DNA(inter)/acpcPNA-C3 probe combination by Exo III, lane 1: lane G-DNA(inter) 2: DNA target, lane 3: G-DNA(inter)+acpcPNA-C3, lane 4: G-DNA(inter)+DNA target, lane 5: G-DNA(inter)+acpcPNA-C3+DNA target lane 6: G-DNA(inter)+Exo III, lane 7: DNA target +Exo III, lane 8: G-DNA(inter)+acpcPNA-C3+Exo III, lane 9: G-DNA(inter)+DNA target +Exo III, lane 10: G-DNA(inter)+acpcPNA-C3+DNA target+Exo III under UV light. The quantities of G-DNA(inter) = 0.4 nmol, acpcPNA-C3 = 0.8 nmol, DNA target = 1.2 nmol, Exo III = 5 U in 66 mM Tris-HCl buffer, 0.66 mM $MgCl_2$, pH 8.0 (total volume = 10 µL), (B) Schematic representation of the propose structure for this experiment

To confirm that the target recycling was possible in the absence of the acpcPNA probe, labeled DNA sequences (FAM-DNA probe and TAMRA-DNA target with the sequence shown in **Table 3.4** were used to demonstrate that Exo III was able to successfully digest the DNA-DNA duplex under the experimental conditions. The G-quadruplex forming region was removed from the FAM-DNA probe to simplify the result interpretation. According to **Figure 3.16** lanes 1-3, the FAM-G-DNA(inter) probe (green band) and TAMRA-target (red band) formed a hybrid and appeared yellow under UV light. In the presence of sub-stoichiometric amounts of DNA target, the green excess probe band was clearly visible as seen in lane 4. The green band of the FAM-G-DNA(inter) and red band of the TAMRA-target were still the same in the presence of Exo III (lanes 5 and 6), indicating that they were not digested by Exo III. On the other hand, the yellow band with low mobility completely disappeared in lane 7, with the concomitant formation of new green and red bands with higher mobilities. The same result was observed when the DNA target was present in sub-stoichiometric quantities (lane 8). Importantly, the original FAM-DNA band was completely digested even when the amount of the DNA target was smaller than the amount of the probe. These results clearly indicated that the target recycling was indeed accomplished, at least in the absence of the G-quadruplex region and the acpcPNA inhibitor strand.

Table 3.4 FAM-DNA probe and TAMRA-DNA target sequences[a]

Name	DNA sequence
FAM-DNA probe	5’-FAM-TTC AGT CTA GGT ATA AGC TAA CGA GTT CCG TGA CGC-3’
TAMRA-DNA target	3’-TT TTT ATT GCT CAA GGC ACT GCG TA CCG-TAMRA-5’

[a]The binding regions for the DNA targets are highlighted. Non-pairing bases are presented in normal text.

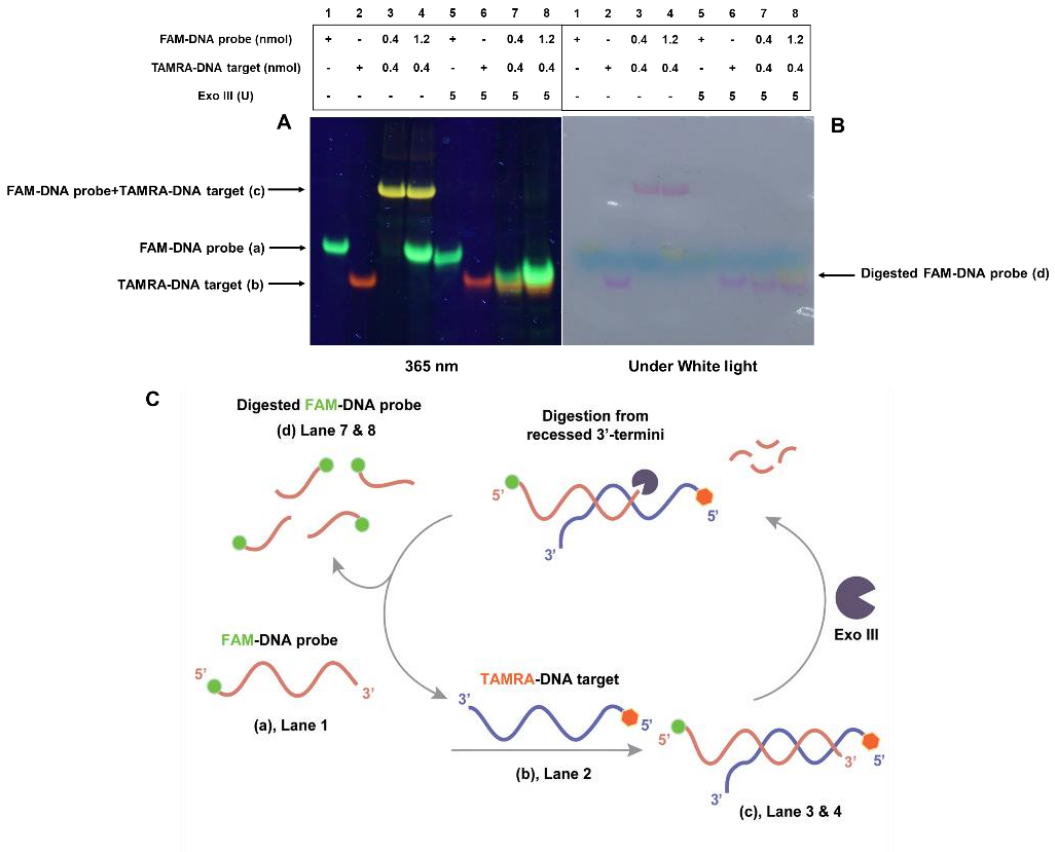

Figure 3.16 Non-denaturing PAGE of digestion of FAM-DNA probe and TAMRA-DNA target by Exo III, lane 1: FAM-DNA probe, lane 2: TAMRA-DNA target, lane 3: FAM-DNA probe+TAMRA-DNA target (1:1), lane 4: FAM-DNA probe+TAMRA-DNA target (3:1), lane 5: FAM-DNA probe+Exo III, lane 6: TAMRA-DNA target+Exo III, lane 7: FAM-DNA probe+TAMRA-DNA target (1:1)+Exo III, lane 8: FAM-DNA probe+TAMRA-DNA target (3:1)+Exo III under (A) UV light 365 nm, (B) white light. The quantities of FAM-DNA probe = 0.4 or 1.2 nmol, DNA target = 0.4 nmol, Exo III = 5 U in 66 mM Tris-HCl buffer, 0.66 mM $MgCl_2$, pH 8.0 (total volume = 10 µL), (C) Schematic representation of the propose structure for this experiment

To investigate the possibility of the formation of ternary complexes between G-DNA(inter)/acpcPNA-C3/DNA target, the labeled acpcPNA probe FAM-acpcPNA-C3 was employed instead of acpcPNA-C3 to allow visualization of the acpcPNA-C3. As shown in **Figure 3.17**, the FAM-acpcPNA-C3 which had an uncharged backbone did not move into the gel as shown by the fluorescence band at the baseline in lane 2 when viewed under UV light (365 nm). In the presence of G-DNA(inter), the

hybridization of G-DNA(inter) and FAM-acpcPNA-C3 occurred, as evidenced by the formation of a new fluorescent band with greater mobility (lane 4) together with the excess FAM-acpcPNA-C3. This G-DNA(inter)/acpcPNA-C3 band disappeared and a smearing fluorescent band appeared at the baseline (lane 6) in the presence of all components (G-DNA(inter), acpcPNA-C3, and DNA target). This experiment suggested that the FAM-acpcPNA-C3 might not be completely displaced by the DNA target, thus providing evidence in favor of the formation of ternary complexes.

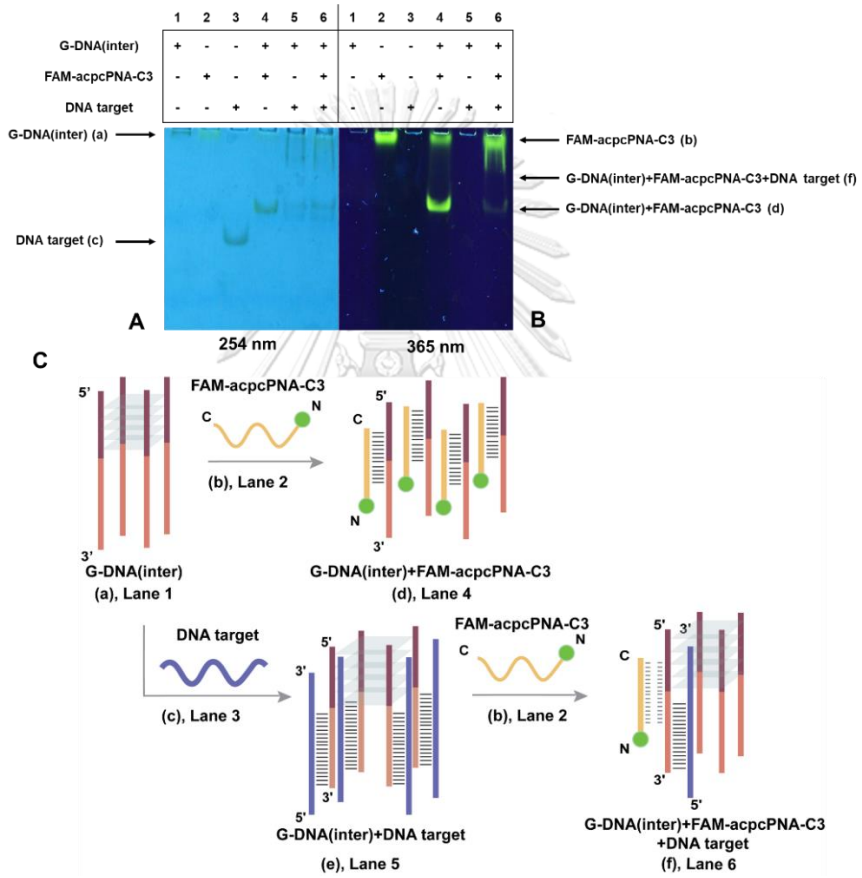

Figure 3.17 Non-denaturing PAGE of the DNA target displacement with G-DNA/acpcPNA-C3 probe combination, lane 1: G-DNA(inter), land 2: FAM-acpcPNA-C3, lane 3: DNA target, lane 4: G-DNA(inter)+FAM-acpcPNA-C3, lane 5: G-DNA(inter)+DNA target, lane 6: G-DNA(inter)+FAM-acpcPNA-C3+DNA target under (A) UV light (254 nm), (B) UV light (365 nm). The quantities of G-DNA(inter) = 0.4 nmol, FAM-acpcPNA-C3 = 0.8 nmol, DNA target = 0.4 nmol, NH_4OAc = 200 mM in 66 mM Tris-HCl buffer, 0.66 mM $MgCl_2$, pH 8.0 (total volume = 10 µL), (C) Schematic representation of the propose structure for this experiment

3.6.3 Effect of $MgCl_2$ concentration on the target recycling

The stability of the hybrid between G-DNA(inter) and acpcPNA-C3 was reduced at high concentrations of salt (high ionic strength).[69, 70] Thus, the increasing of $MgCl_2$ concentration was performed for reduction of the stability of G-DNA(inter) and acpcPNA-C3. In addition, Mg^{2+} is a normally supporting metal required for the digestion of DNA-DNA duplex by Exo III.[71] Thus, it might increase the chance of the target recycling. From the study of the effects of different salts on DNAzyme activity **(section 3.3.2)**, the colorless solution was observed in the presence of G-DNA(inter) and $MgCl_2$. Thus, the effect of $MgCl_2$ on the DNAzyme activity was first tested. The results in **Figure 3.18 (A)** showed that the blue color and the absorbance at 680 nm were stable when the concentration of $MgCl_2$ was increased. The increase in $MgCl_2$ concentration did not affect the DNAzyme activity. However, increased background signals were observed at increased $MgCl_2$ concentrations due to the reduction of the stability of the hybrid between G-DNA(inter) and acpcPNA-C3. Thus, the effect of the addition of $MgCl_2$ to the inhibition of DNAzyme activity of G-DNA(inter) by acpcPNA-C3 was next investigated. **Figure 3.18 (B)** showed that increasing $MgCl_2$ concentration before the addition of acpcPNA-C3 resulted in a blue color and the absorbance at 680 nm was slightly increased. The results showed that the addition of more than 2 mM $MgCl_2$ produced a significant background signal (blue color) visible to the naked eye. Thus, 2 mM $MgCl_2$ was selected for further experiments.

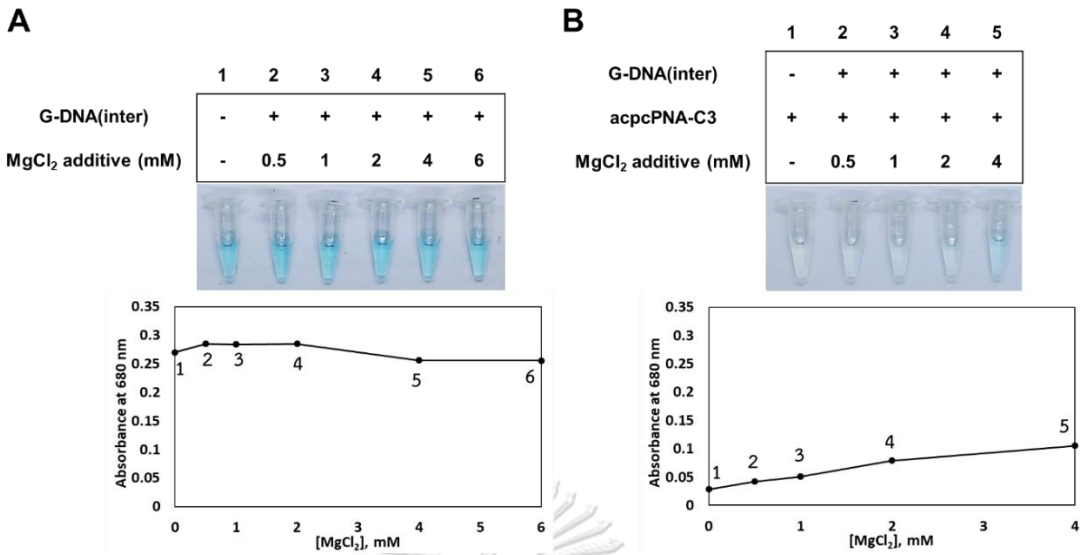

Figure 3.18 Effect of $MgCl_2$ concentration with DNAzyme activity and G-DNA(inter)/acpcPNA-C3 hybridization. Photographs and UV-vis spectra of the DNAzyme-catalyzed oxidation of TMB (0.05 mM) in the presence of G-DNA(inter) (0.25 μM), H_2O_2 (5 mM), hemin (0.0125 μM), NH_4OAc (200 mM), SDS (0.02 %w/v), $MgCl_2$ (2 mM) in 66 mM Tris-HCl buffer, 0.66 mM $MgCl_2$, pH 8.0. (A) without acpcPNA-C3 (0.5 μM) and (B) with acpcPNA-C3 (0.5 μM)

Figure 3.19 showed the effect of 2 mM $MgCl_2$ on the target recycling experiments. The blue color solution in **Tube #5** and the absorbance at 680 nm in **Graph #5** were similar to the results obtained from G-DNA(inter) alone **(Tube and Graph #2)**. The results indicated that the addition of 2 mM $MgCl_2$ did not affect the DNAzyme activity under this condition**.** However, the restoration of DNAzyme activity did not occur because the blue color and absorbance at 680 nm were still not noticeably increased **(Tube and Graph #6)**. Moreover, increasing of Exo III did not help as the results in **Tube and graph #8, #10** are similar to the experiment without Exo III **(Tube and Graph #4)**.

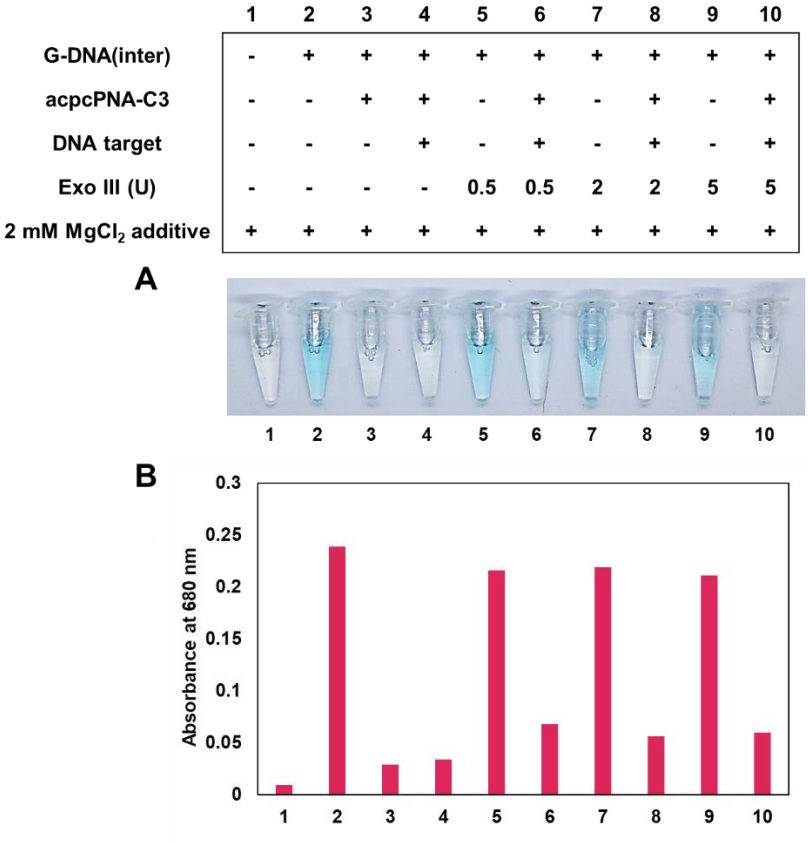

Figure 3.19 (A) Photographs and (B) Bar graph of the DNAzyme-catalyzed oxidation of TMB (0.05 mM) in the presence of H_2O_2 (5 mM), hemin (0.0125 μM), NH_4OAc (200 mM), SDS (0.02 %w/v), $MgCl_2$ (2 mM) in 66 mM Tris-HCl buffer, 0.66 mM $MgCl_2$, pH 8.0 with (1) no G-DNA(inter), (2) G-DNA(inter), (3) G-DNA(inter)+acpcPNA-C3, (4) G-DNA(inter)+acpcPNA-C3+DNA target, G-DNA(inter)+ (5) 0.5 U, (7) 2 U, (9) 5 U Exo III, G-DNA(inter)+acpcPNA-C3+DNA target+ (6) 0.5 U, (8) 2 U, (10) 5 U Exo III with incubation for 30 minutes at 40 °C. Conditions: G-DNA(inter) (0.25 μM), acpcPNA-C3 (0.5 μM), DNA target (0.10 μM)

3.6.4 Variation of incubation time

From the gel electrophoresis experiment in **Figure A8**, The DNA-DNA duplex was completely digested at 40 °C for 30 minutes. However, the target recycling did not occur under this optimal condition as shown by both colorimetric detection **(Figure 3.14)** and gel electrophoresis assay **(Figure 3.15)**. Thus, the incubation time with Exo III was varied from 30 to 180 minutes in this experiment. As shown in **Figure**

3.20 (Tubes and Graphs #7, #9, #11), the intensity of blue color and absorbance at 680 nm were similar for all different incubation times. However, the colorless solution was still observed in the presence of Exo III when the incubation time was increased from 30 to 180 minutes **(Tubes and Graphs #6, #8, #10, #12)**.

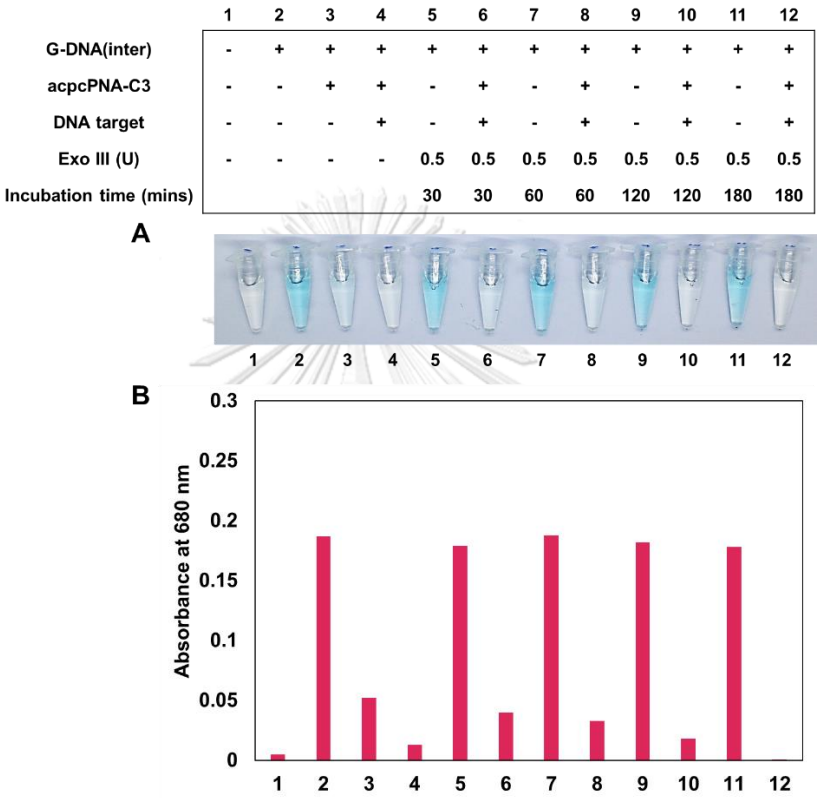

Figure 3.20 (A) Photographs and (B) Bar graph of the DNAzyme-catalyzed oxidation of TMB (0.05 mM) in the presence of H_2O_2 (5 mM), hemin (0.0125 μM), NH_4OAc (200 mM), SDS (0.02 %w/v) in 66 mM Tris-HCl buffer, 0.66 mM $MgCl_2$, pH 8.0 with (1) no G-DNA(inter), (2) G-DNA(inter), (3) G-DNA(inter)+acpcPNA-C3, (4) G-DNA (inter)+acpcPNA-C3+DNA target, G-DNA(inter)+0.5 U Exo III with incubation for (5) 30, (7) 60, (9) 120, (11) 180 minutes, G-DNA(inter)+acpcPNA-C3+DNA target +0.5 U Exo III with incubation for (6) 30, (8) 60, (10) 120, (12) 180 minutes at 40 °C. Conditions: G-DNA(inter) (0.25 μM), acpcPNA-C3 (0.5 μM), DNA target (0.10 μM)

To summarize, the DNAzyme-based DNA detection system using G-DNA(inter) /acpcPNA-C3 probe combination was successfully developed. The peroxidase activity of the DNAzymer was inhibited by the acpcPNA probe resulting in the inability to convert the TMB substrate into the blue-colored oxidized product. In the presence of the DNA target, the DNAzyme activity was restored resulting in the formation of the blue solution in a sequence-specific fashion. Additionally, the DNA target could be detected in the signal-on mode with an LOD of 7 nM. However, all attempts to improve the sensitivity by employing the Exo III enzyme for DNA target recycling failed despite many variations of several parameters including unit of Exo III, $MgCl_2$ concentration, and incubation time. Gel electrophoresis experiments suggested that the incompletely digested G-DNA(inter) probe might dissociate from the DNA target and was subsequently captured by the acpcPNA probe again, resulting in the failure of the DNAzyme activity restoration.

CHAPTER IV
CONCLUSION

In this work, a new colorimetric DNA detection system DNA was successfully developed based on the combination of a G-quadruplex/hemin DNAzyme and a pyrrolidinyl PNA inhibitor probe. In combination with hemin, the intermolecular G-quadruplex-forming DNA sequence (G-DNA(inter)) which contains a G-rich sequence at the 5'-terminus catalyzed the oxidation of the chromogenic substrate TMB, providing a distinctive blue color visible to the naked eyes. Under the optimal conditions, the color of the solution and the absorbance at 680 nm were 6-fold higher than the blank experiment without the G-DNA(inter) probe. The DNAzyme activity was completely inhibited by the acpcPNA-C3 inhibitor probe which could bind to the G-DNA(inter) and prevented the intermolecular G-quadruplex formation as shown by the complete inhibition of the blue color generation. The addition of the DNA target displaced and prevented the acpcPNA-C3 from binding to the G-DNA(inter) and resulted in the reformation of the G-quadruplex, thus the DNAzyme activity was restored. The absorbance at 680 nm increased linearly as a function of DNA target concentration with a linear range from 0.25 μM to 0.025 μM with a limit of detection (LOD) of 7 nM. For the specificity evaluation, the G-DNA(inter)/acpcPNA-C3 detection system could discriminate the complementary DNA target from non-complementary DNA targets, although not to the single base mismatch resolution. When compared to an aegPNA with the same sequence, the acpcPNA system gave a better specificity as shown by the ability to distinguish more closely related DNA targets of the latter. Attempts have been made to improve the sensitivity of the DNA detection further by coupling the DNAzyme assay with the Exo III-assisted target recycling under various conditions. Unfortunately, the target recycling was not successful. Gel electrophoresis studies suggested that the partially digested G-DNA(inter) recombined with the acpcPNA probe, which prevented the formation of G-quadruplex and thus the DNAzyme activity was still inhibited.

APPENDIX

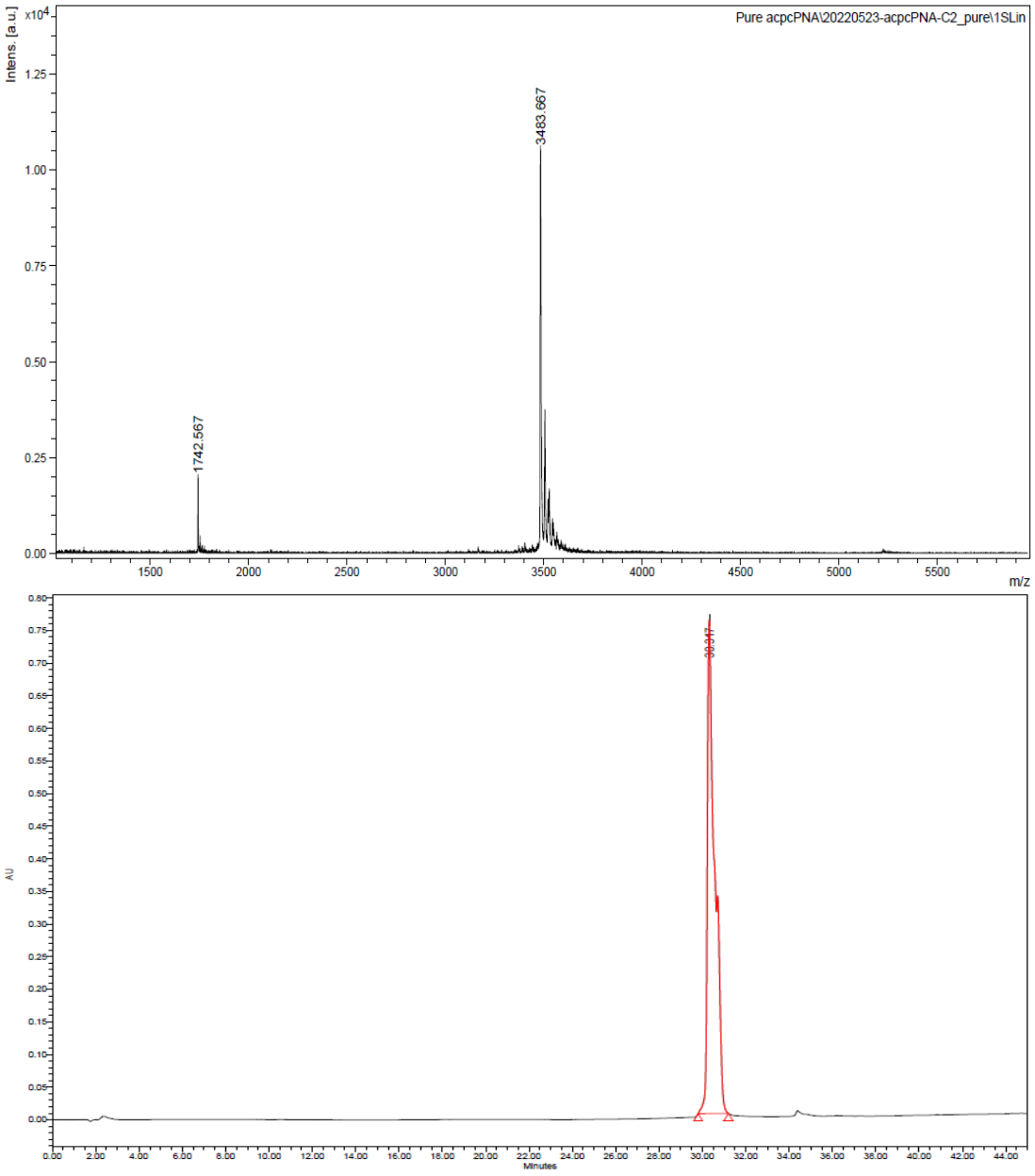

Figure A1 (A) Mass spectrum and (B) chromatogram of acpcPNA-C2.

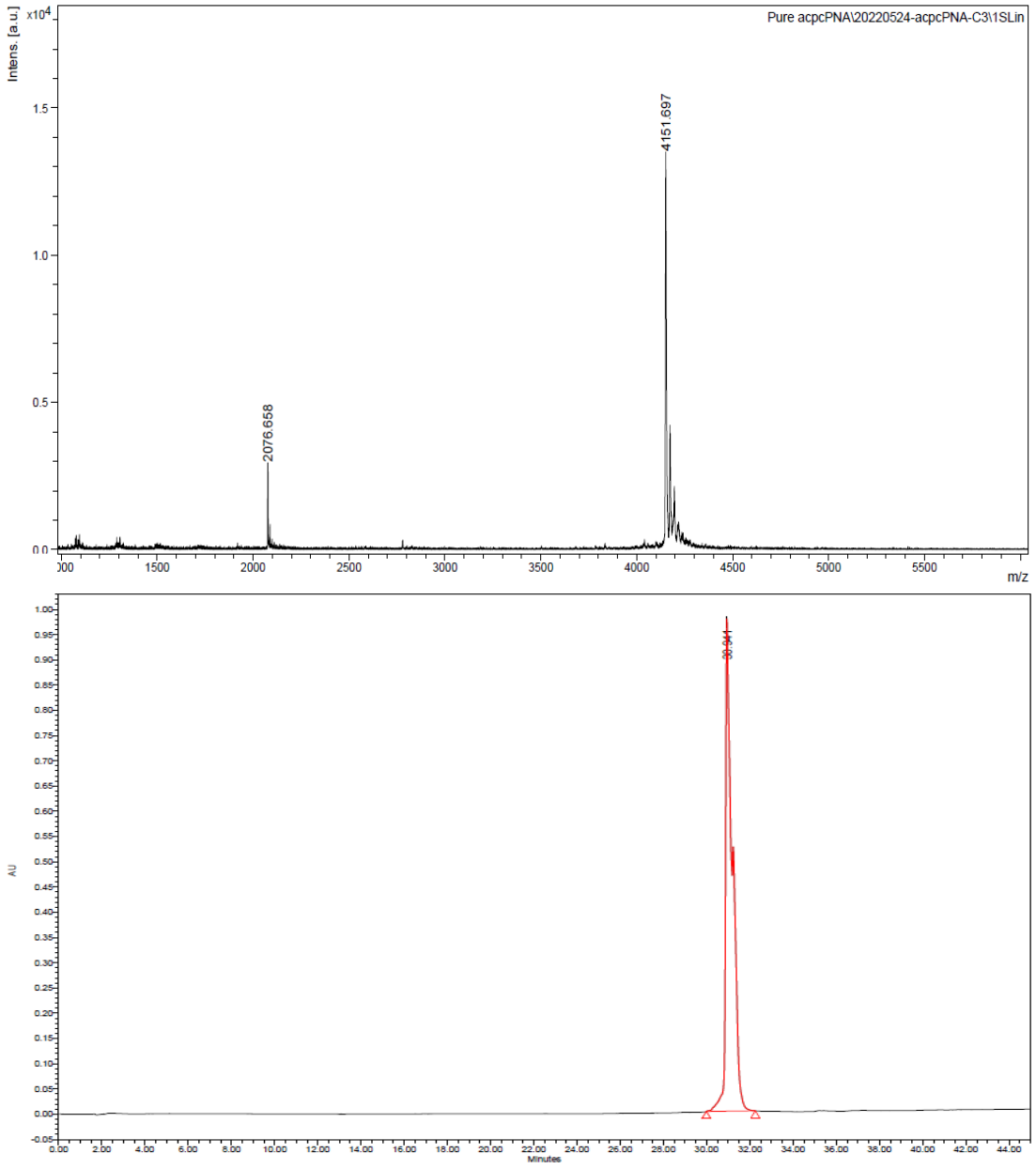

Figure A2 (A) Mass spectrum and (B) chromatogram of acpcPNA-C3.

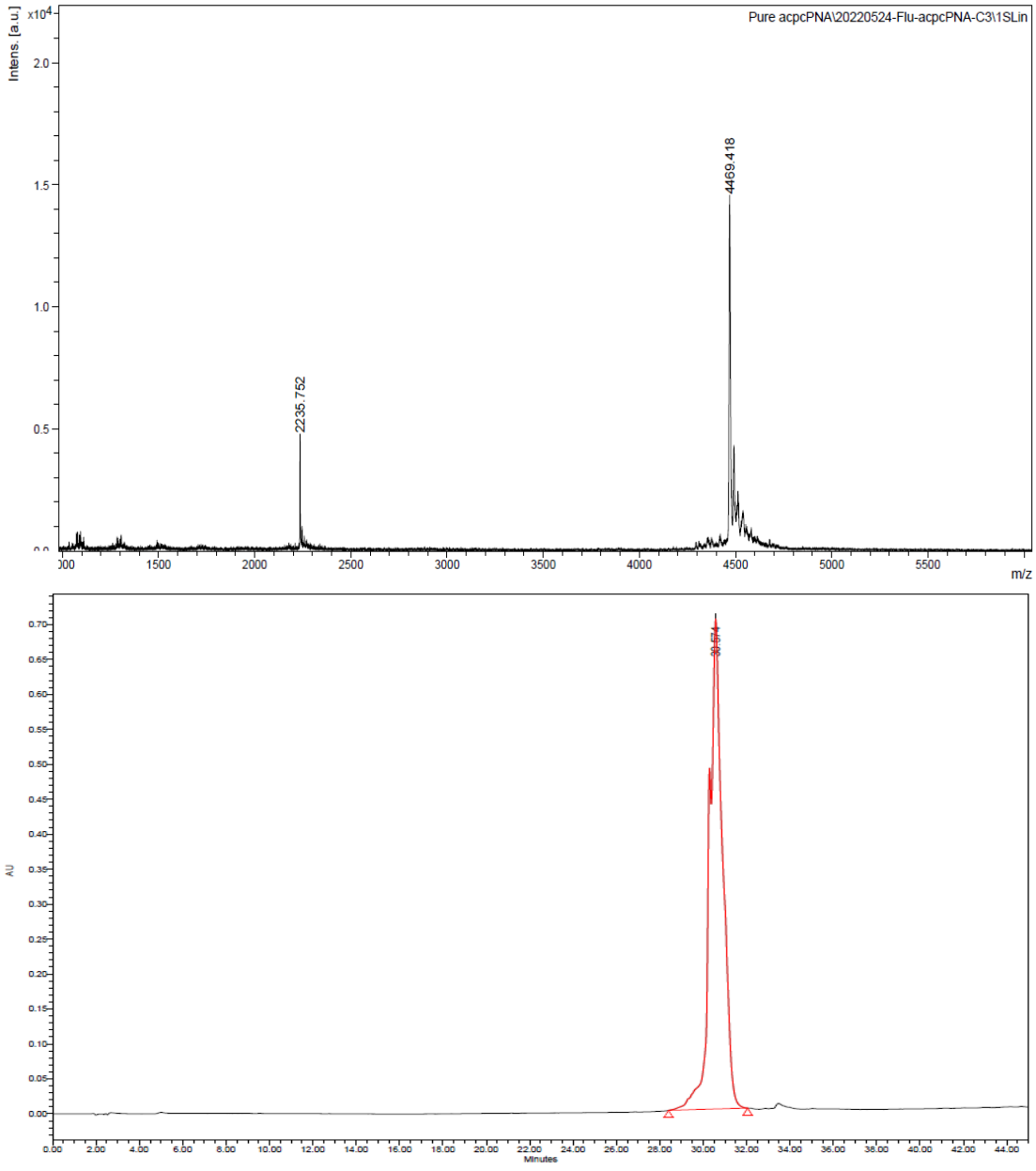

Figure A3 (A) Mass spectrum and (B) chromatogram of FAM-acpcPNA-C3.

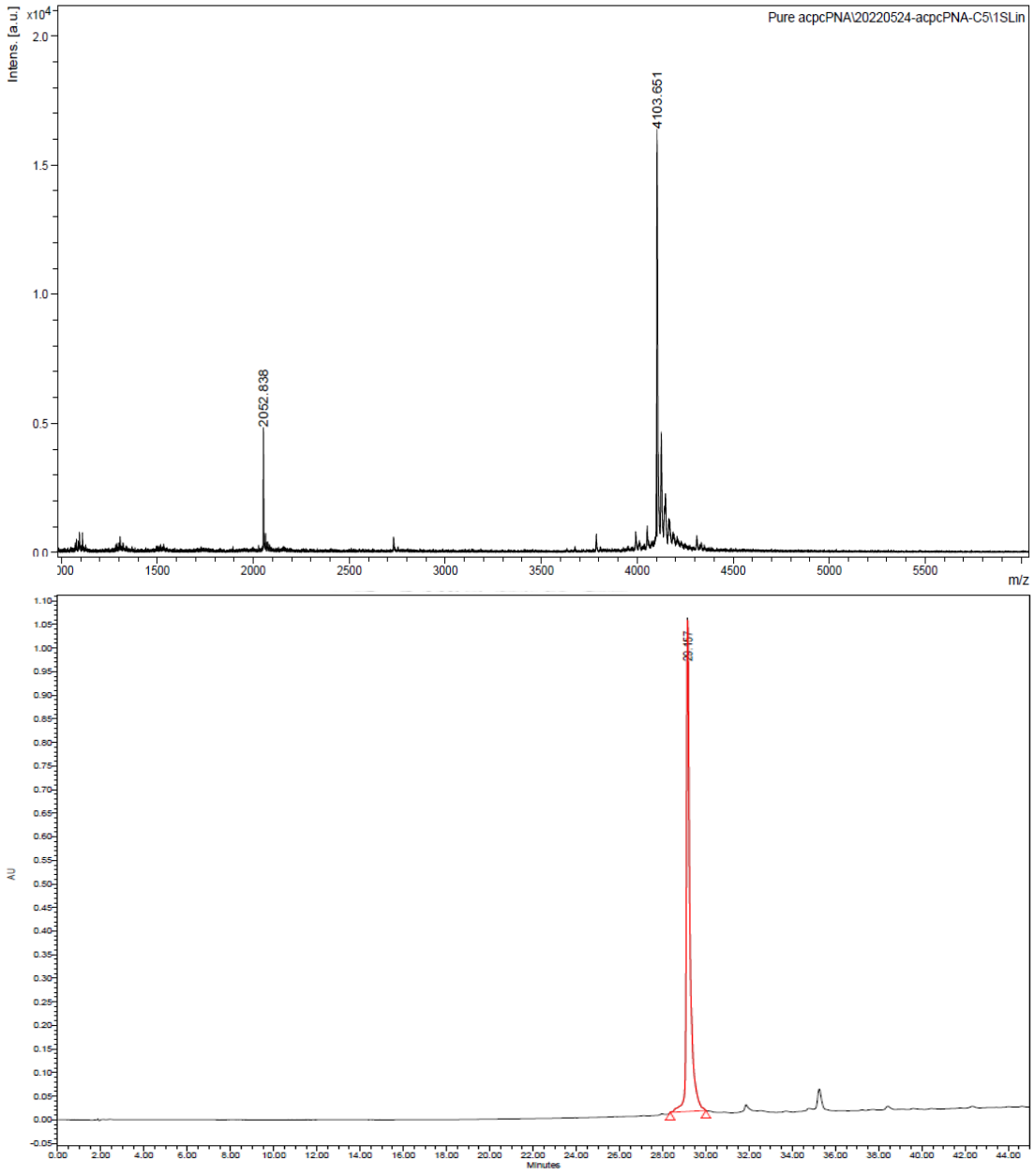

Figure A4 (A) Mass spectrum and (B) chromatogram of acpcPNA-C5.

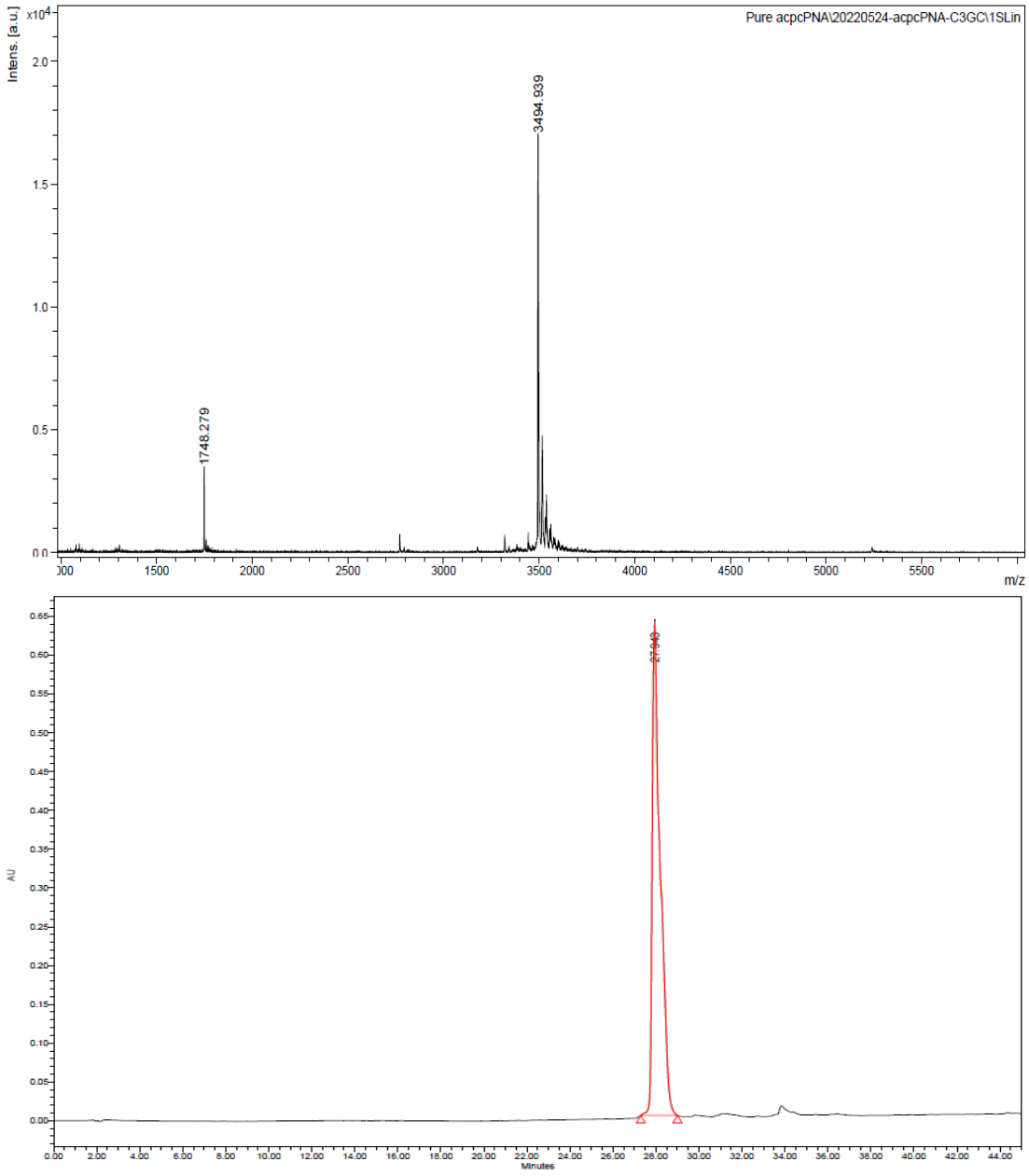

Figure A5 (A) Mass spectrum and (B) chromatogram of acpcPNA-C3GC.

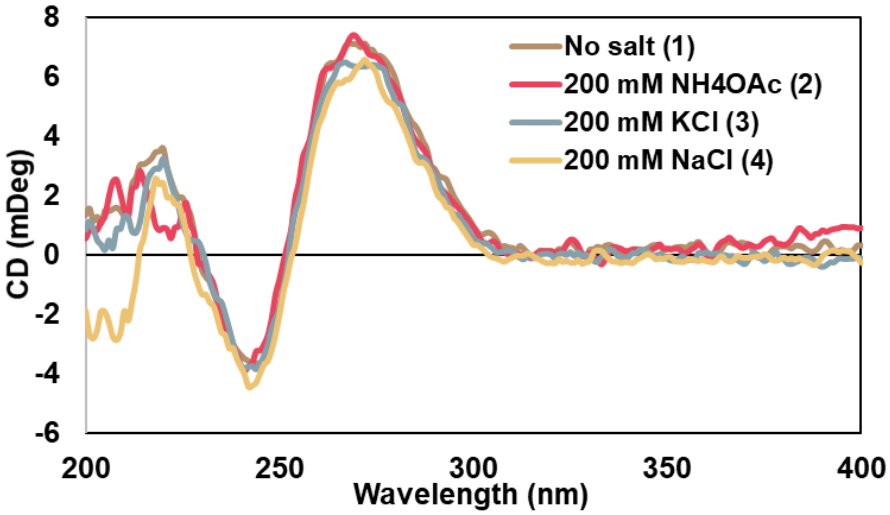

Figure A6 CD spectra of G-DNA(inter) in 66 mM Tris-HCl buffer, 0.66 mM $MgCl_2$, pH 8.0 with (1) no salt, (2) NH_4OAc, (3) KCl, (4) NaCl. The concentration of G-DNA(inter) = 2 μM, salt = 200 mM.

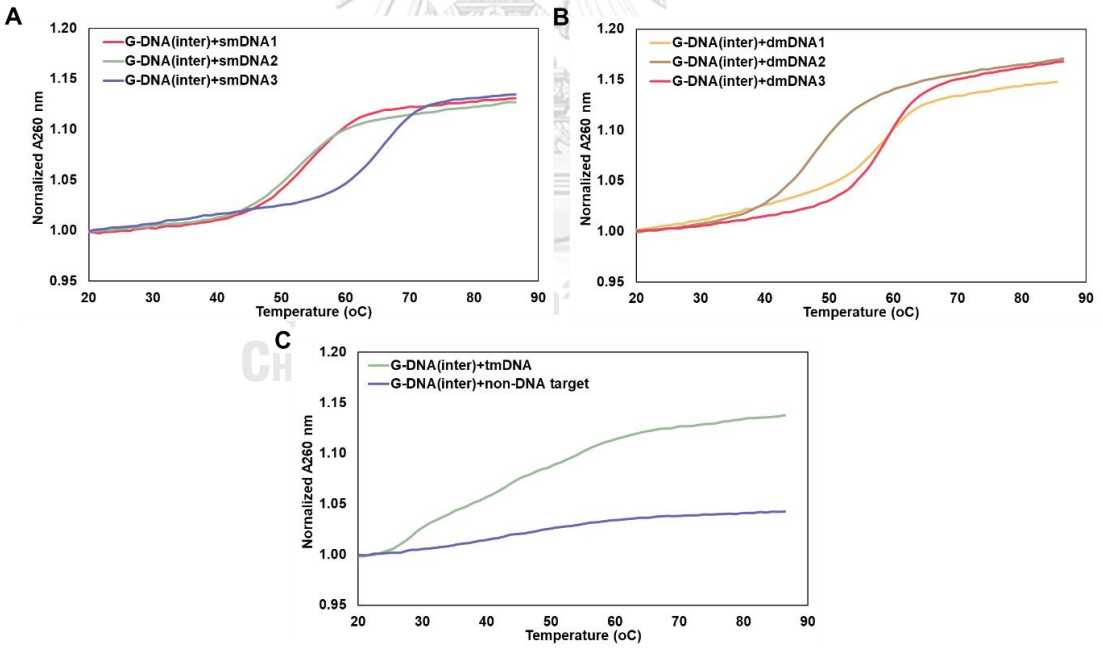

Figure A7 Melting temperature of G-DNA(inter) with (A) (a) smDNA 1, (b) smDNA 2, (c) smDNA 3, (B) (a) dmDNA 1, (b) dmDNA 2, (c) dmDNA 3, (D) (a) tmDNA, (b) non-DNA target in 200 mM NH_4OAc, 0.02% SDS, 66 mM Tris-HCl buffer, 0.66 mM $MgCl_2$, pH 8.0. The concentration of G-DNA(inter) = mmDNAs =1 μM.

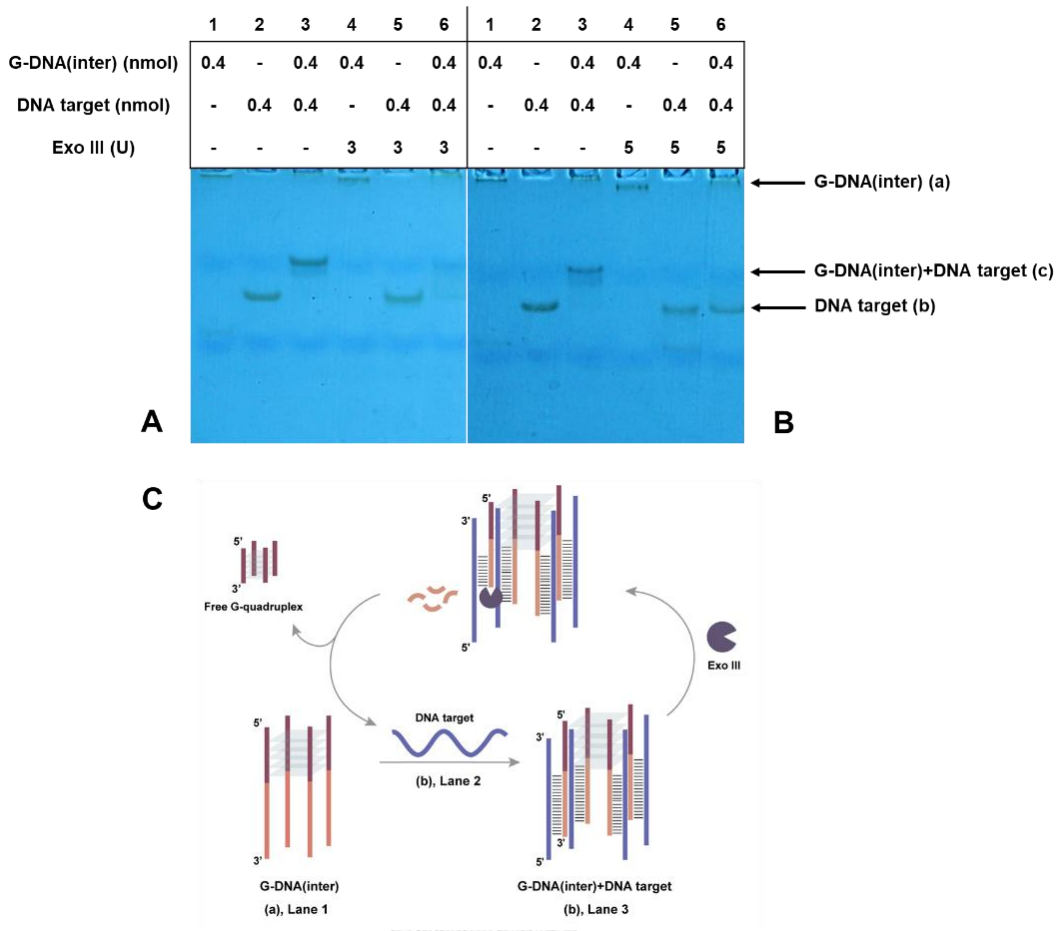

Figure A8 Non-denaturing PAGE of digestion of G-DNA(inter) and DNA target by Exo III, lane 1: G-DNA(inter), lane 2: DNA target, lane 3: G-DNA(inter)+DNA target, lane 4: G-DNA(inter)+Exo III, lane 5: DNA target+Exo III, lane 6: G-DNA(inter)+DNA target+Exo III under UV light. The quantities of G-DNA(inter) = 0.4 nmol, DNA target = 0.4 nmol, Exo III = (A) 3 U, (B) 5 U, NH_4OAc = 200 mM in 66 mM Tris-HCl buffer, 0.66 mM $MgCl_2$, pH 8.0 (total volume = 10 µL), (C) Schematic representation of the propose structure for this experiment

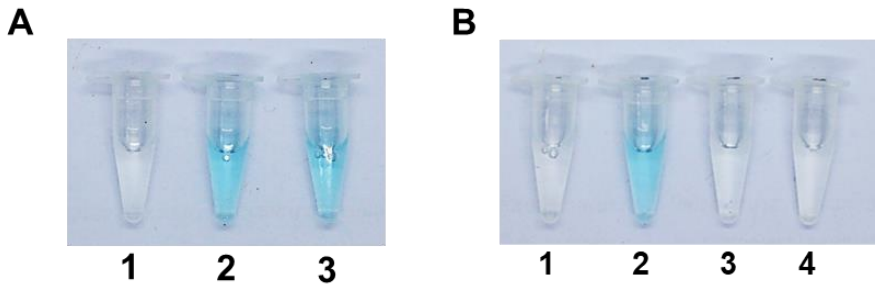

Figure A9 Photographs of (A) the Inhibition of DNAzyme acitivity of single mismatched G-DNA(inter), (1) no G-DNA(inter), (2) single mismatched G-DNA(inter), (3) single mismatched G-DNA(inter)+acpcPNA-C3, (B) the DNA target displacement by the increasing of complementary bases DNA target, (1) no G-DNA(inter) (N83), (2) G-DNA(inter) (N83), (3) G-DNA(inter) (N83)+acpcPNA-C3, (4) G-DNA(inter)+acpcPNA-C3+ DNA target (N82). The quantities of G-DNA(inter) = 0.25 μM, acpcPNA-C3= 0.50 μM, DNA target = 0.75 μM, TMB = 0.05 mM, H_2O_2 = 5 mM, hemin = 0.0125 μM, NH_4OAc = 200 mM, SDS = 0.02 %w/v in 66 mM Tris-HCl buffer, 0.66 mM $MgCl_2$, pH 8.0

Table A1 G-DNA and PNA sequences for the Inhibition of DNAzyme acitivity by single mismatched G-DNA(inter) and the DNA target displacement by the increasing of complementary bases DNA target experiments **(Figure A9)**[a]

Name	DNA and acpcPNA sequence
Single mismatched G-DNA(inter)	5'-GG GGG TAT CGA GTT CCG TGA CGC-3'
G-DNA(inter) (N83)	5'-GG GGG TAA CGA GTT CCG TGA ATA GCC ATC GG-3'
acpcPNA-C3	C-NH_2Lys-AA CCC ATT GCT C-Ac-N
DNA target (N82)	3'-TTT TT ATT GCT CAA GGC ACT TAT CGG TAG CC-5'

[a]The binding regions for the DNA targets are highlighted. The binding regions for the acpcPNA probe are underlined. Mismatched bases are shown in red. Non-pairing bases are presented in normal text.

REFERENCES

1. Zhang, M.; Guan, Y. M.; Ye, B. C. Ultrasensitive Fluorescence Polarization DNA Detection by Target Assisted Exonuclease III-Catalyzed Signal Amplification. *Chem. Commun.* **2011**, *47* (12), 3478-3480.

2. Yang, L.; Zhao, M.; Zhang, R.; Dong, J.; Zhang, T.; Zhan, X.; Wang, G. Synthesis and Fluorescence Study of a Quaternized Copolymer Containing Pyrene for DNA-Hybridization Detection. *ChemPhysChem.* **2012**, *13* (18), 4099-4104.

3. Miyamoto, S.; Sano, S.; Takahashi, K.; Jikihara, T. Method for Colorimetric Detection of Double-Stranded Nucleic Acid using Leuco Triphenylmethane Dyes. *Anal. Biochem.* **2015**, *473*, 28-33.

4. Amini, B.; Kamali, M.; Salouti, M.; Yaghmaei, P. Spectrophotometric, Colorimetric and Visually Detection of Pseudomonas Aeruginosa Eta Gene Based Gold Nanoparticles DNA Probe and Endonuclease Enzyme. *Spectrochim. Acta, Part A.* **2018**, *199*, 421-429.

5. Wang, J.; Cai, X.; Rivas, G.; Shiraishi, H.; Farias, P. A. M.; Dontha, N. DNA Electrochemical Biosensor for the Detection of Short DNA Sequences Related to the Human Immunodeficiency Virus. *Anal. Chem.* **1996**, *68* (15), 2629-2634.

6. Zhang, J.; Lao, R.; Song, S.; Yan, Z.; Fan, C. Design of an Oligonucleotide-Incorporated Nonfouling Surface and Its Application in Electrochemical DNA Sensors for Highly Sensitive and Sequence-Specific Detection of Target DNA. *Anal. Chem.* **2008**, *80* (23), 9029-9033.

7. Jaklevic, M. C. Molecular COVID-19 Test Gains First EAU for At-home Use. *JAMA.* **2021**, *325* (15), 1499-1499.

8. Ensafi, A. A. Chapter 1 - An Introduction to Sensors and Biosensors. In *Electrochemical Biosensors*, Elsevier, 2019; pp 1-10.

9. Rhodes, D.; Lipps, H. J. G-Quadruplexes and Their Regulatory Roles in Biology. *Nucleic Acids Res.* **2015**, *43* (18), 8627-8637.

10. Małgowska, M.; Gudanis, D.; Teubert, A.; Dominiak, G.; Gdaniec, Z. How To Study G-Quadruplex Structures. *BioTechnologia.* **2012**, *93* (4), 381-390.

11. Bhattacharyya, D.; Mirihana Arachchilage, G.; Basu, S. Metal Cations in G-Quadruplex

Folding and Stability. *Front Chem.* **2016**, *4*, 38-38.

12. Wright, W. E.; Tesmer, V. M.; Huffman, K. E.; Levene, S. D.; Shay, J. W. Normal Human Chromosomes Have Long G-rich Telomeric Overhangs at One End. *Genes Dev.* **1997**, *11*, 2801-2809.

13. Mohanty, J.; Barooah, N.; Dhamodharan, V.; Harikrishna, S.; Pradeepkumar, P. I.; Bhasikuttan, A. C. Thioflavin T as an Efficient Inducer and Selective Fluorescent Sensor for the Human Telomeric G-Quadruplex DNA. *J. Am. Chem. Soc.* **2013**, *135* (1), 367-376.

14. Yett, A.; Lin, L. Y.; Beseiso, D.; Miao, J.; Yatsunyk, L. A. N-Methyl Mesoporphyrin IX as a Highly Selective Light-Up Probe for G-quadruplex DNA. *J. Porphyrins Phthalocyanines.* **2019**, *23*, 1195-1215.

15. Achenbach, J. C.; Chiuman, W.; Cruz, R. P.; Li, Y. DNAzymes: from Creation *in vitro* to Application *in vivo*. *Curr. Pharm. Biotechnol.* **2004**, *5* (4), 321-336.

16. Travascio, P.; Li, Y.; Sen, D. DNA-Enhanced Peroxidase Activity of a DNA Aptamer-Hemin Complex. *Chem. Biol.* **1998**, *5* (9), 505-517.

17. Ruttkay-Nedecky, B.; Kudr, J.; Nejdl, L.; Maskova, D.; Kizek, R.; Adam, V. G-Quadruplexes as Sensing Probes. *Molecules.* **2013**, *18* (12), 14760-14779.

18. Yang, X.; Fang, C.; Mei, H.; Chang, T.; Cao, Z.; Shangguan, D. Characterization of G-Quadruplex/Hemin Peroxidase: Substrate Specificity and Inactivation Kinetics. *Chem. Eur. J.* **2011**, *17*, 14475-14484.

19. Ren, W.; Zhang, Y.; Huang, W. T.; Li, N. B.; Luo, H. Q. Label-Free Colorimetric Detection of Hg^{2+} based on Hg^{2+}-Triggered Exonuclease III-Assisted Target Recycling and DNAzyme Amplification. *Biosens. Bioelectron.* **2015**, *68*, 266-271.

20. Wang, G.; Zhu, Y.; He, X.; Chen, L.; Wang, L.; Zhang, X. Colorimetric and Visual Determination of Melamine by Exploiting the Conformational Change of Hemin G-quadruplex-DNAzyme. *Microchim. Acta.* **2014**, *181*, 411-418.

21. Wang, Z. H.; Lu, C. Y.; Liu, J.; Xu, J. J.; Chen, H. Y. An improved G-quadruplex DNAzyme for Dual-Functional Electrochemical Biosensing of Adenosines and Hydrogen Peroxide from Cancer Cells. *Chem. Commun.* **2014**, *50*, 1178-1180.

22. Li, W.; Li, Y.; Liu, Z.; Lin, B.; Yi, H.; Xu, F.; Nie, Z.; Yao, S. Insight into G-Quadruplex-Hemin DNAzyme/RNAzyme: Adjacent Adenine as the Intramolecular Species for Remarkable Enhancement of Enzymatic Activity. *Nucleic Acids Res.* **2016**, *44* (15), 7373-

7384.

23. Fu, R.; Li, T.; Lee, S. S.; Park, H. G. DNAzyme Molecular Beacon Probes for Target-Induced Signal-Amplifying Colorimetric Detection of Nucleic Acids. *Anal. Chem.* **2011**, *83* (2), 494-500.

24. Yan, L.; Yan, Y.; Pei, L.; Wei, W.; Zhao, J. A G-quadruplex DNA-based, Label-Free and Ultrasensitive Strategy for microRNA Detection. *Sci. Rep.* **2014**, *4* (1), 7400.

25. Zhang, L.; Zhu, J.; Li, T.; Wang, E. Bifunctional Colorimetric Oligonucleotide Probe based on a G-Quadruplex DNAzyme Molecular Beacon. *Anal. Chem.* **2011**, *83* (23), 8871-8876.

26. Ma, X.; He, S.; Zhang, Y.; Xu, J.; Zhang, H.; Wang, Z.; Xue, J.; Li, X.; Yu, W.; Fan, X. Signal-Off Tuned Signal-On (SF-T-SN) Colorimetric Immunoassay for Amantadine using Activity-Metalmodulated Peroxidase-Mimicking Nanozyme. *Sens. Actuators, B.* **2020**, *311*, 127933.

27. Hu, D.; Huang, Z.; Pu, F.; Ren, J.; Qu, X. A Label-Free, Quadruplex-based Functional Molecular Beacon (LFG4-MB) for Fluorescence Turn-on Detection of DNA and Nuclease. *Chem. Eur. J.* **2011**, *17* (5), 1635-1641.

28. Shen, C.; Shen, B.; Mo, F.; Zhou, X.; Duan, X.; Wei, X.; Li, J.; Duan, Y.; Cheng, W.; Ding, S. High-Sensitive Colorimetric Biosensing of *PIK3CA* Gene Mutation based on Mismatched Ligation-Triggered Cascade Strand Displacement Amplification. *Sens. Actuators, B.* **2018**, *273*, 377-383.

29. Li, R.; Liu, Q.; Jin, Y.; Li, B. Sensitive Colorimetric Determination of MicroRNA Let-7a Through Rolling Circle Amplification and a Peroxidase-Mimicking System Composed of Trimeric G-Triplex and Hemin DNAzyme. *Microchim. Acta.* **2020**, *187* (2), 139.

30. Li, R.; Zou, L.; Luo, Y.; Zhang, M.; Ling, L. Ultrasensitive Colorimetric Detection of Circulating Tumor DNA using Hybridization Chain Reaction and the Pivot of Triplex DNA. *Sci. Rep.* **2017**, *7* (1), 44212.

31. Li, R.; Liu, Q.; Jin, Y.; Li, B. G-triplex/Hemin DNAzyme: an Adeal Signal Generator for Isothermal Exponential Amplification Reaction-Based Biosensing Platform. *Anal. Chim. Acta.* **2019**, *1079*, 139-145.

32. Zhang, D.; Wang, W.; Dong, Q.; Huang, Y.; Wen, D.; Mu, Y.; Yuan, Y. Colorimetric Detection of Genetically Modified Organisms based on Exonuclease III-Assisted Target

Recycling and Hemin/G-quadruplex DNAzyme Amplification. *Microchim. Acta.* **2017**, *185* (1), 75.

33. Nielsen, P. E.; Egholm, M.; Berg, R. H.; Buchardt, O. Sequence-Selective Recognition of DNA by Strand Displacement with a Thymine-Substituted Polyamide. *Science.* **1991**, *254* (5037), 1497-1500.

34. Nielsen, P. E.; Egholm, M. An Introduction to Peptide Nucleic Acid. *Curr. Issues Mol. Biol.* **1999**, *1*, 89-104.

35. Demidov, V. V.; Potaman, V. N.; Frank-Kamenetskil, M. D.; Egholm, M.; Buchard, O.; Sönnichsen, S. H.; Nlelsen, P. E. Stability of Peptide Nucleic Acids in Human Serum and Cellular Extracts. *Biochem. Pharmacol.* **1994**, *48* (6), 1310-1313.

36. Liu, Y.; Braasch, D. A.; Nulf, C. J.; Corey, D. R. Efficient and Isoform-Selective Inhibition of Cellular Gene Expression by Peptide Nucleic Acids. *Biochemistry.* **2004**, *43* (7), 1921-1927.

37. Suparpprom, C.; Vilaivan, T. Perspectives on Conformationally Constrained Peptide Nucleic Acid (PNA): Insights into the Structural Design, Properties and Applications. *RSC Chem. Biol.* **2022**, *3* (6), 648-697.

38. Dragulescu-Andrasi, A.; Rapireddy, S.; Frezza, B. M.; Gayathri, C.; Gil, R. R.; Ly, D. H. A Simple γ-Backbone Modification Preorganizes Peptide Nucleic Acid into a Helical Structure. *J. Am. Chem. Soc.* **2006**, *128* (31), 10258-10267.

39. Pokorski, J. K.; Witschi, M. A.; Purnell, B. L.; Appella, D. H. (*S*,*S*)-*trans*-Cyclopentane-Constrained Peptide Nucleic Acids. A General Backbone Modification that Improves Binding Affinity and Sequence Specificity. *J. Am. Chem. Soc.* **2004**, *126* (46), 15067-15073.

40. Vilaivan, T.; Srisuwannaket, C. Hybridization of Pyrrolidinyl Peptide Nucleic Acids and DNA: Selectivity, Base-Pairing Specificity, and Direction of Binding. *Org. Lett.* **2006**, *8* (9), 1897-1900.

41. Vilaivan, T. Pyrrolidinyl PNA with α/β-Dipeptide Backbone: From Development to Applications. *Acc. Chem. Res.* **2015**, *48* (6), 1645-1656.

42. Vilaivan, T.; Suparpprom, C.; Harnyuttanakorn, P.; Lowe, G. Synthesis and Properties of Novel Pyrrolidinyl PNA carrying β-amino acid Spacers. *Tetrahedron Lett.* **2001**, *42*

(32), 5533-5536.

43. Argueta-Gonzalez, H. S.; Swenson, C. S.; Song, G.; Heemstra, J. M. Stimuli-Responsive Assembly of Bilingual Peptide Nucleic Acids. *RSC Chem. Biol.* **2022**, *3* (8), 1035-1043.

44. Kaewarsa, P.; Vilaivan, T.; Laiwattanapaisal, W. An Origami Paper-Based Peptide Nucleic acid Device Coupled with Label-Free DNAzyme Probe Hybridization Chain Reaction for Prostate Cancer Molecular Screening Test. *Anal. Chim. Acta.* **2021**, *1186*, 339130.

45. Suparpprom, C.; Srisuwannaket, C.; Sangvanich, P.; Vilaivan, T. Synthesis and Oligodeoxynucleotide Binding Properties of Pyrrolidinyl Peptide Nucleic Acids Bearing Prolyl-2-Aminocyclopentanecarboxylic Acid (ACPC) Backbones. *Tetrahedron Lett.* **2005**, *46* (16), 2833-2837.

46. Li, S.; Liu, C.; Gong, H.; Chen, C.; Chen, X.; Cai, C. Simple G-quadruplex-based 2-Aminopurine Fluorescence Probe for Highly Sensitive and Amplified Detection of MicroRNA-21. *Talanta.* **2018**, *178*, 974-979.

47. Li, B.; Du, Y.; Li, T.; Dong, S. Investigation of 3,3′,5,5′-Tetramethylbenzidine as Colorimetric Substrate for a Peroxidatic DNAzyme. *Anal. Chim. Acta.* **2009**, *651* (2), 234-240.

48. Zhang, L. M.; Cui, Y. X.; Zhu, L. N.; Chu, J. Q.; Kong, D. M. Cationic Porphyrins with Large Side Arm Substituents as Resonance Light Scattering Ratiometric Probes for Specific Recognition of Nucleic Acid G-Quadruplexes. *Nucleic Acids Res.* **2019**, *47* (6), 2727-2738.

49. Zhou, H.; Wu, Z. F.; Han, Q. J.; Zhong, H. M.; Peng, J. B.; Li, X.; Fan, X. L. Stable and Label-Free Fluorescent Probe based on G-triplex DNA and Thioflavin T. *Anal. Chem.* **2018**, *90* (5), 3220-3226.

50. Koirala, D.; Mashimo, T.; Sannohe, Y.; Yu, Z.; Mao, H.; Sugiyama, H. Intramolecular Folding in Three Tandem Guanine Repeats of Human Telomeric DNA. *Chem. Commun.* **2012**, *48* (14), 2006-2008.

51. Hou, X. M.; Fu, Y. B.; Wu, W. Q.; Wang, L.; Teng, F. Y.; Xie, P.; Wang, P. Y.; Xi, X. G. Involvement of G-triplex and G-hairpin in the Multi-Pathway Folding of Human Telomeric G-quadruplex. *Nucleic Acids Res.* **2017**, *45* (19), 11401-11412.

52. Li, M.; He, Y.; Meng, H.; Dong, Y.; Shang, Y.; Liu, H.; Qu, Z.; Liu, Y. Multiple Effects of

Sodium Dodecyl Sulfate on Chromogenic Catalysis of Tetramethylbenzidine with Horseradish Peroxidase. *J. Dispersion Sci. Technol.* **2021**, *42* (4), 526-536.

53. Kireyko, A. V.; Veselova, I. A.; Shekhovtsova, T. N. Mechanisms of Peroxidase Oxidation of O-Dianisidine, 3,3′,5,5′-Tetramethylbenzidine, and O-Phenylenediamine in the Presence of Sodium Dodecyl Sulfate. *Russ. J. Bioorg. Chem.* **2006**, *32* (1), 71-77.

54. Li, M.; Huang, X. R.; Guo, Y.; Shang, Y. Z.; Liu, H. L. A Novel Efficient Medium for Chromogenic Catalysis of Tetramethylbenzidine with Horseradish Peroxidase. *Chin. Chem. Lett.* **2017**, *28* (7), 1453-1459.

55. Jiang, H. X.; Cui, Y.; Zhao, T.; Fu, H. W.; Koirala, D.; Punnoose, J. A.; Kong, D. M.; Mao, H. Divalent Cations and Molecular Crowding Buffers Stabilize G-Triplex at Physiologically Relevant Temperatures. *Sci. Rep.* **2015**, *5* (1), 9255.

56. Schultze, P.; Hud, N. V.; Smith, F. W.; Feigon, J. The Effect of Sodium, Potassium and Ammonium Ions on the Conformation of the Dimeric Quadruplex Formed by the Oxytricha Nova Telomere Repeat Oligonucleotide d($G_4T_4G_4$). *Nucleic Acids Res.* **1999**, *27* (15), 3018-3028.

57. Hardin, C. C.; Watson, T.; Corregan, M.; Bailey, C. Cation-Dependent Transition between the Quadruplex and Watson-Crick Hairpin Forms of d(CGCG3GCG). *Biochemistry.* **1992**, *31* (3), 833-841.

58. Paramasivan, S.; Rujan, I.; Bolton, P. H. Circular Dichroism of Guadruplex DNAs: Applications to Structure, Cation Effects and Ligand Binding. *Methods.* **2007**, *43* (4), 324-331.

59. Vorlíčková, M.; Kejnovská, I.; Sagi, J.; Renčiuk, D.; Bednářová, K.; Motlová, J.; Kypr, J. Circular Dichroism and Guanine Quadruplexes. *Methods.* **2012**, *57* (1), 64-75.

60. Vorlíčková, M.; Kejnovská, I.; Bednářová, K.; Renčiuk, D.; Kypr, J. Circular Dichroism Spectroscopy of DNA: From Duplexes to Quadruplexes. *Chirality.* **2012**, *24* (9), 691-698.

61. Tang, W.; Zhou, H.; Li, W. Silver and Cyanine Staining of Oligonucleotides in Polyacrylamide Gel. *PLOS ONE.* **2015**, *10* (12), e0144422.

62. Wang, G. L.; Jin, L. Y.; Wu, X. M.; Dong, Y. M.; Li, Z. J. Label-Free Colorimetric Sensor for Mercury(II) and DNA on the Basis of Mercury(II) Switched-on the Oxidase-Mimicking Activity of Silver Nanoclusters. *Anal. Chim. Acta.* **2015**, *871*, 1-8.

63. Liu, Y. L.; Fu, W. L.; Li, C. M.; Huang, C. Z.; Li, Y. F. Gold Nanoparticles Immobilized

on Metal–Organic Frameworks with Enhanced Catalytic Performance for DNA Detection. *Anal. Chim. Acta.* **2015**, *861*, 55-61.

64. Dong, H.; Gao, W.; Yan, F.; Ji, H.; Ju, H. Fluorescence Resonance Energy Transfer between Quantum Dots and Graphene Oxide for Sensing Biomolecules. *Anal. Chem.* **2010**, *82* (13), 5511-5517.

65. Loo, A. H.; Sofer, Z.; Bouša, D.; Ulbrich, P.; Bonanni, A.; Pumera, M. Carboxylic Carbon Quantum Dots as a Fluorescent Sensing Platform for DNA Detection. *ACS Appl. Mater. Interfaces.* **2016**, *8* (3), 1951-1957.

66. Shi, H.; Jin, T.; Zhang, J.; Huang, X.; Tan, C.; Jiang, Y.; Tan, Y. A Novel Aptasensor Strategy for Protein Detection based on G-quadruplex and Exonuclease III-Aided Recycling Amplification. *Chin. Chem. Lett.* **2020**, *31* (1), 155-158.

67. Ling, Y.; Zhang, X. F.; Chen, X. H.; Liu, L.; Wang, X. H.; Wang, D. S.; Li, N. B.; Luo, H. Q. A Dual-Cycling Biosensor for Target DNA Detection based on the Toehold-Mediated Strand Displacement Reaction and Exonuclease III Assisted Amplification. *New J. Chem.* **2018**, *42* (6), 4714-4718.

68. Chen, P.; Huang, K.; Zhang, P.; Sawyer, E.; Wu, Z.; Wei, X.; Ying, B.; Geng, J. Exonuclease III-Assisted Strand Displacement Reaction-Driven Cyclic Generation of G-Quadruplex Strategy for Homogeneous Fluorescent Detection of Melamine. *Talanta.* **2019**, *203*, 255-260.

69. Tomac, S.; Sarkar, M.; Ratilainen, T.; Wittung, P.; Nielsen, P. E.; Nordén, B.; Gräslund, A. Ionic Effects on the Stability and Conformation of Peptide Nucleic Acid Complexes. *J. Am. Chem. Soc.* **1996**, *118* (24), 5544-5552.

70. De Costa, N. T. S.; Heemstra, J. M. Evaluating the Effect of Ionic Strength on Duplex Stability for PNA Having Negatively or Positively Charged Side Chains. *PLOS ONE.* **2013**, *8* (3), e58670.

71. Beese, L. S.; Steitz, T. A. Structural Basis for the 3′-5′ Exonuclease Activity of Escherichia coli DNA Polymerase I: a Two Metal Ion Mechanism. *EMBO J.* **1991**, *10* (1), 25-33.

VITA

NAME	Somlawan Thipkunthong
DATE OF BIRTH	26 October 1995
PLACE OF BIRTH	Bangkok
INSTITUTIONS ATTENDED	Bachelor's Degree of Science (Chemistry) in 2018
HOME ADDRESS	25 Satriwit soi 10 Chochi 4 Road Ladprao Bangkok 10230